Oxygen-dependent regulation of the activating transcription factor-4 (ATF-4)

Dissertation

zur Erlangung des mathematisch-naturwissenschaftlichen Doktorgrades

"Doctor rerum naturalium"

der Georg-August-Universität zu Göttingen

vorgelegt von

Marieke Claudia Wottawa

aus Kaufbeuren

Göttingen 2009

Mitglieder des Betreuungsausschusses:

Referent: Prof. Dr. G. Braus
Koreferentin: Prof. Dr. F. Melchior
Koreferentin: Prof. Dr. D. M. Katschinski

Tag der mündlichen Prüfung: 23. Oktober 2009

Abbreviations

3-AT	3-amino-1,2,4-triazole
4E-BP1	suppressor of eIF4E
5'-UTR	5'-untranslated region
aa	amino acid
AD	activation domain
ANP	atrial natriuretic peptide
ARD1	arrest-defective-1 protein
ARNT	aryl hydrocarbon receptor nuclear translocator
ATF-4	activating transcription factor-4
ATP	adenosine triphosphate
Asn	asparagine
att	attachment site
BD	DNA-binding domain
bHLH	basic helix-loop-helix
BNP	brain natriuretic peptide
BSA	bovine serum albumin
β-TRCP	β-transducin repeat-containing F-box protein
°C	degrees Celsius
cAMP	cyclic adenosine monophosphate
cDNA	complementary DNA
CHOP	CCAAT/enhancer-binding protein homologous protein
CMV	cytomegalovirus
CO_2	carbondioxid
CRE	cAMP response elements
CREB	cAMP response element-binding protein
C-TAD	C-terminal transactivation domain of HIF-1α
C-terminus	carboxy-terminus
Da	Dalton
DEPC	diethyl pyrocarbonate
DFO	desferrioxamine
DMEM-HG	Dulbecco's Modified Eagle Medium high glucose
DMOG	dimethyl-oxalyl-glycine
DMSO	dimethyl sulfoxid
DNA	deoxyribonucleic acid
dNTP	deoxynucleotide phosphate
EDTA	ethylendiamintetra acidic acid
eIF2	eukaryotic initiation factor 2
eIF4E	eukaryotic initiation factor 4E
EPO	erythropoietin
ER	endoplasmatic reticulum
F	force
FBP	F-box protein
FCS	fetal calf serum
Fig.	figure
FIH	factor inhibiting HIF-1
FL	firefly luciferase
g	gram
GADD153	growth arrest and DNA-damage-inducible protein 153
Gal4AD	activation domain of the transcription factor Gal4

Gal4BD	DNA-binding domain of the transcription factor Gal4
GFP	green fluorescent protein
GLUT1	glucose transporter 1
GTP	guanosine triphosphate
hrs	hours
HBS	HEPES-buffered saline
HeLa	human cervical cancer cell line
HEPES	4-(2-hydroxyethyl)-1-piperazineethanesulfonic acid
HEK293T	human embryonic kidney cell line expressing T-antigen of SV40
HepG2	human hepatocellular liver carcinoma cell line
HIF	hypoxia-inducible factor
HRE	hypoxia responsive element
IB	immunoblot
IKKβ	inhibitor of NF-κB kinase-β
iNOS	inducible nitric oxide synthase
IP	immunoprecipitation
IPTG	isopropyl-beta-D-thiogalactopyranosid
k	kilo
K_M	Michaelis-Menten constant
LB	Luria Bertani broth
Lys	lysine
M	molar (moles per litre)
MBP	maltose binding protein
MAPK	mitogen-associated protein kinase
MEF	mouse embryonic fibroblast
min	minute
ml	millilitre
mRNA	messenger RNA
NEM	N-ethylmaleimide
NF-κB	nuclear factor kappa-light-chain-enhancer of activated B-cells
N-TAD	N-terminal transactivation domain of HIF-1α
N-terminus	amino terminus
ODD domain	oxygen-dependent degradation domain
p	p-value
PAS domain	Per-Arnt-Sim domain
PBS	phosphate-buffered saline
PCR	polymerase chain reaction
PHD	prolyl-4 hydroxylase domain enzyme
Pro	proline
pVHL	von Hippel-Lindau tumor suppressor protein
RING	really interesting new gene
RL	Renilla luciferase
RNA	ribonucleic acid
Rnase	ribonuclease
RPB1	large subunit of RNA polymerase II
rpm	rounds per minute
RSK2	growth factor-regulated kinase
Sc medium	synthetic complete medium
SD	standard deviation
SDS	sodium dodecyl sulphate
SDS-PAGE	SDS-polyacrylamide gel electrophoresis

sec	second
Ser	serine
Siah2	seven in absentia homolog 2
siRNA	silencing RNA
SKP1	S-phase-kinase-associated protein-1
SUMO	Small ubiquitin-related modifier
Tab.	table
TAE	tris-acetate-EDTA
TAD	transactivation domain
TBE	tris-borate-EDTA
TEMED	tetramethyl ethylene diamine
TRiC	cytosolic chaperonin TCP-1 ring complex
Tris	tris-(hydroxymethyl)-aminomethane
U	unit
uORF	upstream open reading frame
UPR	unfolded protein response
UV	ultraviolet
V	volts
VEGF	vascular endothelial growth factor
YPDA	yeast peptone dextrose adenine

Summary

The prolyl-4 hydroxylase domain enzymes 1-3 (PHD1-3) are involved in regulating the protein stability of the α subunit of the hypoxia inducible factor (HIF), which is the master regulator of oxygen-dependent gene expression. Increasing evidence has been found that the PHDs are involved in regulating additional, HIF-independent, oxygen-dependent signal transduction pathways. Additionally, several hints for isoform-specific functions of the PHDs were observed. Therefore, members of the Department of Cardiovascular Physiology performed a yeast two-hybrid screen in which the activating transcription factor-4 (ATF-4) was identified as a novel interaction partner of the oxygen sensor PHD3. ATF-4 is involved in the cellular stress response and its expression is shown to be induced by different stress signals. ATF-4 is also regulated by phosphorylation and at the level of protein stability. In this thesis the oxygen-dependent regulation of the ATF-4 stability was characterized. Yeast two-hybrid assays revealed the isoform specificity of this interaction. The interaction of ATF-4 is restricted to PHD3 whereas no interaction was observed with PHD1, PHD2 or factor inhibiting HIF-1 (FIH). Furthermore, exposure to hypoxia or silencing PHD3 mRNA expression, but not PHD2 expression, resulted in increased ATF-4 proteins levels compared to normoxia in a HIF-independent manner. Reoxygenation experiments revealed a slower degradation of the ATF-4 protein after inhibiting PHD activity by DMOG treatment or silencing PHD3 expression, indicating the involvement of PHD3 in regulating ATF-4 protein stability. A newly identified oxygen dependent degradation (ODD) domain in the ATF-4 protein sequence is responsible for the oxygen-dependent ATF-4 protein stability. A degradation of ATF-4 by the ubiquitin-proteasome system mediated by the ubiquitin E3 ligase SCF beta-transducin repeat containing protein (β-TRCP) has been described earlier, but its function for the normoxic degradation of ATF-4, was not known. This thesis shows that the normoxic destabilisation of ATF-4 is mediated via PHD3-dependent degradation by the ubiquitin-proteasome system. However, pull-down assays and silencing β-TRCP expression by siRNAs showed that the normoxic degradation of ATF-4 is not mediated by the E3 ligases β-TRCP or von-Hippel Lindau tumor suppressor (pVHL). Therefore further studies will be needed to identify the E3 ligase responsible for the normoxic degradation of ATF-4. Studies of ATF-4 target gene expression under hypoxia revealed an involvement of oxygen-dependent ATF-4 regulation in cell fate decision. This knowledge of PHD regulated pathways can be helpful for the development of clinically applicable small molecule PHD inhibitors that can be used for the treatment of anemia or that may be applied because of their cytoprotective effects in damaged tissues.

1. Introduction

1.1 Hypoxia

Oxygen is needed by all multicellular organisms to produce energy in form of ATP. In mammals the transport of oxygen into tissues involves oxygen uptake by the lungs, transport and distribution via the blood, the cardiovascular system and finally diffusion to the oxygen consuming cells. To maintain their physiological function cells need the ability to adapt to a changing oxygen supply. An insufficient oxygen availability in relation to oxygen consumption is termed hypoxia. The complete absence of oxygen is called anoxia.

Several adaptation mechanisms, which are activated in response to hypoxia, are known. The respiratory rate can be increased to elevate the oxygen uptake and cells can switch to anaerobic metabolism. Additionally, erythropoiesis and angiogenesis into the ischemic tissues can be enhanced.

The hypoxia-inducible factor (HIF) has been identified to be the master transcriptional mediator to maintain oxygen homeostasis (Semenza, 1998).

1.2 The hypoxia-inducible factor (HIF)

HIF is involved in regulating the transcription of many genes involved in the cellular and systemic response to hypoxia by affecting the anaerobic metabolism, oxygen delivery, angiogenesis as well as cellular survival and proliferation. Oxygen homeostasis is maintained by HIF physiologically. However, HIF also affects oxygen homeostasis in pathophysiological situations like tumor growth, ischemia and tissue repair. HIF-1α knockout in mice results in embryonic lethality (embryonic day E 9.5). The embryos show an impaired vascularization, reduction of somites and neural fold defects (Iyer et al., 1998; Ryan et al., 1998).

1.2.1 Structure of HIF

HIF is a heterodimer that consists of three alternative oxygen-regulated α subunits (HIF-1α, HIF-2α and HIF-3α) and a constitutively expressed β subunit (HIF-β or aryl hydrocarbon receptor nuclear translocator (ARNT)). HIF-α and HIF-β belong to the basic helix-loop-helix (bHLH) transcription factors and contain two Per-Arnt-Sim (PAS) domains (Wang et al., 1995).

In addition, HIF-1α contains two transactivation domains (TAD). One is located at the N-terminus (N-TAD, aa 531-575) and the other at the C-terminus (C-TAD, aa 786-826). At these TADs the binding of co-activators takes place (Jiang et al., 1997; Pugh et al., 1997) (see Figure 1).

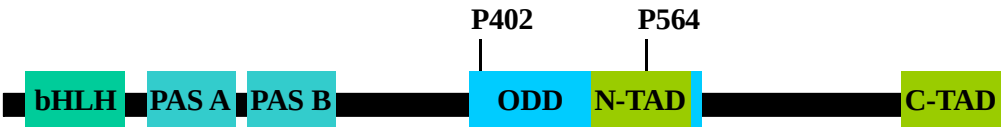

Fig. 1: Domain structure of the HIF-1α protein. The bHLH domain and the PAS domains are involved in dimerization and DNA binding. Two transactivation domains (TAD) are present in the HIF-1α protein. The N-TAD resides in the oxygen-dependent degradation (ODD) domain and the other TAD at the C-terminal end (C-TAD). The ODD domain is responsible for the oxygen-dependent instability of HIF-1α. It contains two proline residues, which are hydroxylated by the Prolyl-4 Hydroxylase domain enzymes (PHDs) in an oxygen-dependent manner.

All HIF-α isoforms are encoded by distinct gene loci. HIF-1α was the first identified isoform. It was discovered by analyzing proteins, which bind to the hypoxia responsive element (HRE) of the erythropoietin (EPO) gene (Wang et al., 1995). Later on HIF-2α and HIF-3α were identified by homology searches and by studying protein interaction partners of HIF-1β. HIF-2α is also known as endothelial PAS domain protein 1 (EPAS1), HIF-1-like factor (HLF) or HIF-1 related factor (HFR) (Ema et al., 1997; Flamme et al., 1997; Gu et al., 1998; Hogenesch et al., 1997; Tian et al., 1997). HIF-1α and HIF-2α are closely related. Both bind to HREs to induce the transcription of their target genes. HIF-3α is less related to HIF-1α. It negatively regulates the HIF-1α response when present as an alternative splice variant termed inhibitory PAS domain protein (Makino et al., 2007). This variant is not involved in activation of target gene transcription due to the lack of a TAD and acts as a HIF-1α inhibitor.

1.2.2 HIF-1 target genes

HIF-1 is the major transcriptional regulator of the oxygen-dependent gene expression. Until now more than one hundred genes are known to be regulated by HIF-1. These genes are involved in processes that regulate vasculogenesis, angiogenesis, metabolism, vasodilatation, cell migration, cell signalling and cell fate. All these processes lead to a decreased oxygen consumption of the cells or an increased oxygen delivery to maintain an adequate oxygen supply of the tissue.

The oxygen transport is influenced by HIF-1 via regulating the expression of EPO. EPO stimulates erythroid progenitor cells to increase erythropoiesis and is also involved in proliferation and differentiation of non-erythroid cells like endothelial cells, vascular smooth muscle cells, neurons and neuronal progenitor cells (Li et al., 2004).

By influencing the expression of transferrin and its corresponding receptor, the iron transport in the blood and uptake into the cells is also dependent on HIF-1 (Lok and Ponka, 1999; Rolfs et al., 1997; Tacchini et al., 1999; Wang and Semenza, 1993).

One of the most prominent HIF-1 target genes is the vascular endothelial growth factor (VEGF), which stimulates vascularization and angiogenesis (Forsythe et al., 1996; Liu et al., 1995). To further mediate the VEGF signal, the expression of the VEGF receptor 1 is also HIF-1-dependently upregulated under hypoxic conditions (Gerber et al., 1997). Furthermore, vascular tone is influenced by induction of the inducible nitric oxide synthase (iNOS) (Melillo et al., 1995) and the expression of the natriuretic peptides ANP and BNP through HIF-1 (Chun et al., 2003; Luo et al., 2006).

To modulate the oxygen demand of the cells in response to a decreased oxygen supply, HIF-1 also regulates several factors which are involved in the energy metabolism. Target genes are for example the glucose transporter-1 (GLUT1) (Ebert et al., 1995) and enzymes which are involved in the glycolytic pathway (Semenza et al., 1994), like the 6-Phosphofructo-1-kinase L, Phosphoglycerate kinase-1, or the Lactate dehydroxygenase A (Firth et al., 1994; Semenza et al., 1996). Theses enzymes allow the cells to switch to an anaerobic metabolism for a short time when oxygen is depleted. Because of the HIF-dependent upregulation of the anaerobic glycolysis the pH is lowered in the affected tissue. However, HIF-1 also regulates the pH by inducing the carbonic anhydrase 9 (CAIX) expression (Wykoff et al., 2000). CAIX catalyzes the buffering of acids by hydrating cell-generated carbon dioxid (CO_2) into bicarbonate (HCO_3^-) and a hydron (H^+).

Another group of HIF-1 target genes is involved in cell differentiation and proliferation. HIF-1 can mediate signals of pro-survival or pro-apoptotic pathways. It has been shown that the insulin-like growth factor (IGF) binding protein 1 and 3, which regulate cell growth and development, are upregulated during fetal hypoxia in a HIF-1-dependent manner (Tazuke et al., 1998). Apoptosis is induced in poorly supplied tissues after prolonged hypoxia. This is also mediated by HIF-1 via induction of for example the transforming growth factor TGF-β (Caniggia et al., 2000) or NIP3 (Bruick, 2000).

1.2.3 Regulation of HIF-1

The HIF-1 signal transduction pathway is tightly regulated. This regulation involves nuclear translocation, heterodimerization, transcriptional activation and recruitment of co-factors (see Figure 2).

Under hypoxic conditions, HIF-1α translocates into the nucleus and heterodimerizes with ARNT to form the transcriptional active HIF-1 complex that binds to HREs to promote and activate its target genes (Kallio et al., 1998).

By searching for interaction partners of the HIF-1α C-TAD, the factor inhibiting HIF-1 (FIH-1) was identified in a yeast two-hybrid screen (Mahon et al., 2001). FIH-1 is an asparaginyl hydroxylase that hydroxylates a conserved asparagine residue in the C-TAD (Asn803) in a strict oxygen-dependent manner. This hydroxylation inhibits the interaction of HIF-1α with the cAMP response element-binding protein (CREB)-binding protein (CBP) and p300 (Lando et al., 2002). CBP and p300 are histone acetyl transferases, which relax the chromatin structure. By inhibiting the recruitment of CBP/p300, FIH acts as a negative regulator of HIF-1 transcriptional activity.

The most crucial step in regulating hypoxia-inducible gene expression is the oxygen-dependent proteasomal degradation of HIF-α. It has been shown by two different groups that the protein stability of HIF-α is regulated via proline hydroxylation (Ivan et al., 2001; Jaakkola et al., 2001). These groups reported that the hydroxylation of HIF-1α takes place in the so called oxygen-dependent degradation (ODD) domain at the two conserved proline residues Pro402 and Pro564. The prolyl-4 hydroxylase domain enzymes (PHDs) were identified to catalyze this hydroxylation reaction (Bruick and McKnight, 2001; Epstein et al., 2001). The K_M values of these enzymes for O_2 are slightly above the atmospheric oxygen concentration and thus makes them suitable oxygen sensors in mammals. The prolyl hydroxylation marks HIF-1α for proteasomal degradation via the ubiquitin proteasome system, which is mediated by the pVHL-E3-ubiquitin-ligase complex. This complex consists of the von Hippel-Lindau tumor suppressor protein (pVHL), elongins B and C, Cullin 2 and the Ring-H2 finger protein Rbx-1. pVHL functions as a F-box protein that is responsible for the target recognition (Maxwell et al., 1999).

Besides hydroxylation, HIF-1α undergoes several other posttranslational modifications like SUMOylation, phosphorylation or acetylation.

A direct acetylation of HIF-1α at the lysine residue 532 was described after overexpression of the acetyl transferase arrest-defective-1 protein (ARD1) (Jeong et al., 2002). This lysine resides in the ODD domain of HIF-1α and it was hypothezised that its acetylation leads to an

enhanced recruitment of pVHL and consequently to an increased degradation of HIF-1α. However, other groups did not confirm a direct acetylation of HIF-1α despite the protein interaction of HIF-1α with ARD1 (Arnesen et al., 2005; Bilton et al., 2005). To date the influence of acetylation is unknown, further studies will be needed to define this issue.

It has been observed that HIF-1α is phosphorylated under hypoxic conditions, which is part of the fine modulation of HIF-1 transactivation activity. Different pathways are known to be involved in mediating this phosphorylation. The FIH-1-mediated hydroxylation is inhibited by phosphorylation of the HIF-1α threonine residue 796, which is mediated by the casein kinase II (Gradin et al., 2002; Lancaster et al., 2004). This phosphorylation leads to an enhanced transactivation activity by increasing the p300 interaction. Furthermore, HIF-1α is phosphorylated by the mitogen activated protein kinase (MAPK) p42/44 (Erk2/Erk1) leading to an enhanced transactivation activity (Richard et al., 1999). Additionally, the translocation of the HIF-1α subunit into the nucleus seems to be regulated by MAPK-dependent phosphorylation of the serine residues 641 and 642 (Mylonis et al., 2006).

SUMOylation of HIF-1α has been shown by different groups with contrary results. The HIF-1α residues Lys391 and Lys477 are found to be SUMOylated in SUMO-1 overexpressing cells. These lysines reside in the ODD domain and therefore SUMOylation might lead to an increased HIF-1α stability and thus increased HIF-1 activity (Bae et al., 2004). However, in another study the authors found a decreased HIF-1 activity after SUMOlyation and could not detect an influence of SUMOylation on the HIF-1α protein stability (Berta et al., 2007). Thus, until now the mechanism of SUMOlyation in regulating the HIF-1α stability and HIF-1 activity is not completely understood.

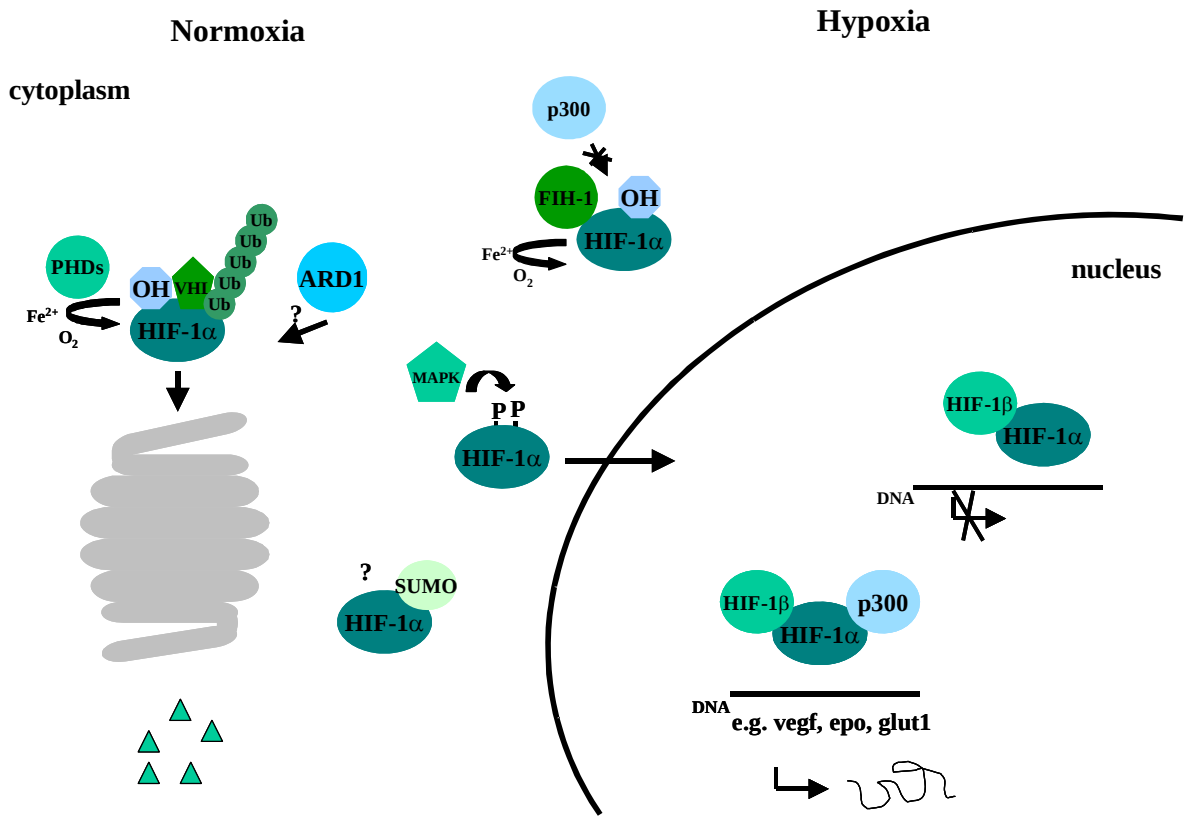

Fig. 2: Summary of the HIF-1α regulation. Under normoxic conditions HIF-1α is located within the cytoplasm. PHD2 hydroxylates the HIF-1α protein on Pro402 and Pro564. This triggers the ubiquitination of HIF-1α by pVHL and consequently leads to the proteasomal degradation of HIF-1α. HIF-1α is hydroxylated by FIH, which blocks the interaction of HIF-1α with p300. Additionally, SUMOylation of HIF-1α was observed, but the function is still discussed controversially. This is also true for the interaction with the acetyl transferase ARD1. Under hypoxic conditions HIF-1α translocates into the nucleus. Its nuclear accumulation is enhanced after MAPK-mediated phosphorylation. In the nucleus HIF-1α dimerizes with HIF-1β. After binding to p300 the transcription of HIF-1 target genes, like epo, vegf and glut1, is induced.

1.3 PHDs act as oxygen sensors in mammalian cells

Three different human PHDs are known (PHD1, PHD2, PHD3) to be responsible for the prolyl hydroxylation of the HIF-α subunit. These belong to the iron- and 2-oxoglutarate-dependent dioxygenases superfamily. The PHDs require oxygen and 2-oxoglutarate as co-substrates for their enzymatic activity. This dependence on oxygen explains their capability to function as oxygen sensors.

In the context of regulating HIF-1α abundance PHD2 is the dominant factor, because it is the rate limiting enzyme that regulates the HIF-1α levels in normoxia (Berra et al., 2003).

PHD1-3 mRNAs are expressed in all tissues but with different expression levels. PHD1 is highly expressed in testis and hormone responsive tissues. In contrast to this, PHD2 is constitutively expressed in all tissues and PHD3 has the highest expression level in skeletal

and heart muscle as well as in placenta (Cioffi et al., 2003; Lieb et al., 2002; Oehme et al., 2002).

In studies using GFP-PHD fusion proteins it was demonstrated that the intracellular localization differs between the three PHD isoforms. PHD1 was found in the nucleus only, PHD2 was mainly localized in the cytoplasm and PHD3 was found in both compartments (Metzen et al., 2003). The expression pattern of the three PHDs varies upon hypoxia. PHD2 is the most abundant isoform in normoxic conditions and consequently PHD2 is mainly responsible for the normoxic hydroxylation of the HIF-α subunit (Berra et al., 2003). The promoters of the *phd2* and *phd3* genes both contain HREs and are transcribed by HIF-1 under hypoxic conditions (Metzen et al., 2005; Pescador et al., 2005). The hypoxia-inducible expression of PHD2 and 3 serves as a negative feedback mechanism and ensures the rapid HIF-α degradation during reoxygenation. Additionally, PHD3 seems to have a higher affinity to HIF-2α compared to HIF-1α (Appelhoff et al., 2004).

In contrast to PHD2 and PHD3, the expression of PHD1 is not induced by hypoxia. It has been shown that PHD1 is inducible in human mammary carcinoma cells by oestrogen (Seth et al., 2002).

1.3.1 PHD activity

PHDs can function as effective oxygen sensors in mammalian cells, because their K_M values for O_2 are between 230-250 μM, which is slightly above the partial atmospheric oxygen pressure at sea level (Hirsila et al., 2003). This ensures their oxygen-dependent hydroxylation activity when all co-factors are present in the cells. PHD activity is tightly regulated at the full range of oxygen concentrations from normoxia (21 % O_2) to severe hypoxia (less than 0,1 % O_2).

The PHDs hydroxylate two proline residues in a conserved LxxLAP motif of HIF-1α. It has been shown that the activity of PHD2 and PHD3 is similar, whereas the PHD1 activity is lower (Tuckerman et al., 2004). In addition, the two proline residues are differently hydroxylated by the PHDs. All three PHD isoforms hydroxylate HIF-1α at Pro564, whereas Pro402 is hydroxylated by PHD1 and PHD2 only (Chan et al., 2005; Epstein et al., 2001). Further studies revealed a much higher affinity of PHD2 for Pro402 than for Pro564 (Huang et al., 2002).

The PHDs catalyze the hydroxylation reaction in which one oxygen atom is added to a peptidyl proline to form hydroxyproline. The other oxygen atom is used in a coupled decarboxylation reaction that converts 2-oxoglutarate to succinate. For this reaction a single

non-haem bound Fe^{2+} that coordinates in an enzyme-Fe^{2+}complex is required. The Fe^{2+}complex binds to 2-oxoglutarate and then to the peptidyl proline. The binding displaces a water molecule and triggers the reaction with molecular oxygen. This leads to the oxidative decarboxylation of 2-oxoglutarate to succinate, CO_2 and the ferrly species Fe=O (Fe^{3+}) at the iron centre. This reactive intermediate then oxidizes the peptiyl proline (see Figure 3).

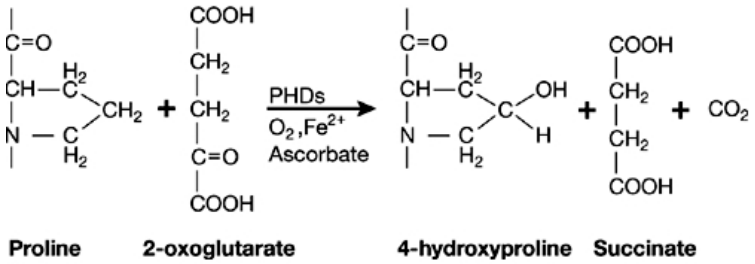

Fig. 3: Reaction catalyzed by the prolyl-4 hydroxylase domain proteins (PHDs). The PHDs use O_2 and 2-oxoglutarate as co-substrates, and Fe^{2+} and ascorbate as co-factors. In the hydroxylation reaction 4-hydroxyproline and succinate are formed (Berra et al., 2006).

The hydroxylation reaction is also dependent on ascorbate, which is needed to recycle the intermediate Fe^{3+} into the reduced Fe^{2+}, which subsequently can be used in the next catalytic cycle and prevents auto-oxidation of the enzyme in an uncoupled reaction (Counts et al., 1978; Nietfeld and Kemp, 1981). Studies in junD deficient cells, in which the antioxidant defense pathways are reduced, showed an enhanced PHD activity resulting in an increased HIF-1α hydroxylation. Furthermore, ascorbate may be involved in mediating the antioxidant reaction and may thereby affect the hypoxia pathway (Gerald et al., 2004).

1.3.2 Modulation of PHD activity

To adapt the HIF activity to a variety of changing conditions, the PHD activity is not only regulated by oxygen availability. An inhibition of PHD function can be achieved by depletion of intracellular ascorbate, with competitive inhibitors of 2-oxoglutarate or inhibiting the Fe^{2+}center of the PHDs.

The 2-oxoglutarate analog N-oxalyl-glycine (NOG) and dimethyl-oxalyl-glycine (DMOG) were the first substances that were found to inhibit PHD enzymatic activity and to stabilize HIF-1α *in vitro* and *in vivo* (Epstein et al., 2001; Jaakkola et al., 2001). For clinical application, however, these substances are not specific and potent enough and thus more screenings were performed to find more efficient PHD inhibitors. By this further 2-oxoglutarate analogs were found to activate HIF *in vivo* leading to an increased expression of HIF target genes: L-mimosine injection leads to HIF-1α induction in the kidney of the

treated rats (Warnecke et al., 2003), FG-2216 treatment elevates EPO levels and increases erythropoiesis (Hsieh et al., 2007), and FG-4487 treatment of rats leads to a HIF-1α induction in the kidneys (Bernhardt et al., 2006). However, before these PHD-inhibitors can be applied clinically the consequences of PHD-inhibition have to be fully understood.

Another approach to stabilize HIF-1α by inhibiting the PHD activity is the use of iron chelators like desferrioxamine (DFO). DFO leads to a stabilization of HIF-1α and expression of its target genes under normoxic conditions (Agani and Semenza, 1998). The clinical application of iron chelators, however, is problematic as iron is an essential co-factor for many enzymes and affects DNA synthesis and cell growth (Le and Richardson, 2002).

The effect of divalent metal ions on PHD activity is not completely understood. It has been shown that the application of cobalt chloride ($CoCl_2$) or nickel chloride ($NiCl_2$) induces EPO production (Goldberg et al., 1988). It has been assumed that $CoCl_2$ or $NiCl_2$ compete with Fe^{2+} for the catalytic center of the PHDs. Recent studies, however, showed that the effect of $CoCl_2$ and $NiCl_2$ could be the result of ascorbate depletion in the cells causing oxidative stress and thereby inhibiting PHD activity (Salnikow et al., 2004).

Reactive oxygen species (ROS) may also influence PHD function by chelating and oxidizing Fe^{2+} to Fe^{3+} (Pan et al., 2007). The role of ROS in hypoxia signaling is discussed controversially. Some groups reported that the production of ROS by mitochondria increases under ongoing hypoxia (Chandel et al., 1998; Guzy et al., 2005; Mansfield et al., 2005). In contrast to this, in other studies a decreased release of H_2O_2 in hypoxia compared to normoxia was detected (Lopez-Barneo et al., 2001).

1.3.3 PHD substrates/interactors

Several PHD protein interaction partners have been identified mainly by yeast two-hybrid screens. These newly found PHD interaction partners might be involved in regulating PHD stability, folding, subcellular localization and enzymatic activity or might themselves be regulated by PHDs.

By performing a yeast two-hybrid screen using full-length PHD3 as bait, the activating transcription factor-4 (ATF-4) was identified as new PHD3 interaction partner (Köditz et al., 2007). The meaning of this interaction was further studied in this thesis. ATF-4 proved to be the up to now only known protein besides HIF-α, for which the protein stability is regulated by PHD3.

PHD3 has been shown to be ubiquitinated and its activity to be regulated by the RING finger E3 ligase seven in absentia homolog 2 (Siah2) (Nakayama et al., 2007; Nakayama et al., 2004). The turnover rate of the other PHD isoforms is not affected by Siah2.

For PHD2 a protein-interaction with the FK506 binding protein 38 (FKBP38) has been described (Barth et al., 2007). It has been hypothesized that FKBP38-bound PHD2 is constantly degraded whereas non-bound PHD2 is not degraded and thus regulates HIF-α abundance. FKBP38 is a peptidyl prolyl cis/trans isomerase that functions as a receptor for the immunosuppressive drugs cyclosporine A and FK506. As member of the FKBP family of immunophilins it interacts in presence of FK506 with calcineurin, which is involved in signal transduction and apoptosis (Liu et al., 1991). Regulation of PHD2 protein stability, however seems to be independent of the peptidyl cis/trans isomerase activity.

PHD3 is the only PHD isoform found to interact with the cytosolic chaperonin TCP-1 ring complex (TRiC) (Masson et al., 2004). Cytosolic chaperonins like TRiC seem to be essential for the correct folding of PHD3 (Fedulova et al., 2007). TRiC is also involved in the assembly of the pVHL-elonginB-elonginC E3 ubiquitin ligase complex, but the interplay of these two functions is not defined yet (Feldman et al., 1999).

To facilitate the interaction between HIF-α and the PHDs, these factors assemble with other proteins to form a multi-protein complex. The osteosarcoma amplified 9 (OS-9) protein which interacts with HIF-1α, PHD2 or PHD3, appears to be one of the scaffolding proteins in this complex (Baek et al., 2005). Another scaffolding protein which might be involved in the assembly of HIF-1α, pVHL and PHDs is the A-kinase anchor protein 12 (AKAP12). An increased AKAP12-dependent HIF-1α degradation was observed which is caused by an enhanced recruitment of PHD2 (Choi et al., 2007). As potential scaffold for the PHD3-HIF-1α interaction the MAPK organizer 1 (Morg1) was identified. Overexpression of Morg1 leads to a decreased HIF target gene expression (Hopfer et al., 2006).

Other not so well studied interaction partners of PHD2, which were also identified by yeast two-hybrid screens, are the iron-only hydrogenase-like protein 1 (IOP1) (Huang et al.,2007) and the inhibitor of growth 4 (ING4) (Ozer et al., 2005). The melanoma antigen 11 and 9 (MAGE-11 and MAGE-9) interact with all three PHD isoforms, but the underlying function is not fully understood to date (Aprelikova et al., 2009).

Especially PHD1 interacts with factors of other signal transduction pathways. These novel PHD1 targets all contain the conserved LXXLAP consensus motif, which is also found in the ODD domain of the HIF-α subunit. One of these novel interaction partners is the inhibitor of NF-κB kinase-β (IKKβ) that is solely regulated by PHD1. Hypoxia activates the NF-κB

pathway by activating IKKβ. This leads to the phosphorylation-dependent degradation of IκBα and thus NF-κB release. Hypoxia mimicking by inhibition of PHD activity or the down regulation of PHD1 expression by siRNA leads also to the activation of the NF-κB pathway. Conversely, overexpression of PHD1 results in a decreased NF-κB activity (Cummins et al., 2006). To date, a PHD1-dependent hydroxylation of IKKβ has not been shown (Cockman et al., 2006). Thus, it is not clear if the PHD1-dependent regulation of IKKβ depends on PHD1 hydroxylation activity comparable to the HIF-α regulation.

The large subunit of RNA polymerase II (RPB1) also contains a LXXLAP consensus motif and forms a complex with PHD1 and PHD2 under oxidative stress. A PHD1-dependent hydroxylation was observed while PHD2 had an inhibitory effect on the degradation of RPB1 (Mikhaylova et al., 2008). The hydroxylation of RPB1 was verified by the use of an anti-hydroxy-RPB1 antibody.

1.3.4 Biological function of PHDs

To study the *in vivo* function of the PHDs several genetically modified PHD mouse models were produced. *Phd1*$^{-/-}$ and *Phd3*$^{-/-}$ mice are viable whereas *Phd2*$^{-/-}$ embryos die at midgestation. The PHD2 knockout leads to an underdeveloped myocardium and trabeculae in the heart and poor labyrinthine branching in the placenta. Thus, PHD2 seems to be the critical regulator of the hypoxic response during embryonic development (Takeda et al., 2006).

To further study the importance of PHD2 in adult animals a tamoxifen-induced Cre-loxP *Phd2*$^{-/-}$ mouse model has been developed. The PHD2 knockout in the adult mice causes an increased vascular density and lumen vessel size together with an increased recruitment of vascular smooth muscle cells (Takeda et al., 2007).

PHD1 knockout mice show no obvious phenotype under non-stressed conditions, except a reduced mitochondrial oxygen consumption in skeletal muscle cells (Aragones et al., 2001). This metabolic adaption protects the muscle cells from an ischemic insult. This effect seems to be mediated by HIF-2α, which indicates a PHD1 HIF-2α isoform specific regulation. A sympathoadrenal phenotype is observed in *Phd3*$^{-/-}$ mice. The symphatic innervation is decreased leading to reduced plasma catecholamine levels and blood pressure in the knockout mice (Bishop et al., 2008).

1.4 The activating transcription factor-4 (ATF-4)

ATF-4 is a member of the ATF/CREB bZIP transcription factor family that binds to cyclic adenosine monophosphat (cAMP) response elements (CRE) (Vallejo et al., 1993). ATF-4 regulates the transcription by forming homo- or heterodimers with other bZIP transcription factors like C/EBP isoforms, FOS, JUN and NRF2 (Chevray and Nathans, 1992).

ATF-4 is crucial for the cellular response to different types of stress, like anoxia, amino acid deprivation, endoplasmatic stress and exposure to oxidants or reactive metals (Rutkowski and Kaufman, 2003). All these stress pathways converge in the phosphorylation of the eukaryotic initiation factor 2 (eIF2), which leads to a general inhibition of protein synthesis, but the selective upregulation of ATF-4 translation. This mechanism is conserved within higher eukaryotes. However, not only the response to stress is regulated by ATF-4, but also cell proliferation and differentiation, vascularization and osteoblast formation (Masuoka and Townes, 2002; Roybal et al., 2005; Yang et al., 2004).

1.4.1 Regulation of ATF-4 expression

Eukaryotic cells respond to diverse stress signals by phosphorylation of the α subunit of eIF2. This phosphorylation inhibits the recycling of eIF2 to its active GTP-bound form, which is crucial for initiation of protein translation. Various eIF2 kinases (PKR, HRI, PERK/PEK and GCN2) are known in mammals and each of them contains unique regulatory regions to recognize different stress conditions. The PKR is part of an antiviral defense mechanism which is mediated by interferon (Garcia et al., 2006). Heme deprivation, oxidative stress and heat shock lead to eIF2α phosphorylation via HRI (Chen, 2007). GCN2 is activated in response to nutrition deprivation, UV irritation, proteasome inhibition and certain viral infections (Berlanga et al., 2006; Deng et al., 2002; Hinnebusch, 2005; Jiang and Wek, 2005). Proteins of the secretory pathway are folded in the endoplasmatic reticulum (ER). When the folding demand exceeds the capacity, unfolded or misfolded proteins accumulate and elicit the unfolded protein response (UPR). ER stress is recognized by the amino terminal region of PERK, which phosphorylates eIF2α at Ser51 and consequently reduces global translation and activates transcription of genes subjected to the UPR (Harding et al., 1999; Harding et al., 2000; Sood et al., 2000). ATF-4 mRNA is one of the selected targets, whose translation is increased in response to ER stress. This enhanced ATF-4 translation is mediated by two upstream open reading frames (uORFs) in the 5'-leader of the ATF-4 mRNA. The 5'-proximal uORF (uORF1) encodes for only three amino acids whereas the second uORF (uORF2) encodes for 59 residues and overlaps with the ATF-4 coding region. uORF1

facilitates ribosome scanning and reinitiation at downstream coding regions of the ATF-4 mRNA. Under non-stressed conditions eIF2α is abundantly present in the GTP-bound form and the uORF1 reinitiates the translation at uORF2, which is an inhibitory element that blocks ATF-4 expression. When eIF2α is phosphorylated under stress conditions, the eIF2α-GTP level is reduced and the time needed by the ribosomes to scan the mRNA increases. This leads to a delay of translational reinitiation and allows the ribosomes to reinitiate at the ATF-4 coding region.

Elevated ATF-4 levels induce the expression of other bZIP transcription factors like ATF-3 and CHOP (CCAAT/enhancer-binding protein homologous protein)/GADD153 (growth arrest and DNA-damage-inducible protein 153) that together induce a set of genes important for cellular remediation and apoptosis.

GADD34 is another ATF-4 target gene, which encodes for the regulatory subunit of the type 1 serine/threonine phosphatase that dephosphorylates eIF2α (Harding et al., 2003; Novoa et al., 2001). The translation of GADD34 is possible because of one uORF in its 5'-untranslated region (5'-UTR) allowing translation under stress conditions (Lee et al., 2009). By regulating GADD34 expression ATF-4 restores translation and allows for the synthesis of proteins which elevate ER capacity.

The dependency on eIF2α-GTP abundance is a shared characteristic of ATF-4 and the transcriptional regulator GCN4 in yeast, where the eIF2α phosphorylation bypasses multiple short uORFs in the 5'-leader of the GCN4 mRNA (Abastado et al., 1991). Accumulation of GCN4 induces the expression of genes involved in metabolism and nutrient production.

1.4.2 ATF-4 target genes

ATF-4 is significantly involved in the regulation of genes belonging to the amino acid metabolism, genes protecting from oxidative stress, genes regulating the switch between apoptosis and autophagy and genes of other bZIP transcription factors like ATF-3 and CHOP/GADD153.

The promoter of the asparagine synthetase (ASNS) contains two *cis*-acting elements. By interacting with one of them, ATF-4 induces ASNS expression eliciting a biological response to amino acid deprivation (Siu et al., 2002).

Another ATF-4-dependent factor is the heme binding oxygenase-1 (HO-1) which mediates a cytoprotective program that is activated by oxidative stress (He et al., 2001). It has also been shown that ATF-4 activates the expression of VEGF during oxidative stress to maintain redox homeostasis (Roybal et al., 2005). This mechanism results in neovascularization, as observed

in retinal pathologies such as age-related macular degeneration (AMD) and diabetic retinopathy.

ATF-4 is also known to be involved in maintaining survival of pancreatic β-cells during ER-stress. ER-stress causes apoptosis, which may be responsible for the loss of pancreatic β-cell mass leading to the development of diabetes. The ATF-4-dependent induction of 4E-BP1, the suppressor of the mRNA 5'-cap-binding protein eIF4E (eukaryotic initiation factor 4E), is involved in β-cell survival under ER-stress. 4E-BP1 upregulation in islets under ER-stress was observed in several mouse models of diabetes. Therefore, ATF-4 might be a therapeutic target for diabetes treatment (Yamaguchi et al., 2008).

The knockout of ATF-4 in mice causes severe fetal anemia based on an impaired fetal-liver hematopoiesis. Further *in vitro* studies showed that ATF-4 is involved in high-rate cell proliferation, which is needed for fetal-liver hematopoiesis (Masuoka and Townes, 2002).

ATF-4 deficiency results also in a delayed bone formation during embryonic development leading to low bone mass in the adult mice. ATF-4 is a substrate of RSK2 (growth factor-regulated kinase) in osteoblasts, which indicates that the lack of ATF-4 phosphorylation via RSK2 is responsible for the skeletal phenotype of the Coffin-lowry syndrome (CLS), in which the gene encoding RSK2 is mutated (Yang et al., 2004). This may be explained by the ATF-4 target gene Osteocalcin (OSE1), which is involved in osteoblast formation.

1.4.3. Regulation of ATF-4

ATF-4 is not only regulated at the translational level but also posttranslationally through phosphorylation and via its protein stability.

As mentioned above, the phosphorylation of ATF-4 at Ser251 by RSK2 leads to an increased transcription of genes involved in osteoblast differentiation, like OSE1 (Yang et al., 2004).

The transcription of another set of ATF-4 target genes is enhanced after protein kinase A (PKA)-mediated ATF-4 phosphorylation at Ser254. This phosphorylation is essential for normal bone formation (Elefteriou et al., 2006).

The expression of ATF-4 is regulated by the G-protein-coupled receptor 48 (GPR48) via activation of the cAMP-PKA pathway leading to an enhanced ATF-4 expression. In line, GPR48 knockout leads to a decreased ATF-4 expression, which results in an impaired erythropoiesis in fetal liver (Song et al., 2008).

Additionally, the ATF-4 transcription activity is regulated by interaction with regulatory proteins like the factor inhibiting ATF4-mediated transcription (FIAT). FIAT contains a leucine zipper domain that mediates binding to ATF-4. This interaction inhibits the activation

of ATF-4 target genes by hindering ATF-4 from binding to DNA. During osteoblast formation FIAT knockout leads to an increased OSE1 expression (Yu et al., 2005).

With a half-life of about 10 min ATF-4 is a very short-lived protein with a high turnover rate. ATF-4 is degradated via the ubiquitin-proteasome system. The chemical inhibition of the proteasome, for example by MG-132, leads to the stabilization of ATF-4. One known F-box protein, which is involved in ATF-4 ubiquitination, is β-Transducin repeat-containing F-box protein (β-TRCP) (Lassot et al., 2001). β-TRCP is part of a SCF E3 ligase complex composed of Skp1, Cul1, Roc1 and the F-box protein (Nakayama and Nakayama, 2005). In ATF-4 the consensus sequence DSGXXS, which is responsible for β-TRCP interaction, resides between the amino acid residues 218 to 224. Mutations within this region increase the ATF-4 stability (Lassot et al., 2001). For the recognition by the E3 ligase, the serine residue 219 within the consensus motif needs to be phosphorylated. For yeast GCN4 the phosphorylation by the cycline-dependent protein kinase PHO85, a functional homologue of mammalien CDK5, has been shown to be crucial for GCN4 ubiquitin-dependent degradation (Shemer et al., 2002). However, the kinase responsible for the phosphorylation of ATF-4 within the DSGXXS motif has not been identified.

The stability of ATF-4 is also regulated via interaction with the histone acetyltransferase p300 (Gachon et al., 2002). Although ATF-4 is acetylated by p300, the stabilizing influence of p300 is independent of its catalytic activity. The mechanism of p300-mediated stabilization is not understood in detail to date. The increased ATF-4 stability could be a result of p300 competing with β-TRCP for ATF-4 or the p300-mediated redistribution of ATF-4 in nuclear speckles. In these nuclear speckles ATF-4 is unavailable for β-TRCP (Lassot et al., 2005).

1.5 Aim of this thesis

The PHDs function as cellular oxygen sensors via regulating the protein stability of the α subunit of HIF, which is the major transcriptional regulator of oxygen-dependent gene expression. The PHD-mediated prolyl hydroxylation marks HIF-α for proteasomal degradation under normoxic conditions. The prolyl hydroxylation of HIF-α is a common characteristic of PHD1-3. Besides this similarity, however, there is increasing evidence for PHD isoform specific properties: (1) enzymatic activity towards HIF-1α and HIF-2α differs among the PHDs. (2) the PHDs show an isoform specific organ expression pattern. (3) PHD knockout mice showed that the different PHD isoforms have specific physiological functions. This might even include HIF-1α-independent oxygen-regulated pathways. (4) PHD isoform-specific protein interaction partners have been identified for PHD1 and PHD2. By searching for new targets of PHD3 the transcription factor ATF-4 was identified as novel protein-interaction partner in a yeast two-hybrid screen. ATF-4 belongs to the ATF/CREB bZIP transcription factor family, which regulates the transcription by forming homo- or heterodimers. In response to different stress stimuli the translation of ATF-4 is upregulated leading to the expression of genes, which are crucial for the response towards the stress conditions. The ATF-4 activity is not only regulated at the translational level, but is additionally modified by phosphorylation, interaction with regulatory proteins and via regulation of its protein stability. The newly identified interaction with PHD3 might now present another possibility to regulate the ATF-4 stability and activity.

Therefore, the aim of this thesis was to characterize the function of the protein-interaction between PHD3 and its novel interaction partner ATF-4. To this end, the following questions and sub-goals were defined:

1. Does ATF-4 interact with PHD3 exclusively? - In first studies it should be examined if the interaction of ATF-4 is limited to PHD3 and is thus PHD-isoform specific.

2. Does PHD3 regulate the protein stability of ATF-4? - The function of the PHD3-ATF-4 interaction should be characterized. Therefore, the influence of PHD3 on ATF-4 stability and activity was determined on mRNA and on protein level to examine on which level ATF-4 is regulated by PHD3.

3. Is the ubiquitination of ATF-4 affected by hypoxia? - The PHD3-dependent ubiquitination of ATF-4 should be defined. Furthermore, the components, involved in the PHD3-dependent ubiquitination of ATF-4, were analyzed.

4. Does PHD3 or hypoxia affect ATF-4 target gene expression? - ATF-4 target genes are involved in cell fate decision. In this regard, one important target gene is GADD153.

Therefore, the impact of the oxygen/PHD3-dependent regulation of ATF-4 for the expression of GADD153 was defined.

2. Materials and methods

2.1 Materials

2.1.1 Chemicals

Most chemicals and materials were obtained from Sigma-Aldrich, Hamburg, Germany; Applichem, Darmstadt, Germany or Carl Roth GmbH & Co. KG, Karlsruhe, Germany. Chemicals obtained from other companies are listed in Table 2.1.

Tab. 2.1: List of chemicals and materials used.

name of the chemical	**provider**
Amylose Resin	New England Biolabs, Inc., Ipswich, USA
Bacto™ Peptone	BD Biosciences, Dendermonde, Belgium
complete Mini EDTA-free Protease Inhibitor Cocktail tablets	Roche Applied Science, Mannheim, Germany
dimethyl pimelimedat dihydrochloride	Fluka Chemie AG, Buchs, Switzerland
DMOG	Frontier Scientific, Carnforth, UK
fetal calf serum	PAN™ biotech GmbH, Passau, Germany
GeneRuler™ 1kb Plus DNA Ladder	Fermentas GmbH, St. Leon-Rot, Germany
Hybond ECL	GE Healthcare, München, Germany
IPTG	Fermentas GmbH, St. Leon-Rot, Germany
lactacystin	Boston Biochem, Cambridge, USA
-Leu/-Trp Do Supplement	BD Biosciences, Dendermonde, Belgium
Lipofectamine™2000	Invitrogen GmbH, Karlsruhe, Germany
PageRuler™ Prestained Protein Ladder	Fermentas GmbH, St. Leon-Rot, Germany
penicillin/streptomycin for cell culture	PAN™ biotech GmbH, Passau, Germany
Prestained Protein Molecular Weight Marker	Fermentas GmbH, St. Leon-Rot, Germany
Protein G Sepharose 4 Fast Flow	GE Healthcare, München, Germany
salmon sperm DNA	Stratagene, La Jolla, USA
Talon Metal affinity resin	BD Biosciences, Dendermonde, Belgium
trypsin/EDTA for cell culture	PAN™ biotech GmbH, Passau, Germany

2.1.2 Buffers

The composition of the buffers used is listed in Table 2.2.

Tab. 2.2: List of the buffers used.

buffer name	composition
borate buffer	200 mM boric acid, 3 M NaCl, pH 9.0 with NaOH
6x DNA sample buffer	30 % glycerin, 0.25 % bromphenol blue, 0.25 % Xylene Cyanole FF in H_20
DEPC-treated water	2 ml DEPC were added to 1 l H_2O
ECL	100 mM Tris/HCl, pH 8.5, 90 mM coumaric acid in DMSO, 250 mM luminol in DMSO, 0,009 % H_2O
ethanolamine buffer	200 mM ethanolamine, pH 8.0 with HCl
glycine solution for IP	200 mM glycine, pH 2.5 with HCl
2x HBS	280 mM NaCl, 12 mM dextrose, 10 mM KCl, 50 mM HEPES, 1.5 mM $Na_2HPO_4 \cdot 2H_2O$, pH 7.05
lysis buffer	400 mM NaCl, 10 mM Tris/HCl, pH 8.0, 0.1 % TritonX100
MBP-buffer	20 mM Tris, pH 7.5, 200 mM NaCl
PBS	137 mM NaCl, 2.7 mM KCl, 4.3 mM $Na_2HPO_4 \cdot 7H_2O$, 1.4 mM KH_2PO_4, pH 7.4
PLATE solution	40 % PEG3350 (w/v), 100 mM lithium acetate, 10x TE yeast, pH 7.5
5x SDS electrophoresis buffer	125 mM Tris, 1.25 M glycine, 0.5 % SDS, pH 8.3
2x SDS-sample buffer	100 mM Tris/HCl, pH 6.8, 4 % SDS, 0.2 % bromphenol blue, 20 % glycerol, 5 % mercaptoethanol
2 M Sodium acetate	dissolve in 75 ml DEPC-H_2O, adjust to pH 4.0 with acetic acid, ad 100 ml with DEPC-H_2O
solution D	4 M guanidine thiocyanate, 25 mM Sodium citrate pH 7.0, 0.5 % sarcosyl, 0.1 M 2-mercaptoethanol
10x TAE	0.4 M Tris acetate, 10 mM EDTA, pH 8.3
0.1x TE	1 mM Tris, 0.1 mM EDTA, pH 8.0
TE yeast	10 mM Tris, pH 7.5, 0.4 mM EDTA
western blot transfer buffer	25 mM Tris, 192 mM glycine, ad 800 ml with H_2O, 200 ml methanol

2.1.3 Enzymes

The enzymes used and the companies they were obtained from are listed in Table 2.3.

Tab. 2.3: List of the enzymes used.

name of the enzyme	provider
PfuTurbo DNA polymerase	Stratagene, La Jolla, USA
lysozyme	Carl Roth GmbH & Co. KG, Karlsruhe, Germany
RiboLock™ ribonuclease inhibitor	Fermentas GmbH, St. Leon-Rot, Germany
restriction endonucleases	Fermentas GmbH, St. Leon-Rot, Germany
T4 DNA Ligase	Fermentas GmbH, St. Leon-Rot, Germany

2.1.4 Antibodies

The antibodies used for immunoblotting are listed in Table 2.4. The antibodies were obtained from SantaCruz Biotechnology, Inc., Heidelberg, Germany; Invitrogen GmbH, Karlsruhe, Germany; BD Biosciences, Dendermonde, Belgium; Novus Biologicals, Littleton, USA; New England Biolabs (NEB) Inc., Ipswich, USA; Clontech Laboratories, Inc. Saint-Germain-en-Laye, France; Acris Antibodies GmbH, Herford, Germany and Sigma-Aldrich, Hamburg, Germany.

Tab. 2.4: List of antibodies used in this study.

antibody against	source	dilution	provider	catalogue number
primary antibodies				
ATF-4	rabbit	1:100 - 1:500	SantaCruz	sc-200
β-TRCP	mouse	1:500	Zymed/Invitrogen	37-3400
GADD153	mouse	1:500	SantaCruz	sc-7351
HIF-1α	mouse	1:1000	BD Transduction Lab	610959
β-actin	mouse	1:10000	Sigma	A 5441
PHD2	rabbit	1:1000	Novus	NB100-137
PHD3	rabbit	1:1000	Novus	NB100-303
V5	mouse	1:2500	Invitrogen	R960
GFP	mouse	1:20000	Clontech	632375
Ubiquitin	rabbit	1:200	SantaCruz	sc-9133
VHL	mouse	1:300	Oncogene	OP102-10046

MBP	rabbit	1:10000	NEB	E8030S
MCL-1	mouse	1:500	BD	559027
SKP1	rabbit	1:2000	Acris	R1521
secondary antibodies				
rabbit HRP	goat	1:16000	Sigma	A 0545
mouse HRP	goat	1:1000	SantaCruz	sc-2005
normal rabbit IgG	-	-	SantaCruz	sc-2027

2.1.5 Cell culture media and supplements

The different media used for the cultivation of bacteria, the yeast two-hybrid assays and the media used in cell culture are listed in Table 2.5.

Tab. 2.5: List of the used media for the cultivation of bacteria, yeasts and cell culture.

name of the medium	**compositon or provider**
bacteria	
Luria-Broth (LB)	10 g NaCl, 10 g tryptone, 5 g yeast extract, to 1 l with ddH_2O, pH 7.0 with 5 N NaOH
SOC	0.5 % yeast extract, 2 % tryptone, 10 mM NaCl, 2.5 mM KCl, 10 mM $MgCl_2$, 20 mM $MgSO_4$, 20 mM glucose
yeast	
YPDA	10 g yeast extract, 20 g Bacto™ peptone, 0.1 g adenine, in 950 ml H_2O, 50 ml 40 % glucose after autoclaving, pH 6.0 with HCl
Synthetic Complete Medium (Sc medium) -Leu-Trp	6.7 g yeast nitrogen base, 0.64 g Do-Leu-Trp in 950 ml H_2O, 50 ml 40 % glucose after autoclaving, pH 5.9 with NaOH
Sc medium -Leu	Sc medium -Leu-Trp, 8 ml tryptophan (40 mM) after autoclaving, pH 5.9 with NaOH
Sc medium -Trp	Sc medium -Leu-Trp, 8 ml leucine (100 mM) after autoclaving, pH 5.9 with NaOH
cell culture	
DMEM-HG	PAN™ biotech GmbH, Passau, Germany
OptiMEM™	Invitrogen GmbH, Karlsruhe, Germany

Solid medium for the cultivation of bacteria was produced by addition of 15 g/l agar agar to LB medium. Agar plates for the yeast two-hybrid assays were produced by the addition of 20 g/l agar agar to the selective medium.

2.1.6 Cell lines

The analyzed cell lines are listed in Table 2.6.

Tab. 2.6: List of used cell lines.

name	description	source
HEK293T	human embryonic kidney cell line, that stable expresses the large T-antigen of SV40; derivate of HEK293 cell line (Lebkowski et al., 1985)	ATTC, Wesel, Germany
HeLa	human epithelia adeno carcinoma cell line	ATTC, Wesel, Germany
HepG2	human hepatocellular carcinoma cell line	ATTC, Wesel, Germany
TS20	TS-20 cells are derivatives of 3T3 fibroblasts, which harbor a temperature sensitive defect in the E1 ubiquitin–activating enzyme (Monney et al., 1998; Oehme et al., 2004).	kindly provided by C. Borner, Freiburg, Germany
H38-5	H38-5 cells are reconstituted with a wild-type allele of the E1 enzyme (Monney et al., 1998; Oehme et al., 2004).	kindly provided by C. Borner Freiburg, Germany
MEF*Hif*$^{-/-}$	mouse embryonic fibroblasts derived from mouse day 9.5 embryos deficient for HIF-1α, SV40 large T antigen immortalized and H-ras transformed cells (Unruh et al., 2003)	kindly provided by R. S. Johnson, San Diego, USA
MEF*Hif*$^{+/+}$	mouse embryonic fibroblasts derived from mouse day 9.5 embryos; SV40 large T antigen immortalized and H-ras transformed cells (Unruh et al., 2003)	kindly provided by R. S. Johnson, San Diego, USA

2.1.7 Bacteria strains

The *Escherichia coli* lines used for plasmid amplification or production of recombinant proteins are listed in Table 2.7.

Tab. 2.7: Genotypes and sources of the *E. coli* strains used.

E. coli	**genotype**	**source**
TOP10	F -*mcr*A Δ(*mrr-hsd*RMS-*mcr*BC) φ80*lacZ*ΔM15 ΔlacX74 *rec*A1 *ara*D139, Δ(*ara-leu*)7697 *gal*U *gal*K *rps*L *end*A1 *nup*G	Invitrogen GmbH, Karlsruhe, Germany
TB1	F^-Δ(lac-proAB) [ϕ80dlacΔ(lacZ)M15]*rpsL thi hsdR*	New England Biolabs, Inc., Ipswich, USA
DB3.1	F^- *gyr*A462 *end*A1 Δ(sr1-*rec*A) *mcr*B *mrr hsd*S20(r_B^-,m_B^-) *sup*E44 *ara*14 *gal*K2 *lac*Y1 *pro*A2 *rpsL*20 *xyl*5 Δ*leu mtl*1	Invitrogen GmbH, Karlsruhe, Germany

2.1.8 Yeast strains

The genotype of the yeast strain used for the yeast two-hybrid assay is given in Table 2.8.

Tab. 2.8: Genotype of the *S. cerevisiae* strain MaV203.

S. cerevisiae	**genotype**	**source**
MaV203	*MAT*α*; leu2-3,112; trp1-901; his3*Δ*200; ade2-101; cyh2R; can1R; gal4*Δ*; gal80*Δ*; GAL1::lacZ; HIS3UASGAL1::HIS3@LYS2; SPAL10::URA3.*	Invitrogen GmbH, Karlsruhe, Germany

2.1.9 Plasmids

Tables 2.9 to 2.12 list the plasmids used for cloning, the yeast two-hybrid assays, the luciferase reporter gene assays, overexpression or production of recombinant proteins.

Tab. 2.9: List of the vectors used to create Gateway® compatible destination vectors.

name of the vector	source
pENTR™4	Invitrogen GmbH, Karlsruhe, Germany
pDEST™22	Invitrogen GmbH, Karlsruhe, Germany
pDEST™32	Invitrogen GmbH, Karlsruhe, Germany
pENTR4 ATF4FL	J. Nesper, Dept. of Cardiovascular Physiology
pENTR4 ATF4 aa 83-175	PCR-product cloned in pENTR4
pENTR4 ATF4 aa 131-175	PCR-product cloned in pENTR4
pENTR4 ATF4 aa 176-270	PCR-product cloned in pENTR4
pENTR4 ATF4 aa 271-351	PCR-product cloned in pENTR4
pDONR221 ATF-4 FL	J. Nesper, Dept. of Cardiovascular Physiology
pDNOR221ATF-4 FL S219N	produced by site-directed mutagenesis using the pDNOR221ATF-4 FL plasmid
pENTR4 hFIH	PCR-product cloned in pENTR4
pENTR4 βTRCP F478S	J. Köditz, Dept. of Cardiovascular Physiology
pGEX-S-x-1 hFIH	kindly provided by D. Stiehl, Zürich, Switzerland

Tab. 2.10: Plasmids used for yeast two-hybrid assays.

vector name	source
pDBleu	Invitrogen GmbH, Karlsruhe, Germany
pExpAD502	Invitrogen GmbH, Karlsruhe, Germany
pDEST32 PHD1	C. Franke, Dept. of Cardiovascular Physiology
pDEST32 PHD2	J. Nesper, Dept. of Cardiovascular Physiology
pDEST32 PHD3	C. Franke, Dept. of Cardiovascular Physiology
pDEST32 FIH	produced by Gateway® cloning
pDEST22 ATF-4 (Fl)	J. Nesper, Dept. of Cardiovascular Physiology
pDEST32 β-TRCP	produced by Gateway® cloning
pDEST22 β-TRCP	produced by Gateway® cloning
pDEST22 PHD3	C. Franke, Dept. of Cardiovascular Physiology
pDEST22 ATF-4 S219N	produced by Gateway® cloning

pDEST22 ATF-4 aa 83-175	produced by Gateway® cloning
pDEST22 ATF-4 aa 131-175	produced by Gateway® cloning
pDEST22 ATF-4 aa 176-270	produced by Gateway® cloning
pDEST22 ATF-4 aa 271-351	produced by Gateway® cloning

Tab. 2.11: Plasmids used for the luciferase reporter gene assays.

vector name	**source**
pATFx2-Luc	kindly provided by T. Hai, Ohio State University, Columbus, USA
pRLSV40	Promega, Madison, USA

Tab. 2.12: Plasmids used for overexpression or production of recombinant proteins.

plamid name	**product**	**source**
pEGFPC1	wild type GFP	Clontech, Laboratories, Inc. Saint-Germain-en-Laye, France
pcDNA3.1Dest-V5 ATF-4	V5-ATF-4	J. Nesper, Dept. of Cardiovascular Physiology
pET3aWT-His-Ubiquitin	His-ubiquitin	kindly provided by F. Melchior, Heidelberg, Germany
pMalc2xHif2αODD	MBP-HIF-2α ODD	J. Nesper, Dept. of Cardiovascular Physiology
pMalc2x ATF4	MBP-ATF-4	J. Nesper, Dept. of Cardiovascular Physiology
pcDNA3.1HA-PHD2	HA-PHD2	kindly provided by W. G. Kaelin Jr., Boston, USA
pDEST17gm PHD3	His-PHD3	C. Franke, Dept. of Cardiovascular Physiology
pST38-His6TrxN-pVhl-elonginB-elonginC	His-Trx-pVHL	kindly provided by S. Tan Pennsylvania, USA (Tan, 2001)
pcDNA3.1 nV5 Dest β-TRCP Δ17-42	V5 β-TRCP	produced by Gateway® cloning

pMalc2x Gateway®	MBP	Invitrogen GmbH, Karlsruhe, Germany
pMalc2x-PHD3	MBP-PHD3	J. Nesper, Dept. of Cardiovascular Physiology

2.1.10 Oligonucleotide primers

Table 2.13 and 2.14 list the primers used for cloning and real time PCR (RT-PCR).

Tab. 2.13: Primers used for RT-PCR.

mRNA	primer name	sequence	annealing
L28	hL28 forward	5'-GCAATTCCTTCCGCTACAAC-3'	58 °C
	hL28 reverse	5'-TGTTCTTGCGGATCATGTGT-3'	58 °C
PHD1	hPHD1 forward	5'-AGCCCCTAAGTCAGGCTCTC-3'	64 °C
	hPHD1 reverse	5'-AGTGGTAGAGGTGGCTGTGG-3'	64 °C
PHD2	hPHD2 forward	5'-TTGCTGACATTGAACCCAAA-3'	56 °C
	hPHD2 reverse	5'-TTACCGACCGAATCTGAAGG-3'	56 °C
PHD3	hPHD3 forward	5'-AGATCGTAGGAACCCACACG-3'	60 °C
	hPHD3 reverse	5'-CAGATTTCAGAGCACGGTCA-3'	60 °C
ATF-4	hATF4 RT forw	5'-TCAAACCTCATGGGTTCTCC-3'	60 °C
	hATF4 RT rev	5'-GTGTCATCCAACGTGGTCAG-3'	60 °C

Tab. 2.14: Primers used for cloning and sequencing.

primer name	primer sequence	annealing
ATF4(83)for	5'-CGGGATCCCAGATTGGATGTTGGAGAAAATG-3'	60 °C
ATF4aa131for	5'-CACCAATAAGCAGCCCCCCCAGAC-3'	60 °C
ATF4(175)rev	5'-CTAATCTGGAGTGGAGGACAGGA-3'	60 °C
ATF4(176)for	5'-CGGGATCCATTCCTTTAGTTTAGAGCTGGGC-3'	58 °C
ATF4(270)rev	5'-CTATGCTACCATCTTCTCTCCAG-3'	58 °C
ATF4(271)for	5'-CGGGATCCCAGCAAAAGTAAAGGGTGAG-3'	58 °C
ATF4rev	5'-CTAGGGGACCCTTTTCTTCC-3'	58 °C
ATF4S219Nfor	5'-CTTCAGATAATGATAATGGCATCTGTATGAGC-3'	62 °C
ATF4S219Nrev	5'-GCTCATACAGATGCCATTATCATTATCTGAAG-3'	62 °C
NcoI hFIHforw	5'-CCCCATGGCGGCGACAGCGGCGG-3'	60 °C
hFIHrev	5'-CTAGTTGTACCGGCCCTTGATC-3'	60 °C

hβTRCPfor	5’-TGAGGAATTGGTGCGTTGTA-3’	53 °C
hβTRCPrev	5’-GGCAGCTGGATCATTTAGGA-3’	53 °C

2.1.11 siRNA sequences

Table 2.15 lists stealth siRNAs and control siRNAs used in this study obtained from Invitrogen GmbH, Karlsruhe, Germany.

Tab. 2.15: List of the stealth siRNAs and control siRNAs used.

name of the siRNA	**sequence of the siRNA**
PHD2 siRNA for	5’-GGACGAAAGCCAUGGUUGCUUGUUA-3’
PHD2 siRNA rev	5’-UAACAAGCAACCAUGGCUUUCGUCC-3’
PHD3 siRNA for	5’-GCUAUCCGGGAAAUGGAACAGGUUA-3’
PHD3 siRNA rev	5’-UAACCUGUUCCAUUUCCCGGAUAGC-3’
ATF-4 siRNA for	5’-GAGUUGGCUUCUGAUUCUCAUUCAG-3’
ATF-4 siRNA rev	5’-CUGAAUGAGAAUCAGAAGCCAACUC-3’
β-TRCP siRNA for	5’-AAUACAACGCACCAAUUCCUCAUGG-3’
β-TRCP siRNA rev	5’-CCAUGAGGAAUUGGUGCGUUGUAUU-3’
SKP1 siRNA for	5’-UAUUCUGCUAAUACAAUUGACUUGC-3’
SKP1 siRNA rev	5’-GCAAGUCAAUUGUAUUAGCAGAAUA-3’
AllStars Neg. Control siRNA	QIAGEN, Hilden, Germany
StealthRNAi Negativ Control Duplexes	Invitrogen GmbH, Karlsruhe, Germany

2.1.12 Kits

The following kits were used for nucleic acid purification, cDNA synthesis, real time PCR and mutagenesis (see Table 2.16).

Tab. 2.16: List of kits used.

application	name of the kit	manufacturer
nucleic acid purification	QIAprep Spin Miniprep kit	QIAGEN, Hilden, Germany
	CompactPrep Plasmid Midi Kit	QIAGEN, Hilden, Germany
	QIAquick Gel Extraction kit	QIAGEN, Hilden, Germany
cDNA synthesis	First Strand cDNA Synthesis Kit #K1612	Fermentas GmbH, St. Leon-Rot, Germany
in vitro translation	TNT® Coupeled Reticulocyte Lysate Systems	Promega, Madison, USA
luciferase assay	Dual-Luciferase® Reporter Assay System	Promega, Madison, USA
mutagenesis	QuikChangeTM Site-Directed Mutagenesis Kit	Stratagene, La Jolla, USA
real time PCR	SYBR® Advantage® qPCR Premix	Clontech Laboratories, Inc. Saint-Germain-en-Laye, France

2.1.13 Software

The software used for different applications is given in Table 2.17.

Tab. 2.17: List of software used.

program	application	reference
Vector NTI	sequence analysis	Invitrogen GmbH, Karlsruhe, Germany
Generunner	sequence reading program	Hastings Software Inc
Blast	Sequence alignment	http://www.ncbi.nlm.nih.gov/BLAST/
GraphPad PRISM	statistical analysis	GraphPad Software Inc.
Multi Gauge	western blot analysis	Fujifilm Corporation

CorelDraw	graphic editor	Corel Corporation
EndNote	managing of bibliographic references	Thomson, Wintertree Software Inc.

2.1.14 Equipment

The equipment used is given in Table 2.18.

Tab. 2.18: List of equipment used.

application	**model**	**manufacturer**
centrifugation	Centrifuge 5415R	Eppendorf AG Hamburg, Germany
	Centrifuge 5810R	Eppendorf AG Hamburg, Germany
	MicroCentrifuge	Carl Roth GmbH + Co. KG, Karlsruhe, Germany
cleanbench	HERAsafe KS 12	Thermo Electron Corporation, Langenselbold, Germany
electroporation of *E. coli* cells	Electroporator 2510	Eppendorf AG, Hamburg, Germany
incubation shaker	Minitron	INFORNS HT, Bottmingen, Switzerland
incubator	CB159	Binder GmbH, Tuttlingen, Germany
micro plate luminometer	Centro LB 960	Berthold Technologies GmbH & Co. KG, Bad Wildbad Germany
micro plate reader	*Model 680*	Bio-Rad, München, Germany
oxygen-controlled work station	Invivo$_2$ 400	Ruskin Technologies, Bridgend, UK
PCR cycler	Primus 96 Thermocycler	Peqlab, Erlangen, Germany
photometer	Smart Spec^{TM} Plus	Bio-Rad, München, Germany
Real-time PCR cycler	Mx3000P	Stratagene, La Jolla, USA
rotator	Rotator RS-24	G.Kisker GbR, Steinfurt, Germany
UV-transilluminator	InGenius	Syngene, Camebridge, UK
western blotting	PerfectBlue Semi-Dry Elektroblotter	Peqlab, Erlangen, Germany
western blot imaging	LAS 3000 Imager	Fujifilm, Düsseldorf, Germany

SDS-PAGE	PerfectBlue Doppelgelsystem Twin M	Peqlab, Erlangen, Germany
sonotrode	Ultra-Turrax® IP18-10	Janke and Kunkel GmbH & Co. KG, Germany

2.2 Methods

2.2.1. Isolation and purification of nucleic acids

2.2.1.1 DNA isolation and purification from *Escherichia coli*

Plasmid harboring *E. coli* cells were incubated in LB medium containing antibiotics according to the resistance given by the plasmids at 37 °C overnight. The isolation of plasmid DNA was done by the principle of alkaline lysis (Sambrook et al., 2000). Therefore, the QIAprep Spin Miniprep Kit from QIAGEN was used. For the isolation of higher amounts of DNA the CompactPrep Plasmid Midi Kit again from QIAGEN was used. These kits are anion exchange resin-based plasmid purification kits and they were used according to the manufactures instructions.

2.2.1.2 RNA isolation from adherent cells

The total RNA of adherent cells was isolated by the principle of phenol-chloroform extraction. $2x10^5$ cells/well were plated in a 6-well plate and incubated under normoxic or hypoxic conditions. The were cells washed with cold PBS and to each well 750 µl solution D was added to solubilize the cells. The cells were homogenized by vortexing. Subsequently on ice 75 µl 2 M sodium acetate (pH 4.0), 750 µl water-saturated acid phenol and 150 µl chloroform-isoamyl alcohol mixture (49:1) were added. In between the samples were thoroughly vortexed. The final suspension was incubated on ice for 20 min and then centrifuged at 12000 rpm for 20 min at 4 °C, which separated the mixture into the lower protein containing organic phenol-chloroform phase, the DNA containing interphase and the upper aqueous phase, which contains the RNA. The aqueous phase was transferred into a new tube and the RNA precipitated by the addition of 750 µl isopropanol. The samples were incubated at -20 °C for 1 hrs. RNA was pelleted by centrifugation at 12000 rpm for 20 min at 4 °C. The supernatant was removed and the pellet dissolved in 75 µl solution D. The samples were transferred into a fresh tube and the RNA precipitated with 75 µl isopropanol at -20 °C for 1 hrs. RNA was pelleted by centrifugation at 12000 rpm for 20 min at 4 °C and the supernatant removed. Washing of the RNA was done by vortexing in -20 °C cold

75 % ethanol. Afterwards the RNA was centrifuged for 20 min at 12000 rpm and 4 °C. The supernatant was removed and the RNA was dried for 30 min. The dry RNA pellet was resuspended in 20 µl DEPC-treated water by heating at 56 °C for 15 min followed by vortexing. The RNA was stored at -80 °C.

2.2.1.3 Photometric measurement of nucleic acid concentration

After the RNA or DNA purification the concentration of the nucleic acids in the samples was determined by measuring the absorption at 260 nm and the ratio 260 nm/280 nm in the Smart Spec^{TM} Plus photometer. Pure DNA or RNA samples have a 260 nm/280 nm ratio of 1.8, while the presence of proteins in the samples lowers this ratio.

2.2.2 Agarose gel electrophoresis

The agarose gel electrophoresis was used to visualize or isolate DNA. Depending on the size of the studied DNA molecules, agarose gels were cast at concentrations of 1 % or 2 % agarose. Electrophoresis was done using the TAE buffer. To load the samples on the gel, 5 µl DNA sample buffer were added to 20 µl sample. Additionally, an appropriate molecular weight marker was loaded on every gel to estimate the fragment size of the DNA. The gel was stained after electrophoresis with 0.1 µg/ml ethidium bromide, which fluoresces under UV light when intercalated into DNA. The DNA was visualized under the UV-transilluminator at 302 nm.

2.2.3 Isolation of DNA fragments from agarose gels

The required DNA fragments, which had been separated via agarose electrophoresis, were excised with a scalpel from the gel. DNA fragments were purified using the QIAquick Gel Extraction kit from QIAGEN, according to the protocols provided.

2.2.4 cDNA synthesis

The synthesis of cDNA utilizes the viral RNA-dependent DNA polymerase reverse transcriptase, which synthesizes DNA from primed RNA templates. Oligo $(dT)_{18}$ primers, which bind to the 3'-end of poly$(A)^+$mRNA, ensure template specificity of mRNA for the cDNA synthesis. The First strand cDNA Synthesis Kit from Fermentas was used for the cDNA synthesis. 2 µg RNA were mixed with 1 µl oligo$(dT)_{18}$ primer (0.5 µg/µl) and DEPC-treated water was added up to a volume of 11 µl. The mixture was gently mixed and incubated at 70 °C for 5 min. The samples were chilled on ice and subsequently 4 µl

5x reaction buffer, 1 µl RiboLock™ ribonuclease inhibitor (20 U/µl) and 2 µl 10 mM dNTP mix were added. The samples were gently mixed and incubated at 37 °C for 5 min allowing the primers to anneal. Then 2 µl M-MuLV reverse transcriptase (20 U/µl) were added and the cDNA synthesis was performed by incubation at 37 °C for 60 min. The reaction was stopped by incubating the samples at 70 °C for 10 min, which inactivated the M-MuLV reverse transcriptase.

2.2.5 Polymerase chain reaction

By performing polymerase chain reaction (PCR) it is possible to amplify specific DNA regions. As template genomic DNA, cDNA, plasmid DNA or lambda DNA can be used. PCR is a three step process of denaturating the double stranded DNA, annealing of the primers to the DNA and elongation, which is performed by a thermo stable DNA polymerase. The annealing temperature depends on the base composition and length of the used primers. The reaction was carried out in the Primus 96 thermocycler.

PCR was performed in a total reaction volume of 50 µl containing 40.6 µl ddH_2O, 5 µl 10x cloned Pfu reaction buffer, 0.4 µl dNTPs (25 mM each dNTP), 1 µl DNA template (100 ng/µl), 1 µl forward primer (20 pmol/µl), 1 µl reverse primer (20 pmol/µl) and 1 µl PfuTurbo DNA polymerase (2.5 U/µl) from Stratagene. The used PCR cycling parameters are described in Table 2.19.

Tab. 2.19: Parameters used for PCR cycling.

step	duration	temperature	number of cycles
initial denaturation	2 min	95 °C	1
denaturation	30 sec	95 °C	
annealing	30 sec	primer specific see Tab. 2.14	30
elongation	1 min per kb	72 °C	
final elongation	10 min	10 min	1

The amplified DNA fragments were separated by size performing agarose gel electrophoresis (see paragraph 2.2.2) and cloned into the pENTR™4 vector, which is Gateway® compatible.

2.2.6 Quantitative real-time RCR

Quantitative real-time PCR is an optimized PCR in which the amount of the amplified product is linked to fluorescence intensity using a fluorescent reporter molecule. For the detection a DNA-intercalating dye, that fluoresces once it binds to double-stranded DNA, was utilized. The most commonly used dye is SYBR Green I. Its fluorescence is detected during the DNA amplification. As a reference dye ROX™ was added to the samples, to normalize the fluorescent signal intensity between the reactions. To measure the exact copy number of the template in the sample a standard curve from 10^2 to 10^{10} copies was made using a control template. The gene for the ribosomal protein L28 was used as normalization control for differences in RNA isolation and in the efficiency of the reverse transcription reaction.

The quantitative real-time PCR was performed by using the SYBR® Advantage® qPCR Premix from Clontech. For the quantitative real-time PCR 2 µl cDNA, 12,5 µl SYBR Advantage qPCR Premix (2x), 0.5 µl forward primer (10 µM), 0.5 µl reverse primer (10 µM) and 0.5 µl ROX reference dye LMP were mixed and dH_2O added to a total volume of 25 µl. The conditions used for the real-time PCR are described in Table 2.20.

Tab. 2.20: Parameters used for the real-time PCR.

	step	temperature	time	detection	cycles
initial denaturation	denaturation	95 °C	30 sec	off	1
three step PCR	denaturation	95 °C	10 sec	off	40
	annealing	see Tab.2.13	20 sec	off	
	extension	72 °C	20 sec	on	
amplification of the dissociation curve	denaturation	95 °C	1 min	off	1
	annealing	see Tab. 2.13	30 sec	off	
	denaturation	95 °C	30 sec	on	

The copy number of the template in the sample was determined using the standards. The normalization with the ribosomal protein L28 was done to compensate differences in the amount of used cDNA.

2.2.7 Recombination to destination vectors using the Gateway® technology

The Gateway® technology from Invitrogen was used for cloning, which takes advantage of the site-specific recombination properties of bacteriophage lambda to insert the gene of interest into multiple vector systems. The lambda recombination occurs between the attachment (*att*) sites *att*B in the *E. coli* chromosome and *att*P on the *lambda* chromosome. The recombination proteins involved in the recombination reaction differ depending whether *lambda* utilizes the lytic or the lyogenic pathway. The BP Clonase™ reaction is catalyzed by the *lambda* Integrase (Int) and the *E. coli* Integration Host Factor (IHF), which catalyze the lysogenic pathway. The lytic pathway is catalyzed by Int and Excisionase (χis) and the *E. coli* IHF, which are used for the LR Clonase™ reaction.

In the Gateway® BP reaction the recombination occurs between the *att*B and the *att*P site creating an *att*L containing entry clone and an *att*R containing by-product. For the LR recombination reaction an *att*L containing entry clone and the *att*R-containing pDEST™ vector is used. The presence of the *ccd*B gene in the donor, destination and entry vectors allows the negative selection in *E. coli*. The CcdB protein inhibits the growth of the *E. coli* strain TOP10, which is used for the plasmid amplification after the recombination, by interfering with the *E. coli* DNA gyrase. In the recombination reaction, the *ccd*B gene is replaced by the gene of interest and the cells survive. Gateway® vectors containing the *ccd*B gene can only be propagated in *E. coli* strains with a gyrase mutation (*gyr*A462) like the DB3.1 *E. coli* strain.

The ATF-4 fragments, used in the yeast two-hybrid assays, were produced by performing PCR with the primers listed in Tab. 2.14 and cloned into the pENTR™4 vector to create Gateway® compatible entry clones. These pENTR™4 clones were then used in LR recombination reactions to obtain the pDEST22 destination vector, which were used in the yeast two-hybrid assays.

The vectors containing the β-TRCP cDNA used in the yeast two-hybrid assays were created by performing the LR recombination reaction with the pENTR4 βTRCP F478S vector, containing the β-TRCP cDNA, and the two destination vectors pDEST™22 and pDEST™32.

The pDEST32 FIH vector used for the yeast two-hybrid assay was produced by performing PCR with the primers NcoI_hFIH_forw and hFIH_rev using pGEX-S-x-1 hFIH as template. The PCR-product was digested with the restriction enzymes *Nco*I and *Eco*RV and then ligated into the pENTR™4 vector. This vector was used in a LR clonase reaction with the pDEST™32 vector and the pDEST32 FIH vector was obtained.

To verify the success of the recombination reaction, the obtained plasmids were analyzed by restriction digestion (see paragraph 2.2.8) and sequencing (see paragraph 2.2.13).

2.2.8 Restriction digestion

Endonucleases are useful tools to specifically cut DNA. The specific recognition sequences of the endonucleases consist of 4, 6 or 8 bases, mostly palindromes. Most restriction enzymes create fragments with a 5'-phosphate and a 3'-OH end, which can be blunt ends or sticky ends. The restriction digestion was performed with endonucleases from Fermentas, following the manufactures specifications for the buffer conditions. The restriction of 1 µg plasmid DNA was performed at 37 °C for 1 hrs and the obtained DNA fragments were analyzed by agarose gel electrophoresis (see paragraph 2.2.3).

2.2.9 Ligation

The ligation of PCR-products into a Gateway® compatible Entry Vector was done by digesting the plasmid DNA and the PCR-product using the *EcoRV* and *Nco*I restriction enzymes. The ligation mixtures contained: 50-400 ng vector, three times more PCR-product, 2 µl 10X Ligation buffer, 1 µl T4 DNA ligase (5 U/µl) and the volume made up to 20 µl with ddH_2O. The ligation mixture was incubated at room temperature for 1 hrs, followed by transformation into *E.coli* cells.

2.2.10 Preparation of high efficiency electro competent *E. coli* cells

To produce electro competent *E.coli* cells, the TOP10F' strain was incubated over night at 37 °C at 180 rpm in a volume of 15 ml LB containing 25 µg/ml streptomycin. 1.5 l LB medium containing 25 µg/ml streptomycin were inoculated with 1/100 volume of the fresh overnight culture. The cells were grown at 37 °C to an ABS_{600} of 0.5 to 1, harvested and chilled on ice for 15 to 30 min. By centrifugation at 5000 rpm for 10 min the cells were pelleted. The pellet was resuspended in 1.5 l ice cold water and again centrifuged as before. Subsequently the pellet was resuspended in 1/2 volume water and again pelleted, followed by resuspendation in 1/50 and 1/500 volume 10 % glycerol. The cells were stored at -70 °C in aliquots of 60 µl.

2.2.11 Transformation of electro competent *E. coli*

The transformation of plasmids into *E. coli* was done to amplify plasmid DNA. The electro competent *E. coli* TOP10F' cells were used. The principle of electroporation was used for the transformation into *E. coli*, which is a process of applying high voltage field pulses of short duration to create temporary holes in the membrane of cells. The cells were thawed on ice and 1-2 µl of the DNA, that should be transformed, were added to the cells. The mixture was transferred into a cold 0.2 cm cuvette and the electroporation of the samples was performed in the Electroporator 2510 using the following settings: 10 µF, 2500 V pulse discharge, 600 Ohms. Immediately after the electroporation 1 ml SOC medium was added to the cells and then transferred into a new tube. Incubation at 37 °C at 225 rpm for 1 hrs allowed the expression of antibiotic resistance. The cells were than plated on selective plates containing 100 µg/ml ampicillin respectively 50 µl/ml kanamycine and incubated overnight at 37°C. The positive clones were plated on new selective plates.

2.2.12 Site-directed mutagenesis

The QuikChange™ Site-Directed Mutagenesis Kit from Stratagene was used to mutate the serine residue 219 of the ATF-4 protein to asparagines (ATF-4 S219N).

Using the QuikChange kit allows site-specific mutation in any double-stranded plasmid, containing the insert of interest. By performing PCR using two oligonucleotide primers containing the desired mutation and using the PfuTubo DNA polymerase, which has a very high fidelity and does not displace the mutant oligonucleotide primers, in which the mutations are introduced. The oligonuclotide primers are complementary to the opposite strands of the vector and are elongated during temperature cycling by PfuTurbo DNA polymerase. The template is then removed by treatment with *Dpn*I, which is specific for methylated and hemimethylated DNA from bacteria and has the target sequence 5'-Gm^{6}ATC-3'. The nicked vector DNA containing the desired mutation is then transformed into *E. coli*, which repair the nicked DNA and amplify it.

For the QuikChange site-directed mutagenesis the plasmid pDONR 221 ATF-4 FL, containing the full length ATF-4 cDNA, and the oligonucleotid primers ATF4S219Nfor and ATF4S219Nrev, containing the desired mutations to replace the serine residue 219 by asparagine, were used.

The cycling reaction mix consisted of 5 µl 10x reaction buffer, 50 ng template plasmid, 125 ng of each oligonucleotide primer, 1 µl dNTP mix, 1 µl *Pfu* DNA polymerase (2.5 U/µl)

and ddH_2O was added to a final volume of 50 µl. The cycling parameters are summarized in Table 2.21.

Tab. 2.21: Cycling parameters used for site-directed mutagenesis.

step	temperature	time	number of cycles
initial denaturation	95 °C	30 sec	1
introduction of a single amino acid change	95 °C	30 sec	
	55 °C	1 min	16
	68 °C	1 min/kb	

After the cycling reaction, the template DNA was digested by adding 1 µl *Dpn*I restriction enzyme (10 U/µl) to the amplification reaction and incubation at 37°C for 1 hrs. Once *Dpn*I digestion was complete the produced vector, containing the mutation, was transformed into *E. coli* (see paragraph 2.2.11) and by performing recombination reaction (see paragraph 2.2.7) the insert was introduced into the pDEST22 vector, which was used in a yeast two-hybird assay (see paragraph 2.2.15).

2.2.13 DNA sequencing and analysis

The sequencing was performed by Seqlab-Sequence Laboratories. The extended HotShot sequencing reactions, which guaranteed a reading length of about 900 base pairs, was chosen to sequence the cloned plasmids. Therefore, 1 µg plasmid DNA was mixed with 20 pmol primer and filled up with water up to a total volume of 7 µl. The obtained sequences were analyzed by different programs, listed in Table 2.14. Sequence homology searches were performed using NCBI/BLAST service.

2.2.14 Luciferase reporter assay

The luciferase reporter gene assay is widely used to study the eukaryotic gene expression and cellular physiology. By using a dual reporter assay containing firefly luciferase (FL) from *Photinus pyralis* and renilla luciferase (RL) from *Renilla reniformis* the experimental accuracy is increased. These two enzymes have a distinct evolutionary origin and their enzymes have dissimilar enzyme substrates and substrate requirements. Therefore, it is possible to discriminate between their respective bioluminescent reactions. FL and RL both do not need posttranslational activation and are active immediately upon translation. FL catalyzes the oxidation of the beetle luciferin in a reaction that emits a photon consuming

ATP and O_2. In the luminescent reaction catalyzed by RL O_2 and coelenterate-luciferin are utilized.

For the luciferase reporter assays HeLa cells were transiently transfected in a 24-well scale by the method of Calcium phosphate transfection as described in paragraph 2.2.19.2, with 250 ng firefly luciferase reporter vector pATFx2-Luc, containing 2 cAMP response element (CRE) sites. For each condition three replicates were made. The pRLSV40 vector encoding RL was co-transfected and used as internal control, the vectors are listed in Tab. 2.11. After transfection the cells were incubated at 1 % O_2 or 20 % O_2 for 24 hrs with and without DMOG treatment. The Dual-Luciferase® Reporter Assay System from Promega was used. The cells were lysed by the addition of 100 µl Passive Lysis Buffer. 10 µl of the samples were transferred into a 96-well plate and the FL activity wass measured by adding 10 µl Luciferase Assay Reagent II. The luminescence was measured in a 10 second measurement period using the Berthold micro plate luminometer Centro LB 960. After quantifying the FL luminescence, the reaction was quenched and the RL reaction was simultaneously initiated by addition of 10 µl Stop&Glow® to the same well. The apparent luminescence was again measured and the mean values of FL/RL ratios were calculated.

2.2.15 Yeast two-hybrid assay

The interaction between two proteins can by identified by performing a yeast two-hybrid assay. Interaction between two proteins leads to the reconstitution of an active transcription factor by forming a dimer. The first protein of interest is fused to the Gal4 DNA-Binding domain (BD) and the other to the Gal4 Activation domain (AD). The functional transcription factor activates chromosomally-integrated reporter genes driven by promoters containing the relevant BD binding site. When a histidine-auxothrophic yeast strain is used in a yeast two-hybrid assay the HIS3 gene, which encodes for an enzyme involved in histidine synthesis, can be used as reporter gene. The growth of the cells is screened on selective plates without histidine.

The Gateway® compatible ProQuest™ Two-Hybrid System from Invitrogen was used for the yeast two-hybrid assays. In this system the BD containing vector is the pDEST™32 vector and the AD containing vector is the pDEST™22 vector.

These two vectors allow a specific selection of transformed yeast on media without the amino acids leucine and tryptophan. The pDEST™32 contains the LEU2 gene allowing selection of the transformed yeast cells by plating on media without leucine and the pDEST™22 vector includes the TRP1 gene which allows selection on media lacking tryptophan. For the yeast

two-hybrid assays the *S. cerevisiae* strain MaV203 was used. This strain is leucine and tryptophan auxotroph and therefore co-transformants of the pDEST^{TM}22/ pDEST^{TM}32 can be screened by plating on medium lacking tryptophan and leucine.

For the transformation YPDA medium was inoculated with the MaV203 strain and incubated for 24-48 hrs at 30 °C and 250 rpm until saturation of the culture was reached. To exclude a possible contamination of the MaV203 strain, an overnight culture using Sc medium -Leu-Trp media was also inoculated. In this media no growth of the MaV203 cells was expected. The plasmids used for the performed yeast two-hybrid assays are listed in Tab. 2.10. Full length ATF-4 cDNA, the ATF-4 fragments and the ATF-4 S219N mutant fused to the Gal4AD were expressed by the pDEST22^{TM} vector and the PHDs, FIH respectively β-TRCP were fused to the Gal4BD and were expressed by the pDEST22^{TM}. Additionally, PHD3 was fused to the Gal4AD expressed by the pDEST22^{TM} vector. The whole transformation was performed on ice starting with the centrifugation of 500 µl starter culture for each sample at 8000 rpm for 1 min. The supernatant was removed and the cells were resuspended in 5 µl salmon sperm DNA (10 mg/ml). The salmon DNA was preheated at 100 °C for 5 min to obtain single stranded DNA. 1 µg plasmid DNA was added to the cells, the samples were mixed and 500 µl PLATE solution were added. The samples were mixed by pipetting followed by incubation at 30 °C for 24 hrs. Cells were collected by centrifugation for 1 min at 8000 rpm, the supernatant discarded. 200 µl sterile TE yeast were added to resuspend the cells. The transformants were screened on synthetic drop-out medium lacking tryptophan, leucine, and histidine, as well as medium containing 10 mM, 25 mM or 50 mM 3-amino-1,2,4-triazole (3-AT). After two days five transformed colonies were restreaked on new selection plates.

2.2.16 Purification of recombinant proteins

2.2.16.1 *In vitro* translation

The TNT® Coupled Reticulocyte Lysate Systems from Promega were used to produce recombinant proteins in an *in vitro* translation reaction. In this system the transcription and the translation are coupled by incorporating transcription directly in the translation mix. The cDNA of the protein to be amplified is directly cloned downstream of the T7 RNA polymerase promoter and circular plasmid DNA is then used to perform the *in vitro* translation. Therefore, the DNA of the desired protein is mixed with the T7 RNA polymerase, amino acids, salts, recombinant RNasin® ribonuclease inhibitor and reticulocyte lysate is added. The reticulocyte lysate contains the cellular components necessary for protein synthesis, like tRNA, ribosomes, amino acids, initiation, elongation and termination factors

and may also contain a variety of post-translational processing activities, including acetylation, isoprenylation and some phosphorylation activity.

For the *in vitro* translation of HA-PHD2, 1 µg of the pcDNA3.1-HAPHD2 vector was used; and for the translation of V5-βTRCP, 1 µg of the pcDNA3.1nV5 Dest β-TRCP vector was used. To the DNA 25 µl TNT® rabbit reticulocyte lysate, 2 µl TNT® reaction buffer, 1 µl T7 RNA polymeras, 0.5 µl 1 mM amino acid mixture without leucine, 0.5 µl 1 mM amino acid mixture without metheonine and 1 µl RNasin® ribonuclease inhibitor (40 U/µl) were added and the mixture was filled up with nuclease-free water to a total volume of 50 µl. The *in vitro* translation reaction was performed at 30 °C for 90 min. The obtained protein was stored at -70 °C.

2.2.16.2 Expression and purification of MBP-fusion proteins from *E. coli*

The N-terminal fusion of a target protein to the maltose binding protein (MBP) allows the production of recombinant protein in *E. coli* and purification via an affinity matrix. The purification of the MBP-fusion proteins from whole cell lysate is then done using amylose conjugated agarose beads. The elution from the agarose beads is done by competition with free maltose. The expression of recombinant MBP-ATF-4, MBP-PHD3, MBP-HIF-2αODD and MBP was done using the pMalc2x plasmid from NEB. These plasmids allow translation via the strong *tac*-promoter. The *tac*-promoter is a functional hybrid derived from the tryptophan- (*trp*) and the lactose-*lac* operon, which are inducible by isopropylthiogalactoside (IPTG).

The corresponding pMalc2x derivates or the pMalc2x plasmid (see Tab. 2.12) were transformed into *E. coli* TB1 cells and an overnight culture was inoculated. The cultivation was done at 37 °C and 220 rpm. The overnight culture was used to inoculate 3 l LB containing ampicillin and 0.2 % glucose and the culture was incubated at 25 °C until an OD_{600} of approximately 0.5 was obtained. The addition of 0.3 mM IPTG to the culture led to the induction of MBP-fusion proteins. The production was done overnight at room temperature. The next day, cells were harvested by centrifugation at 5000 rpm for 20 min, the supernatant was discarded and the pellet frozen at -20 °C to facilitate cell disruption. The pellet was thawed and 200 ml MBP-buffer, EDTA-free protease inhibitor and 0.2 mg lysozyme were added. The cells were disrupted by sonication using short pulses of 8 sec and undissolved particles were removed by centrifugation at 13000 rpm for 1 hrs at 4 °C. To 50 ml of the supernatant, 1.5 ml amylose resin, which was previously washed with 50 to 100 ml MBP-buffer, were added and incubated for 3 hrs at 4 °C on a rotator. The mixture was then

transferred onto a column and washed with 100 ml MBP-buffer. The elution of the MBP-fusion proteins from the amylose resin was done by the addition of 25 ml MBP-buffer containing 10 mM maltose. The elution fraction was collected in 1 ml aliquots and the protein concentration was measured by a Bradford protein assay (see paragraph 2.2.19). The protein containing fractions were pooled and dialyzed against 5 l buffer containing 20 mM Tris pH 7.5 with 200 mM NaCl and PEG 30000 was used to increase the protein concentration. The produced recombinant proteins were stored at –70 °C.

2.2.16.3 Expression and purification of His-PHD3 from insect cells and His-Trx-pVHL from *E. coli*

The expression and purification of His-PHD3 and His-Trx-pVHL was previous to this study done in the Department of Cardiovascular Physiology by Dr. J. Nesper and Dr. J. Köditz.

Spodoptera frugiperda Sf9 cells were used to produce the recombinant His-PHD3 protein, used for the pull-down assays. These cells were grown as suspension cultures in Sf900IISFM serum-free medium. The Sf9 cells were transfected with the pDEST17gm PHD3 plasmid, containing His-tagged PHD3 cDNA. The cells were harvested 72 hrs after the transfection. Cells were washed with 0.15 M NaCl and 0.02 M phosphate pH 7.4 and homogenized in a buffer containing 0.1 M NaCl, 0.1 M glycine, 10 µM dithiothreitol, 0.1 % Trition X-100 and 0.01 M Tris, pH 7.8. The samples were centrifuged and the pellets were sobulized in 1 % SDS.

The recombinant His-Trx-pVHL protein was expressed in *E.coli* BL21-AI from Invitrogen using the pST38-His6TrxN-pVhl-elonginB plasmid. His-Trx-pVHL protein was purified by Ni-affinity. Therefore 5 ml HiTrap chelating HP column from Amersham Biosiences were used. Additionaly a purification by anion-exchange chromatography, using 1 ml Econo-Pac High Q cartridge from BioRad was performed as published previously (Tan et al., 2005) using a BioLogic DuoFlow chromatography system from BioRad.

2.2.17 Cell culture

The adherent HeLa, HEK293T, HepG2, MEF*Hif*$^{-/-}$and MEF*Hif*$^{+/+}$ cells were cultured in high glucose Dulbecco's modified Eagle's medium containing 10 % fetal calf serum, 100 U/ml penicillin G and 100 µg/ml streptomycin (Pen/Strep) in a humidified 5 % CO_2, 20 % O_2 air atmosphere at 37°C. Cells were subcultivated every second day. Therefore, the medium was removed and 2 ml of a solution containing 0.05 % trypsin and 0.02 % EDTA in PBS was added to the cells. The flasks were incubated at 37 °C until the cells detached. HeLa,

HEK293T and HepG2 cells were transferred to a new flask with a subcultivation ratio of 1:5. The MEF*Hif*$^{-/-}$and MEF*Hif*$^{+/+}$ were subcultivated at a ratio of 1:10.

The TS-20 cells, which harbor a temperature sensitive defect in the E1 ubiquitin activating enzyme, and the H38-5 cells, which are reconstituted with a wild-type allele of the E1 enzyme, were cultured as described above. To study the influence of ubiquitination on ATF-4 protein stability, the TS-20 cells and H38-5 cells were cultured under normoxic conditions at 34 °C and then exposed to 39 °C for 2 or 4 hrs.

For hypoxic conditions, O_2 levels were decreased to 1 % or 0.2 % O_2 with N_2 in the oxygen-controlled work station from Ruskin. In some experiments, cells were treated with 30-50 µM lactacystin or 25 µM MG-132 to inhibit the proteasome or 1 mM DMOG to inhibit the PHD activity for the indicated time periods. As a positive control for ATF-4 expression, some cells were treated with 300 nM thapsigargin for 2 hrs.

To maintain a backup of cells the principle of cryogenic preservation was used. Therefore the cells were again detached from the flasks by trypsin/EDTA, the medium was removed and 1 ml of a mixture of 90 % fetal calf serum and 10 % DMSO was added. In this solution the cells could be stored below -100 °C in liquid nitrogen.

2.2.18 Protein sample isolation from adherent cells

The preparation of protein extracts from adherent cells was done by the principle of osmotic lysis. Therefore the medium was removed from the cells and washed with cold PBS to remove the remaining medium. Samples, used for the measurement of polyubiquitinated proteins, were washed with PBS containing 20 mM N-Ethylmaleimide (NEM) to inhibit the deubiquitinating enzymes. The PBS was removed from the cell culture dish and 200 µl respectively 500 µl lysis buffer were added to each well of a 6-well plate respectively a 10 cm dish. An EDTA-free protease-inhibitor cocktail from Roche was added to the lysis buffer to prevent protein degradation. Again 20 mM NEM were added to the lysis buffer, when polyubiquitinated proteins were studied. The cells were scraped from the dishes and the cell lysate was transferred into a 1.5 ml tube. The samples were placed on ice for about 10 min. The lysed cells were pelleted by centrifugation at 12000 rpm for 10 min at 4 °C and the cell lysate was transferred into a new tube. The protein concentration was measured by performing a Bradford protein assay (see paragraph 2.2.19).

2.2.19 Bradford protein assay

The Bradford protein assay is a colorimetric protein assay, based on the absorbance shift of the Coomassie Blue G dye after protein binding. At a very low pH this dye is most stable in its double-protonated form, which appears red with a maximal absorbance at 450 nm. After protein binding, however, the dye donates the protons and its color turns blue with a maximal absorbance at 595 nm. The Bradford assay is linear between 2 µg/ml and 120 µg/ml. The increase of absorbance at 595 nm in this range is proportional to the amount of protein in the sample. To measure the protein concentration of a sample, a regression curve was derived from a series of standards between 0.5 µg and 5 µg bovine serum albumin (BSA) and used as the basis to estimate the unknown concentrations. For the Bradford assay, 2 µl of the sample were added to 200 µl Protein Assay Reagent from Bio-Rad and the absorbance was measured at 595 nm using the micro plate reader from Bio-Rad. The concentration was determined by using the regression curve.

2.2.20 Transient transfection of adherent cells

2.2.20.1 Lipid-mediated transfection

Cationic lipid reagents are used to create artificial membrane vesicles, called liposomes, which bind to the to be transfected DNA. These cationic complexes adhere to the negatively charged cell membrane and fuse with it. The DNA is transiently overexpressed in the cells, but is not necessarily integrated into the genome of the recipient cell. This method also allows the transfection of siRNAs, which are used to silence gene expression. In this work stealth siRNAs were used, which are duplexes of 25mer RNA oligonucleotides with chemical modifications. These modifications increase the siRNA stability and reduce the nonspecific stress response. The endogenous siRNAs interact with protein components to form the RNA-induced silencing complex (RISC). The siRNA is unwound and a single stranded RNA remains bound to the RISC. Activated RISC binds to complementary transcripts by base pairing interactions between the siRNA antisense strand and the mRNA. The RISC cleaves the homologous mRNA and by this prevents its translation.

The used stealth siRNAs, which are listed in Tab. 2.15, were purchased from Invitrogen. As negative control All Star-control siRNA from QIAGEN or StealthRNAi Negativ Control Duplexes from Invitrogen were used. For the siRNA transfection $1x10^6$ for 10-cm dish scale or $2x10^5$ cells for 6-well scale were seeded in DMEM containing 10 % FCS and Pen/Strep. The following day the medium was removed and DMEM containing 10 % FCS was added. For the transfection of a 6-well 80 pmol siRNA and 4 µl Lipofectamine^{TM}2000 were mixed

with 500 µl OptiMEM™. For the transfection of a 10-cm dish 600 pmol siRNA and 24 µl Lipofectamine™2000 were mixed with 2 ml OptiMEM™. The mixtures were incubated at room temperature for 20 min to allow the formation of the oligo-Lipofectamine™2000 complexes. The mixture was then added to the cells and 6 hrs after transfection the medium was again changed. The cells were further incubated under normoxic or hypoxic conditions. The cells were usually harvested 24 hrs after transfection (see paragraph 2.2.18).

2.2.20.2 Calcium phosphate-mediated transfection of adherent cells

The calcium phosphate-mediated transfection was used to transiently transfect HeLa cells with plasmid DNA. The DNA-calcium phosphate coprecipitate enters the cytoplasm of the cells via endocytosis and the DNA reaches the nucleus when the cells divide. The calcium phosphate-mediated transfection was used to transfect plasmids for the luciferase reporter assay. $5x10^4$ cells were plated in a 24-well containing 0.5 ml DMEM medium with 10 % FCS and Pen/Strep and incubated at 37 °C. The following day the medium was removed and DMEM containing 10 % FCS was added. For each well to be transfected 0.25 µg pATFx2-Luc plasmid-DNA, which contains two cAMP response element (CRE) sites and 0.025 µg pRLSV40 plasmid-DNA, containing the renilla luciferase gene, were mixed with 0.1xTE up to a volume of 22 µl. To this mixture 25 µl 2x HBS were carefully added, followed by 3 µl 2 M $CaCL_2$. The incubation at room temperature for 20 min allowed the formation of DNA-calcium phosphate coprecipitates. The solution was again carefully mixed and added drop wise to the cells to be transfected. The medium was changed 6 hrs after transfection. Cells were further incubated under normoxic or hypoxic conditions with and without addition of 1 mM DMOG. The cells were harvested 24 hrs after transfection (see paragraph 2. 2.14).

2.2.21 SDS-Polyacrylamide gel electrophoresis

The SDS-polyacrylamide gel electrophoresis (SDS-PAGE) was used to separate proteins according to their molecular weight. The anionic detergent sodium dodecyl sulphate (SDS) is used to denaturate the proteins by disrupting the non-covalent bonds and the use of the reducing agent β-mercaptoethanol in the sample buffer leads to the dissociation of subunits of the multimeric proteins. SDS charges the unfolded proteins negatively, which makes them migrate to the positive electrode in electrophoretic gel. The use of a discontinuous SDS-PAGE, in which a stacking gel is casted onto the resolving gel, leads to a decrease in sample spread. The pH conditions in the stacking gel result in the samples to stack between the fast migrating chloride ions and the slower migrating glycine from the sample buffer at the

starting point above the resolving gel. For the separation of polyubiquitinated proteins gradient gels with higher concentrations of acrylamide at the bottom of the gel were used. Usually gels with a gradient between 5 to 10 % acrylamide were used. The composition of the stacking and resolving gel is given in Tab. 2.21.

Tab. 2.21: Solutions for the preparation of one gel containing resolving and stacking gel for discontinuous SDS-PAGE.

	resolving gel			**stacking gel**
	5 %	10 %	12 %	5 %
H_2O	15.9 ml	11.9 ml	9.9 ml	6.8 ml
30 % acrylamide mix	6.0 ml	10 ml	12 ml	1.7 ml
1.5 M Tris pH 8.8	7.5 ml	7.5 ml	7.5 ml	-
1.0 M Tris pH 6.8	-	-	-	1.25 ml
10 % SDS	0.3 ml	0.3 ml	0.3 ml	0.1 ml
10 % ammonium persulfate	0.3 ml	0.3 ml	0.3 ml	0.1 ml
TEMED	0.024 ml	0.012 ml	0.012 ml	0.01 ml

50-120 µg of the sample were mixed with 2x SDS sample buffer. The samples were boiled at 70°C for 10 min and loaded onto the discontinuous SDS polyacrylamide gel. The prestained molecular weight marker or the prestained PageRuler^{TM} from Fermentas were loaded in a separate lane. The electrophoresis was done at a constant current of 50 mA with maximum voltage set at 300 V.

2.2.22 Western blot/ECL

Western blots were performed to further analyze the by SDS-PAGE separated samples with an immunostaining. Therefore, the separated proteins are transferred from the gel to a nitrocellulose membrane and analyzed by specific primary antibodies. The primary antibodies are then detected by horseradish peroxidase conjugated secondary antibodies which are raised against the Fc region of the primary antibody. The conjugated peroxidase catalyzes the oxidation of luminol resulting in a chemiluminescence emitting reaction that can be used for the specific detection of the target proteins.

To perform the western blot after the electrophoresis, the gel and the nitrocellulose membrane were equilibrated in western blot transfer buffer. The gel and the membrane were then sandwiched between filter papers previously soaked in blotting buffer. The western blot was

performed in the PerfectBlue Semi-Dry Electroblotter from Peqlab with a constant current setting of 2 mA/cm^2 for 1 hrs.

The membrane was washed with PBS after the transfer and the quality of the transfer was controlled by Ponceau S staining. The Ponceau S was washed off with PBS. To prevent unspecific binding of the antibodies, used for the detection of the target proteins, the blot was incubated with 5 % milk in PBS for 1 hrs at 4 °C. The primary antibody solution was then applied to the membrane and incubated overnight at 4 °C. For the used antibodies the applied dilutions are listed in Tab. 2.4.

Subsequently the membrane was washed thrice for 10 min with PBS. Incubation with the secondary, peroxidase conjugated antibody diluted in PBS containing 5 % milk (see Tab. 2.4) was done for 2 hrs at 4 °C. Again the blot was three times washed with PBS for 10 min. For the detection 10 ml ECL solution were applied to the membrane and incubated for 1 minute. The blot was developed by using the LAS3000 Imager from Fujifilm or by using chemiluminescence sensitive films from GE health care.

2.2.23 MBP pull-down

The maltose binding protein (MBP) is part of the maltodextrin transport system in *E. coli* and fusion proteins with MBP can be purified by using amylose columns.

For the pVHL or β-TRCP pull-down assays, 40 µl amylose-resin from NEB previously washed with MBP-buffer were incubated with 20 µg MBP-proteins and *in vitro* translated HA-PHD2 or purified His-PHD3 in a buffer containing 20 mM Tris/HCl, pH 7.5, 5 mM KCl, 1.5 mM $MgCl_2$, 100 µM α-Ketoglutaric acid, 1 mM $FeSO_4$, 2 mM ascorbate for 1 hrs. This buffer facilitates the hydroxylation reaction, mediated by recombinant PHD2 or PHD3. The resins were washed thrice with 900 µl MBP-buffer and incubated with the purified His-Trx-pVHL or *in vitro* translated V5-β-TRCP in 500 µl buffer containing 50 mM Tris/HCl, pH 7.5 and 120 mM NaCl for 1 hrs at 30 °C. Subsequently the resins were washed five times with MBP-buffer. The bound proteins were resuspendend in 50 µl SDS-sample buffer and immunoblot analysis was performed.

2.2.24 His pull-down

The His pull-down uses the principle based on the reversible interaction between various amino acid side chains and immobilized metal ions. Depending on the immobilized metal ions different side chains can be involved in the adsorption. The used Talon Metal affinity resin from BD Biosciences utilizes a tetradentate chelator of the Co^{2+} metal ion for purifying recombinant polyhistidine-tagged proteins.

For the His-ubiquitin pull-down HeLa cells were transfected with the pET3aWT-His-Ubiquitin plasmid overexpressing 6xHis-tagged ubiquitin. The cells were incubated with and without 1 mM DMOG for 24 hrs at 37 °C and 2 hrs before lysis 25 µM MG-132 was added to inhibit the proteasome. 650 µg of the cell lysate were incubated with 60 µl resin for 4 hrs at 4 °C. Subsequently the resin was washed 4 times with PBS and bound proteins were eluted by addition of 70 µl SDS-sample buffer. The cell lysates and the bound fractions were then analyzed by performing immunoblots against ATF-4.

2.2.25 Immunoprecipitation

Immunoprecititation (IP) is a method by which the quantity or physical characteristics of a protein from a mixture can be examined by using the antigen-antibody reaction principle. Sepharose beads, to which Protein G is crosslinked, are used for the precipitation. Protein G is a cell surface protein from *Streptococci* that binds to the Fc region of IgG antibodies from a variety of mammalian species and is therefore used in the immunoprecipitation reaction.

Protein G sepharose with a binding capacity of 10 to 20 mg/ml from GE was used for the ATF-4 IP. The antibody was covalently coupled to the sepharose. Therefore, the sepharose was washed twice with PBS and sedimented by centrifugation at 5000 rpm for 5 min at room temperature between washes. For each IP 50 µl Protein G sepharose were resuspended in 500 µl PBS and 5 µg antibody were added. As negative control 5 µg non-immunogenic rabbit sera were used (see Tab.2.4). The sepharose was incubated with the antibodies at room temperature for 1 hrs in a rotator to allow the binding of antibodies by Protein G. By centrifugation at 5000 rpm for 5 min the sepharose-bound antibodies were sedimented and washed twice with 900 µl borate buffer. The covalent coupling was done by incubation with 1 ml 20 mM dimethylpimelimidate in borate buffer for 30 min at room temperature in a rotator. The sepharose was again washed with 900 µl borate buffer, followed by washing with ethanolamine buffer. To stop the coupling reaction the sepharose was incubated with 900 µl ethanolamine buffer for 2 hrs in a rotator at room temperature. Subsequently the sepharose was washed twice with PBS and the uncoupled antibodies were removed by washing with

900 µl of a 200 mM glycine solution. The glycine was removed by washing with 900 µl PBS twice and unspecific binding sites were blocked by incubation with 3 % BSA in PBS containing 0.05 % ammonium azide for 1 hrs at 4 °C.

Before the IP was performed a preclearing of the protein extract was done. Incubation with 50 µl washed Protein G sepharose without antibody for 1 hrs was done to capture the proteins that would bind unspecifically to the Protein G sepharose. For each IP 800 µg protein extract were used. 50 µl Protein G sepharose covalently bound to the antibody were added and the volume was filled up to 1 ml with lysis buffer containing a protease inhibitor cocktail. The samples were incubated overnight at 4 °C in a rotator. The next day the sepharose was washed with lysis buffer thrice and the supernatant discarded. By addition of 75 µl 2x SDS sample buffer to the Protein G sepharose, the proteins bound to the immune complex dissociated from the antibodies. The samples were transferred to centrifuge filter units to remove the sepharose and centrifuged for one min at 5000 rpm. The samples were heated for 10 min at 70 °C and analyzed by immunoblotting against ubiquitin and ATF-4.

3. Results

3.1 Work performed in the Department of Cardiovascular Physiology previous to this thesis

Increasing amount of data has been obtained over the last years indicating the additional involvement of the PHD isoforms 1-3 in oxygen-dependent, but HIF-independent, signal transduction pathways. To further characterize isoform-specific functions of the PHDs, yeast two-hybrid screens using PHD1, PHD2 or PHD3 as baits were performed in the Department of Cardiovascular Physiology by Dr. J. Nesper and Dr. J. Köditz.

To this end, a human brain cDNA library fused to the Gal4AD domain was screened with full length PHD1, PHD2 or PHD3 fused to the Gal4BD domain as baits. HIF-2α was identified as PHD interaction partner in all screens demonstrating the reliability of the method. Several transcription factors or transcriptional co-regulators were identified as PHD3 protein interaction partners, which were not identified in the PHD1 or PHD2 screen.

In total 35 different potential PHD3 protein-interaction partners were identified. Among these were eight transcription factors or transcriptional regulators (ATF-4, NUDR8, MKL-1, FOG-2, SNW1, TBR-1, ZNF282, and HIF-2α). Four different cDNA clones of ATF-4 were identified. The protein interaction of PHD3 and ATF-4 was validated by pull-down assays using recombinant proteins.

ATF-4 comprises a basic leucine zipper domain and a zipper II domain (Figure 3.1). Using ATF-4 deletion variants the zipper II domain of ATF-4 was determined to be responsible for the interaction with PHD3. The C-terminal basic leucine zipper domain, which is needed for homo- or heterodimerization with other members of the ATF/CREB family, is not needed for the interaction with PHD3.

Fig. 3.1: Domain structure of the ATF-4 protein. The zipper II domain was identified to be responsible for the interaction with PHD3. Via the basic leucine zipper, ATF-4 forms hetero- or homodimers with other bZIP transcription factors.

Based on these preliminary data, the presented thesis was conceptualized to functionally characterize the protein interaction of PHD3 and ATF-4.

3.2 The protein interaction of ATF-4 is restricted to PHD3

A protein interaction with all PHD isoforms and the asparaginyl-hydroxylase FIH has been described for the HIF-α subunits (Mazure et al., 2004). To study if the interaction of ATF-4 is restricted to PHD3 or whether ATF-4 also interacts with PHD1 and PHD2 or with FIH, yeast two-hybrid assays were performed. The yeast reporter strain Ma V203 was transformed with the ATF-4 full length protein fused to Gal4AD. The different PHD isoforms and FIH were used as baits (Figure 3.2). The protein interaction was determined by screening for histidine auxothrophy after inhibiting histidine synthesis with 10 mM or 50 mM 3-Amino-1,2,4-triazole (3-AT).

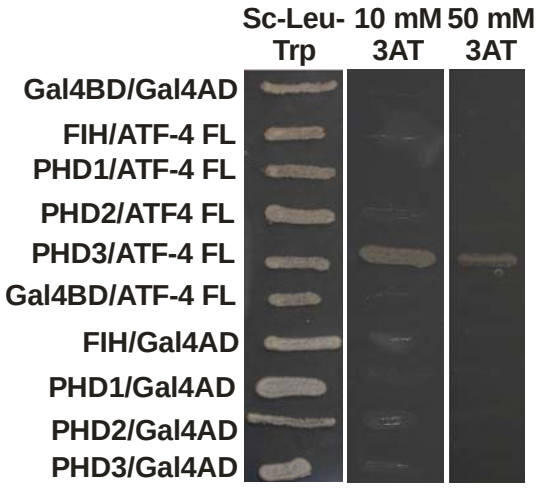

Fig. 3.2: ATF-4 interacts with PHD3 but not with PHD1, PHD2 or FIH. The yeast reporter strain MaV203 expressing Gal4AD ATF-4 and the PHDs or FIH fused to the Gal4BD was assayed for histidine auxotrophy.

These yeast two-hybrid assays revealed the exclusive interaction of ATF-4 with PHD3. No interaction of ATF-4 was observed with the PHD isoforms 1 and 2 or with the asparginyl-hydroxylase FIH. Additionally, no yeast growth was observed using the empty Gal4AD and Gal4BD vectors. The empty Gal4BD vector as bait in combination with Gal4AD ATF-4 or the empty Gal4AD in combination with Gal4BD PHDs or FIH excluded nonspecific signals or self activity.

The exclusive interaction of ATF-4 with PHD3 is an additional hint for different physiological functions of the three PHD isoforms.

3.3 ATF-4 protein levels are elevated in various cell lines by hypoxia and after inhibition of PHD activity

An induction of ATF-4 expression after exposure to severe hypoxia/anoxia (0 % to 0.2 % O_2) has been shown by others (Ameri et al., 2004). To study if the ATF-4 protein levels are not only elevated after anoxia but even after exposure to hypoxia (1 % O_2), various cell lines (HeLa, HepG2 and HEK293T) were exposed to normoxic or hypoxic conditions. Furthermore, PHD activity was inhibited by the addition of the 2-oxoglutarate analog DMOG (Figure 3.3). PHD-mediated prolyl hydroxylation of HIF-α in normoxia is known to mark HIF-α for ubiquitination and subsequent proteasomal degradation. If ATF-4 protein stability is comparable to HIF-α stability regulated by PHD3, one would expect that ATF-4 is more abundant in hypoxia and after inhibition of PHD activity.

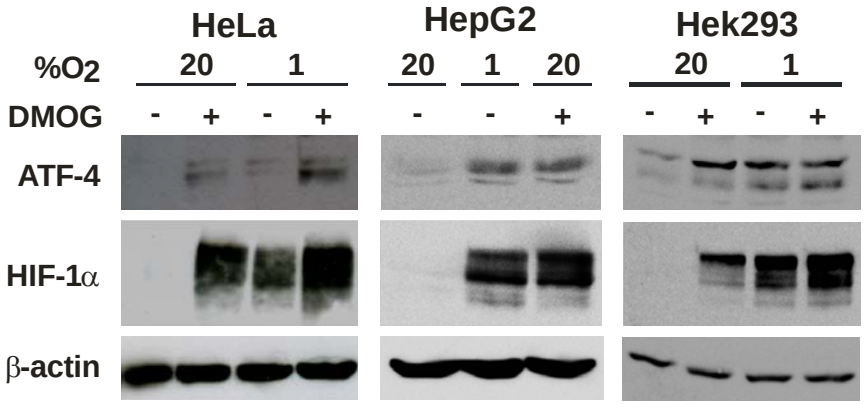

Fig. 3.3 ATF-4 and HIF-1α protein levels are increased by hypoxia and DMOG. HeLa, HepG2 and HEK293T cells were incubated for 4 hrs in 20 % O_2 or 1 % O_2, with or without treatment with 1 mM DMOG. Subsequently the cells were lysed and the protein expression of ATF-4, HIF-1α and β-actin was analyzed by immunoblots.

In all three cell lines the exposure to hypoxia (1 % O_2) for 4 hrs resulted in enhanced ATF-4 and HIF-1α protein levels. ATF-4 and HIF-1α were barely detectable under normoxic conditions, whereas after exposure to hypoxia the ATF-4 and HIF-1α levels were significantly higher. After inhibition of PHD activity, ATF-4 and HIF-1α protein signals were detectable also under normoxic conditions. The addition of DMOG under hypoxic conditions resulted in even stronger ATF-4 and HIF-1α signals than the exposure to hypoxia alone. A cell line-dependent effect of the increased ATF-4 abundance in hypoxia or after treatment with DMOG could be excluded since the same expression pattern was observed in all three cell lines studied.

To analyze if the elevated ATF-4 protein levels in hypoxia are a result of the increased HIF-1α stability, the impact of HIF-1α on ATF-4 protein levels was determined. Therefore, mouse embryonic fibroblasts isolated either from *Hif-1α*$^{+/+}$ or *Hif-1α*$^{-/-}$ embryos (MEF*Hif-1α*$^{+/+}$ and MEF*Hif-1α*$^{-/-}$ (Unruh et al., 2003)) were used to analyze the ATF-4 expression in hypoxia and normoxia (Figure 3.4).

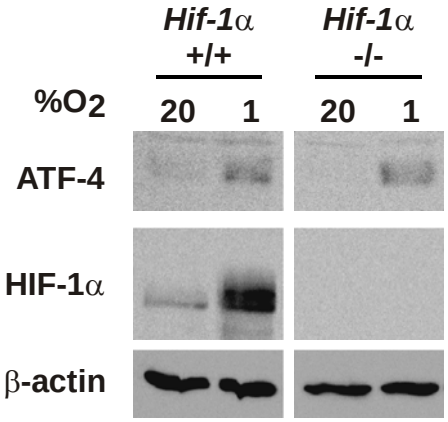

Fig. 3.4: The increase of ATF-4 protein levels in hypoxia is independent of HIF-1α. MEF*Hif*-1α$^{+/+}$ and MEF*Hif*-1α$^{-/-}$ cells were exposed to 20 % O_2 or 1 % O_2 for 4 hrs. Subsequently the cells were lysed and the protein expression of ATF-4, HIF-1α and β-actin was analyzed by immunoblots.

By analyzing the ATF-4 and HIF-1α protein levels under normoxic and hypoxic conditions a HIF-dependent expression of ATF-4 could be excluded. The expression of ATF-4 was induced after exposure to hypoxia in both cell lines. In HIF-1α expressing MEFs and also in the *Hif-1α*$^{-/-}$ MEFs elevated ATF-4 protein levels were observed after exposing the cells to hypoxic conditions for 4 hrs. This indicates that ATF-4 is part of a HIF-independent oxygen-regulated pathway.

To further investigate if the observed elevated ATF-4 protein levels in hypoxia correlate with increased ATF-4 transactivation activity, a luciferase reporter assay was performed. To activate the transcription of its target genes, ATF-4 interacts with a distinct DNA binding site that is named CRE. Therefore, a FL construct, in which the expression of the FL is under the control of two CRE sites, was used. As an independent control a constitutively active RL construct was co-transfected. Transiently transfected HeLa cells were incubated under hypoxic conditions for 4 hrs or treated with 1 mM DMOG (Figure 3.5).

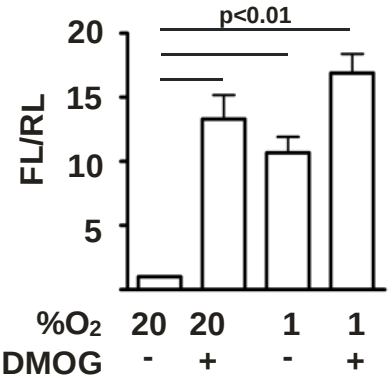

Fig. 3.5: ATF-4 activity is increased in hypoxia and after DMOG treatment. HeLa cells were transiently transfected with an ATF-4 dependent firefly luciferase (FL) reporter gene plasmid (pATFx2-Luc). As control the renilla luciferase (RL) plasmid pRLSV40 was co-transfected. The cells were incubated in 20 % or 1 % O_2 for 4 hrs, with or without treatment with 1 mM DMOG. Subsequently the cells were lysed and luciferase activities were determined. Shown are mean values of the FL/RL ratios (± SD) of three independent experiments.

As expected from the western blot analysis, only little ATF-4 transactivation activity was measured under normoxic conditions. Exposure to hypoxia, however, led to an enhanced FL activity. The inhibition of the PHD enzymatic activity by treatment of the cells with the 2-oxoglutarate analog DMOG also resulted in an increased FL activity even under normoxic conditions. These results suggest that the ATF-4 protein is not only more abundant after inhibition of PHD activity by hypoxia or DMOG, but is present in an active form in which it is able to induce target gene expression.

3.4 The ATF-4 protein level is dependent on PHD3 but not PHD2

To gain insight into the mechanism of hypoxia/DMOG-induced increase of ATF-4 protein levels, the kinetics of the hypoxic/DMOG stabilisation were determined. Cells were incubated under normoxic (20 % O_2) or hypoxic conditions (1 % or 0.2 % O_2), for 4 and 24 hrs (Figure 3.6). I experienced a lot of variation in the quality of the commercially available polyclonal anti-ATF-4 antibody. Therefore, I used cell extracts obtained from HeLa cells, which were treated with 300 nM thapsigargin for 4 hrs, as a positive control for the reliable detection of ATF-4 expression. Thapsigargin is a well described inducer of enhanced ATF-4 expression (Ord and Ord, 2003).

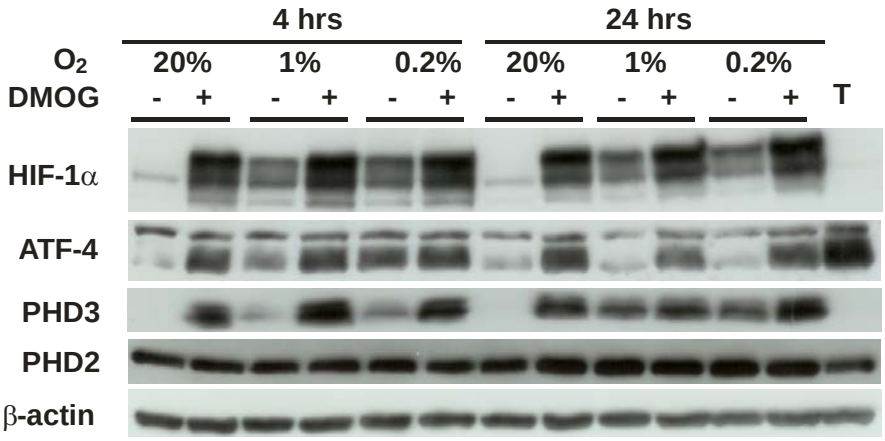

Fig. 3.6: ATF-4 protein levels are elevated in hypoxia and after treatment with DMOG. HeLa cells were incubated for 4 or 24 hrs in 20 %, 1 %, or 0.2 % O_2, with or without the addition of 1 mM DMOG. Subsequently cells were lysed. The protein levels of HIF-1α, ATF-4, PHD2, PHD3 and β-actin were analyzed by immunoblots. To obtain a positive control for the detection of ATF-4, HeLa cells were treated with 300 nM thapsigargin (T) for 4 hrs as indicated.

HIF-1α and ATF-4 were barely detectable under normoxic conditions, but after 4 hrs of exposure to hypoxia (1 % O_2), both proteins showed strong western blot signals. These signals were even stronger after exposure of the cells to 0.2 % O_2 for 4 hrs. In contrast to PHD2, PHD3 is barely detectable in normoxia. After treating the HeLa cells with DMOG, ATF-4 and HIF-1α were also detectable under normoxic conditions and even stronger signals were observed after DMOG treatment and the exposure to hypoxia.

In contrast to 4 hrs hypoxia, ATF-4 was not detectable after 24 hrs of hypoxia. This correlates with the increased PHD3 expression after 24 hrs of hypoxia. However, inhibition of PHD activity with DMOG resulted in an enhanced ATF-4 and HIF-1α abundance under hypoxic and normoxic conditions. This leads to the suggestion that ATF-4 stability is not only dependent on the interaction with PHD3 but also on the PHD hydroxylation activity.

To further study the functional impact of PHDs in ATF-4 expression, PHD2 or PHD3 expression was repressed via siRNA (Figure 3.7). The influence of PHD1 was not further investigated because it was not detectable at the protein level in HeLa cells in considerable amounts.

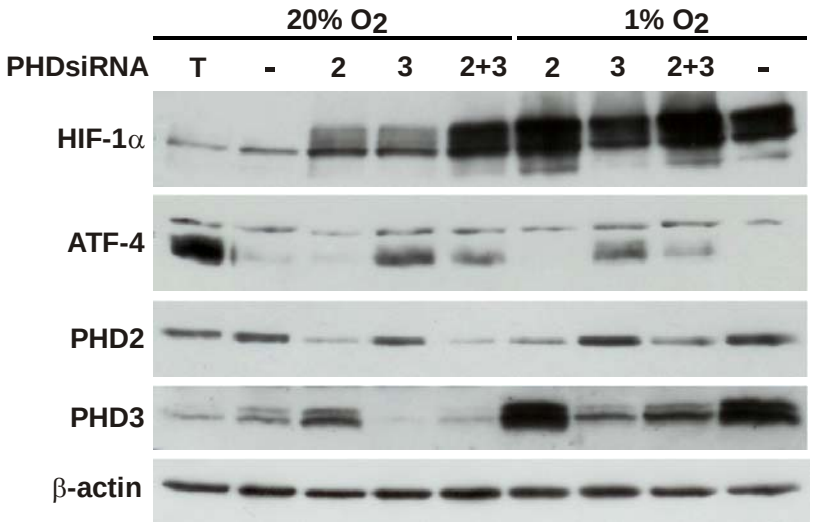

Fig. 3.7: ATF-4 protein levels are elevated after silencing PHD3 expression. HeLa cells were transiently transfected with siRNAs against PHD2, PHD3 or PHD2 and PHD3 together. The cells were incubated in 20 % or 1 % O_2 for 24 hrs and subsequently the cells were lysed. The protein levels of ATF-4, PHD2, PHD3, HIF-1α and β-actin were analyzed by immunoblots and compared to the untreated cells (-). To obtain a positive control for the detection of ATF-4, HeLa cells were treated with 300 nM thapsigargin (T) for 4 hrs as indicated.

ATF-4 expression was, comparable to the results described above, barely detectable under normoxic conditions. In contrast to HIF-1α, which is stabilized in normoxia after PHD2 down-regulation, silencing of PHD2 expression had no influence on ATF-4 protein levels. Elevated ATF-4 protein levels were detected only after silencing PHD3 expression in normoxia and hypoxia. The normoxic induction of ATF-4 is therefore restricted to PHD3, in contrast to HIF-1α protein levels, which are upregulated after PHD2 or PHD3 silencing.

To determine if the PHD3-mediated elevated ATF-4 protein levels are a result of an increased ATF-4 mRNA expression, the ATF-4 mRNA levels were measured. To this end, HeLa cells were transiently transfected with siRNA against PHD2, PHD3, a combination of both or a non-targeting control siRNA. Subsequently the cells were incubated in normoxia (20 % O_2) or hypoxia (1 % O_2) for 24 hrs and the mRNA levels of PHD2, PHD3 and ATF-4 were determined (Figure 3.8).

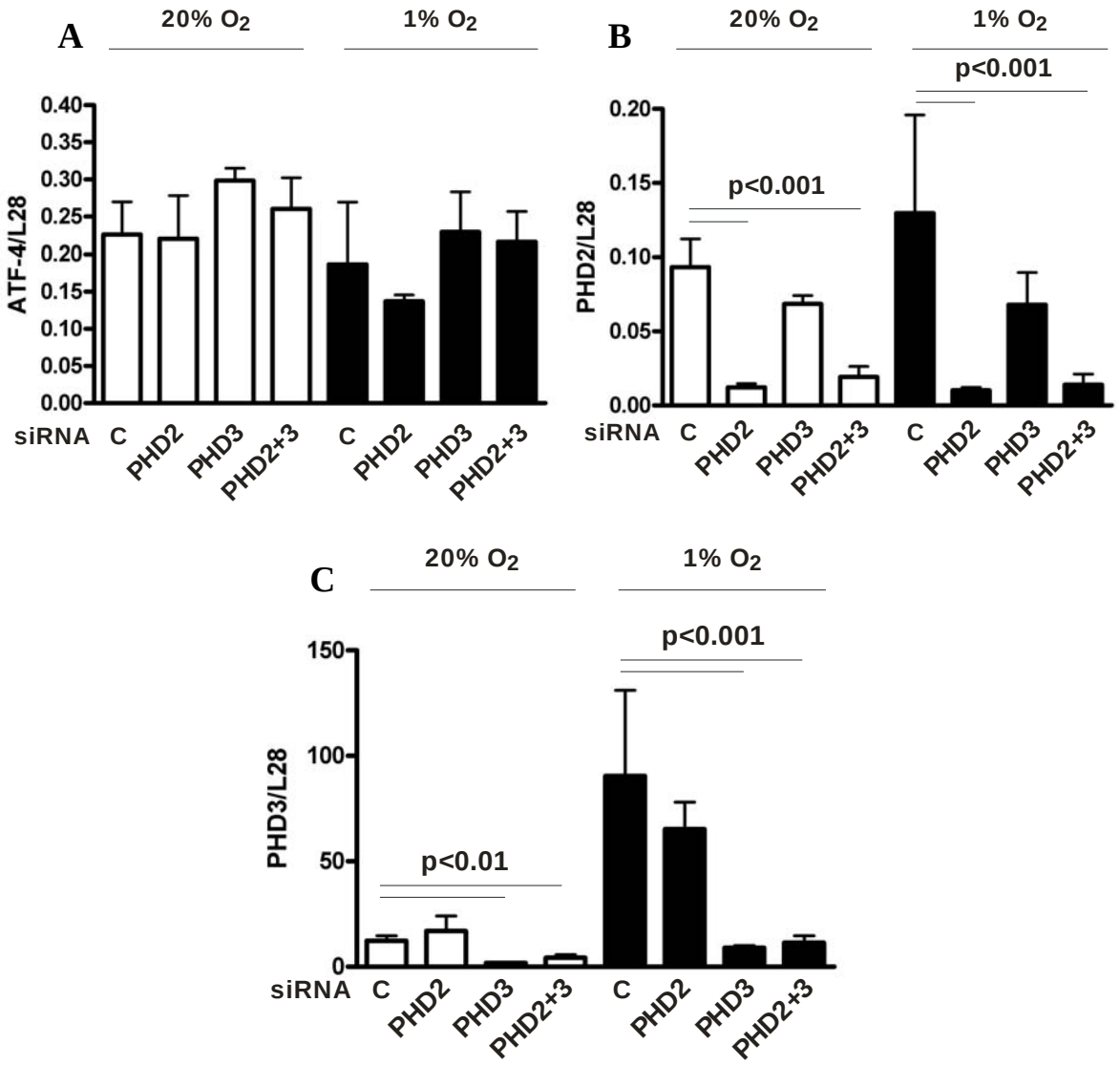

Fig. 3.8: ATF-4 mRNA levels are not increased by hypoxia or after the knockdown of PHD2 or PHD3 expression. HeLa cells were transiently transfected with the indicated siRNAs. Subsequently cells were incubated for 24 hrs in 20 % or 1 % O_2. The mRNA levels of ATF-4 (A), PHD2 (B), PHD3 (C) and L28 (housekeeping control RNA) were measured by quantitative RT-PCR. Shown are mean values ± SD of 3 independent experiments (ratios to the ribosomal protein L28 mRNA levels).

The mRNA levels were normalized in relation to the mRNA levels of the housekeeping gene L28, which encodes a ribosomal protein. No significant differences in the ATF-4 expression were observed after exposure of the HeLa cells to hypoxia compared to normoxia (see Figure 3.8 A). As expected, PHD3 expression was elevated after exposing the cells to hypoxia (Figure 3.8 C). The hypoxic induction of PHD2 mRNA was not that strong, which is in line with the literature (Cioffi et al., 2003) (Figure 3.8 B). For PHD2 and PHD3, a significant reduction of the mRNA levels was observed after transfection of the respective siRNA. Neither down-regulation of PHD2 nor PHD3, however, affected ATF-4 mRNA levels. These results indicate, that the elevated ATF-4 protein level under hypoxia or PHD3 knockdown is

not the result of an increased mRNA expression, but might be the consequence of a change in ATF-4 protein stability.

3.5 Inhibition of PHD activity or PHD3 expression leads to a slower degradation rate of ATF-4

In all experiments presented so far, ATF-4 protein expression was barely detectable under normoxic conditions, but the inhibition of PHD activity by DMOG or hypoxia led to enhanced ATF-4 protein levels. If this is due to PHD3-mediated normoxic destabilization, the elevated ATF-4 protein levels under hypoxic conditions should become unstable upon reoxygenation of the cells.

To test this hypothesis, HeLa cells were exposed to hypoxia (0.2 % O_2) followed by reoxygenation in normoxic conditions. To study the protein stability upon reoxygenation, protein synthesis was inhibited by the addition of cycloheximide shortly before reoxygenation. The cells were harvested at eleven different time points from 0 min to 40 min after reoxygenation to determine the protein half-life (Figure 3.9). Additionally, the ATF-4 protein half-life was measured after inhibition of PHD activity by DMOG, to clarify if the ATF-4 protein stability is regulated by PHD activity.

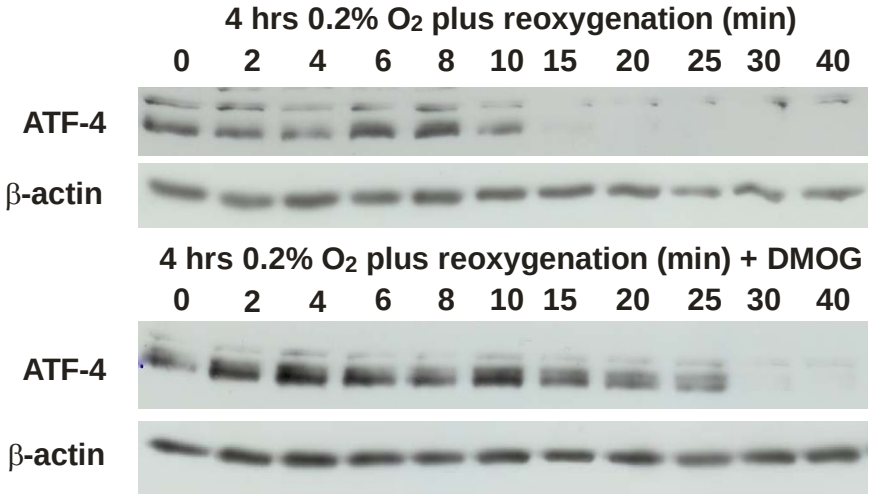

Fig. 3.9: Degradation of ATF-4 is decreased by DMOG. HeLa cells were incubated for 4 hrs in 0.2 % O_2 with or without treatment with 1 mM DMOG. Subsequently 20 µg/mL cycloheximide were added, and the cells were reoxygenated at 20 % O_2. The cells were lysed after the indicated time points and the ATF-4 and β-actin protein levels were analyzed by immunoblots.

Upon reoxygenation, the ATF-4 protein levels decreased rapidly with a half-life of roughly 9 min. Inhibiting PHD activity with DMOG elevated the ATF-4 half-life measured after

reoxygenation. DMOG treatment resulted in a prolonged protein half-life of roughly 21 min, indicating that the degradation of ATF-4 upon reoxygenation is regulated by PHD activity.

To further study the specific role of PHD3 in ATF-4 protein stability upon reoxygenation, HeLa cells were transiently transfected with siRNA targeting PHD3 mRNA or non-targeting siRNA. After 4 hrs of incubation under hypoxic conditions (1 % O_2), the cells were subsequently reoxygenated at 20 % O_2. The synthesis of new proteins was inhibited by addition of cycloheximide (Figure 3.10).

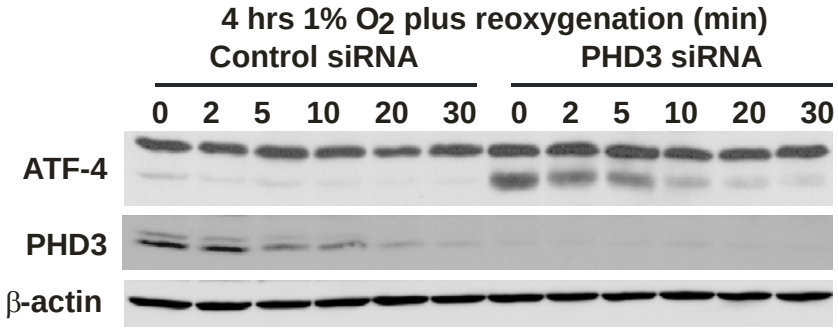

Fig. 3.10: Degradation of ATF-4 is decreased after PHD3 knockdown. HeLa cells were transfected with siRNA against PHD3 or a control siRNA. Subsequently cells were incubated in 1 % O_2 for 4 hrs, followed by the addition of 20 µg/mL cycloheximide and reoxygenation at 20 % O_2. The cells were lysed after the indicated time points and the ATF-4, PHD3 and β-actin protein levels were analyzed by immunoblots.

The down-regulation of PHD3 expression by siRNA led to an enhanced protein half-life compared to the control siRNA transfected cells. Taken together these results strongly indicate that the ATF-4 degradation under normoxic conditions is dependent on PHD3 activity.

The half-life of HIF-1α in normoxia is about 5 to 8 min. This results from its rapid degradation via the ubiquitin proteasome system (Berra et al., 2001). The E3 ubiquitin ligating enzyme pVHL is responsible for the ubiquitination of HIF-α in normoxia (Maxwell et al., 1999). After PHD-dependent prolyl hydroxylation pVHL binds to the ODD domain of HIF-α. Similar to HIF-α, an ODD domain was found in the ATF-4 protein sequence by Dr. J. Nesper and Dr. J. Köditz (Department of Cardiovascular Physiology). The ODD domain resides between the residues 154 to 181 and includes 5 prolyl residues (P156, P162, P164, P167, P174) (Figure 3.11), which are potential targets for PHD-dependent hydroxylation. Deletion of this ODD domain or mutation of the prolyl residues resulted in an increased ATF-4 stability under normoxic conditions (Köditz et al., 2007).

Fig. 3.11: Domain structure of the ATF-4 protein. The zipper II domain was identified to be responsible for the interaction with PHD3. The ODD domain (aa 154-181) is crucial for the oxygen-dependent instability of ATF-4. ATF-4 forms hetero- or homodimers with other bZIP transcription factors via its basic leucine zipper

3.6 ATF-4 is degraded via the ubiquitin proteasome system

The involvement of the ubiquitin proteasome system in regulating ATF-4 abundance has been described earlier (Lassot et al., 2001). Additionally, the translation of ATF-4 is upregulated in response to several stress conditions like amino acid deprivation, anoxia and ER stress (Ameri and Harris, 2008). To check, if the observed normoxic destabilization of ATF-4 is mediated via the ubiquitin proteasome system and to exclude an enhanced translation of the endogenous ATF-4 protein under hypoxic conditions, HeLa cells were transiently transfected with a V5-ATF-4 expression vector (pcDNA3.1Dest-V5ATF-4). This vector contains the CMV promoter fused to the V5-ATF-4 cDNA allowing an ATF-4 expression, which is independent of translational regulation. Equal transfection efficiency was controlled by co-transfection of the pEGFPC1 vector which results in a constitutive expression of GFP. The transfected cells were incubated in normoxia (20 % O_2) or hypoxia (1 % O_2) for 24 hrs. The degradation via the proteasome was inhibited by additional treatment of the cells with the proteasome inhibitor MG-132 for 2 hrs. To further study, if the normoxic destabilization of ATF-4 is mediated by PHDs, PHD activity was inhibited by DMOG treatment (Figure 3.12).

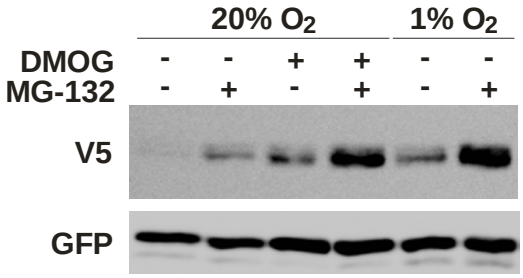

Fig. 3.12: ATF-4 is degraded via the proteasome. HeLa cells were transiently transfected with a V5-ATF-4 expression vector. As a transfection control the pEGFPC1 vector was co-transfected. The cells were incubated in normoxia respectively hypoxia, or treated with 1 mM DMOG for 24 hrs. 2 hrs before cell lysis 25 µM MG-132 were added to the indicated samples. The V5-ATF-4 and the GFP protein levels were analyzed by immunoblots.

Like the endogenous ATF-4 protein, V5-ATF-4 was not detectable under normoxic conditions. Exposure to hypoxia or treatment with 1 mM DMOG resulted in an enhanced

V5-ATF-4 signal, demonstrating that the overexpressed ATF-4 is like the endogenous ATF-4 regulated by hypoxia/DMOG. The pcDNA3.1V5Dest expression vector does not contain a functional HRE. Therefore, the elevated V5-ATF-4 signals are most likely not the result of an enhanced hypoxia-induced ATF-4 expression. The treatment of the cells with MG-132 resulted in an increased V5-ATF-4 abundance in normoxia and in hypoxia, indicating that the normoxic degradation of V5-ATF-4 is mediated by the proteasome.

To further verify the involvement of the proteasome in the normoxic destabilisation of ATF-4, the TS-20 cell line was used (Figure 3.13). This cell line has a temperature-sensitive E1 ubiquitin-activating enzyme defect. The shift from 34 °C to 39 °C stops ubiquitination leading to the accumulation of proteins which are degraded via the ubiquitin proteasome system. As a control the E1-resconstituted cell line H38-5 was used.

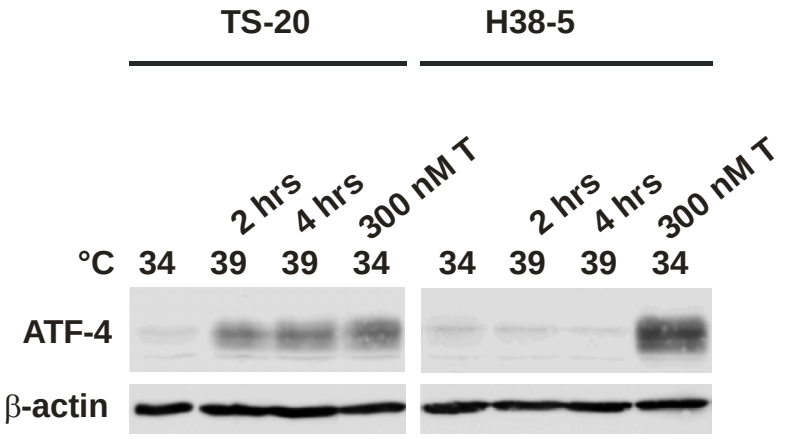

Fig. 3.13: ATF-4 is degraded via the proteasome. TS-20 cells, with a temperature-sensitive E1 ubiquitin-activating enzyme defect, and E1-reconstituted H38-5 cells were incubated at 34 °C or 39 °C for 2 or 4 hrs. As ATF-4 positive control the cells were incubated with 300 nM thapsigargin (T) for 2 hrs. Subsequently cells were lysed and the ATF-4 and β-actin protein levels were analysed by immunoblots.

At 34 °C no ATF-4 expression was observed in the TS-20 cells. Incubation of the thermolabile E1 mutant strain at 39 °C resulted in an increased ATF-4 abundance. No similar effect was observed in the H38-5 E1 reconstituted cells. These results point to an involvement of ubiquitination in regulating normoxic destabilisation of ATF-4.

The previous experiments did not answer if the ubiquitination of ATF-4 in normoxia is dependent on PHD activity. Therefore, HeLa cells were transiently transfected with a His-ubiquitin expressing plasmid. The proteasome was inhibited by MG-132 treatment. To determine an involvement of PHD activity in ATF-4 stabilization, DMOG was additionally

applied to the cells. The precipitated anti-His fractions and the cell lysates were studied by immunoblotting (Figure 3.14).

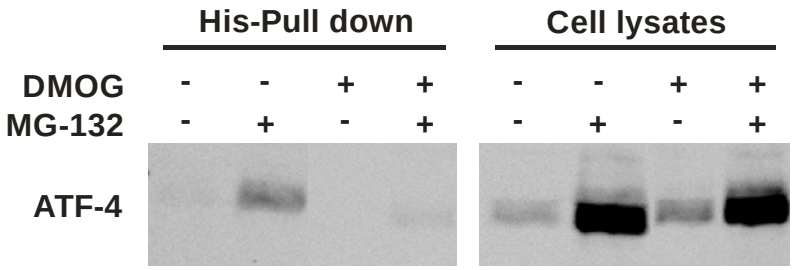

Fig. 3.14: DMOG inhibits the ubiquitination of ATF-4. His-ubiquitin was transiently overexpressed in HeLa cells. The cells were incubated for 24 hrs with 1 mM DMOG. 2 hrs before lysis 25 µM MG-132 were added to the indicated samples. His-ubiquitin was precipitated with Co^{2+} resin. The ATF-4 protein levels were analyzed in the cell lysates and in the Co^{2+} bound fractions by immunoblots.

Inhibition of the proteasome as well as inhibition of PHD activity resulted in an enhanced ATF-4 abundance. Analyzing the precipitated fraction showed that treatment with MG-132 results in an accumulation of ubiquitinated ATF-4. However after simultaneous treatment with MG-132 and DMOG, ubiquitinated ATF-4 was barely detectable, indicating a PHD-dependent regulation of normoxic ATF-4 degradation.

3.7 ATF-4 ubiquitination is inhibited by hypoxia

To test if the observed normoxic destabilization of ATF-4 is a result of an enhanced ubiquitination, HEK293T cells were incubated under normoxic (20 % O_2) and hypoxic conditions (1 % O_2). The proteasome was inhibited by addition of lactacystin to the cells to study the amount of ubiquitinated ATF-4 (Figure 3.15). Lactacystin inhibits the proteasome by binding to the catalytic subunits of the 20 S catalytic core and irreversibly blocks its protease activity (Fenteany et al., 1995). Furthermore, it inhibits the peptide hydrolysis which is mediated by the 26 S complex (Craiu et al., 1997).

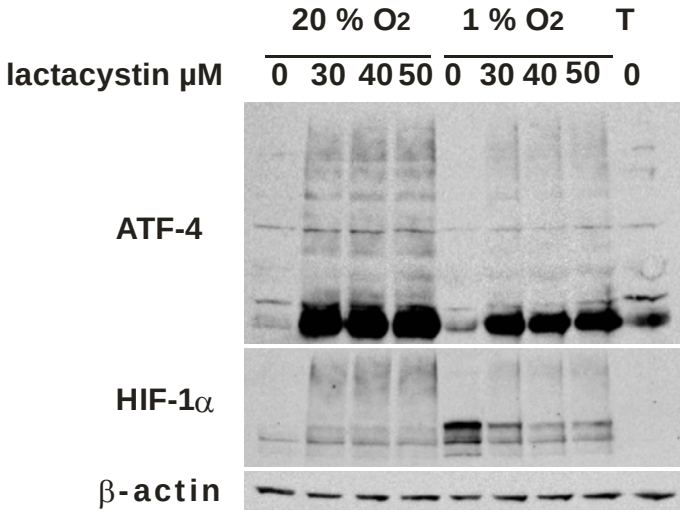

Fig. 3.15: Hypoxia impairs ubiquitination of ATF-4. HEK293T cells were incubated for 4 hrs in 20 % or 1 % O_2 in the presence of absence of 30-50 µM lactacystin. Subsequently cells were lysed and protein expression of ATF-4, HIF-1α, and β-actin was analyzed by immunoblot.

Analyzing the obtained cell lysates by using an ATF-4 specific antibody showed higher molecular weight bands in addition to the unmodified ATF-4 protein band. The intensity of these higher molecular weight bands was reduced in hypoxic conditions compared to normoxia. Similar results were observed for HIF-1α, which also appeared as higher molecular weight bands in addition to the unmodified protein. Similar to ATF-4 the intensity of the bands was decreased in hypoxic conditions.

To verify that the higher molecular weight bands of ATF-4, observed after lactacystin treatment, refer to polyubiquitinated ATF-4, HEK293T cell were again treated with lactacystin after exposure to normoxia (20 % O_2) or hypoxia (1 % O_2). ATF-4 was immunoprecipitated and the amount of ubiquitinated ATF-4 was detected by immunoblot using a specific anti-ubiquitin antibody (Figure 3.16). To confirm the specificity of the performed ATF-4 immunoprecipitation, normal rabbit serum, instead of the specific antibody, was used in an additional immunoprecipitation reaction as a negative control.

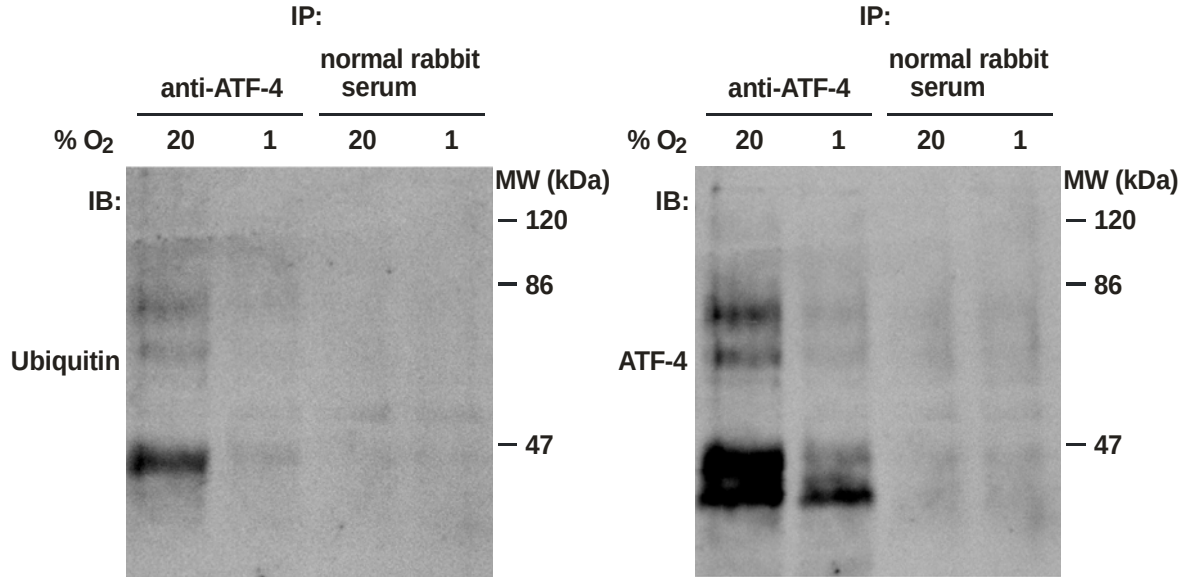

Fig. 3.16: The ubiquitination of ATF-4 is decreased in hypoxia. HEK293T cells were incubated for 4 hrs in 20 % or 1 % O_2 in the presence or absence of 30 µM lactacystin. Subsequently cells were lysed and cell lysates were immunoprecipitated with an anti-ATF-4 antibody and analyzed by immunoblots.

By analyzing the ubiquitin immunoblot, a diminished ubiquitination of ATF-4 in hypoxia was found. These results show that the previously observed normoxic destabilization of ATF-4 is a result of an increased polyubiquitination, which is abolished in hypoxia.

3.8 ATF-4 is not a target of pVHL

The ubiquitination of HIF-α is mediated via the E3 ubiquitin ligating enzyme pVHL (Maxwell et al., 1999). This involves a direct protein interaction of HIF-1α/HIF-2α and pVHL. To gain insight into the degradation pathway of ATF-4, a possible protein interaction of ATF-4 with pVHL was tested by performing MBP pull-downs. HIF-α is only ubiquitinated after PHD-dependent hydroxylation (Figure 3.17). Since our results also indicated a PHD3-dependent ubiquitination for ATF-4, the ATF-4 samples were preincubated with PHD2 or PHD3.

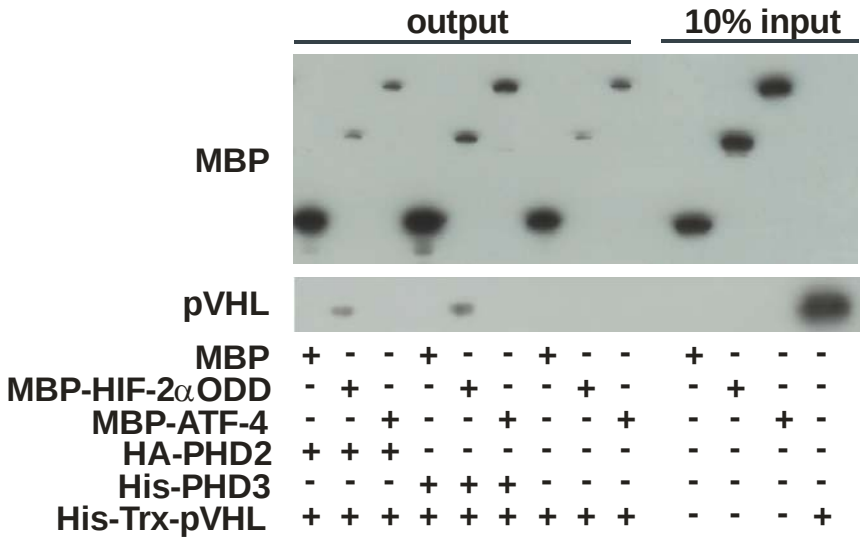

Fig. 3.17: ATF-4 is not a target of pVHL. HIF-2α-ODD-MBP or ATF-4-MBP fusion proteins were bound to amylose resin and incubated with HA-PHD2 or His-PHD3 for 1 hrs at 30°C in the presence of oxygen, ferrous iron, 2-oxoglutarate and ascorbate for a sufficient hydroxylation reaction. The binding to the pVHL was tested by MBP pull-down assay. Antibodies against MBP or pVHL were used for immunoblot detection.

As expected, an interaction of pVHL with the HIF-2α-ODD, preincubated with PHD2 or PHD3, was observed. This interaction was not detectable without incubating the HIF-2αODD with PHD2 or PHD3. In contrast, no protein interaction of ATF-4 and pVHL was observed. These results indicate that pVHL may not be responsible for the normoxic degradation of ATF-4.

3.9 ATF-4 interacts with the E3 ligase β-TRCP

The presented results imply that the normoxic degradation of ATF-4 is mediated via the ubiquitin proteasome system. But in contrast to HIF-α, this degradation is not dependent on pVHL (Figure 3.18). The SCF E3 ligase β-TRCP has been reported to interact with ATF-4 by others (Lassot et al., 2001).

To determine the domain of ATF-4, which is involved in the protein-interaction with β-TRCP, a yeast two-hybrid assay with several ATF-4 variants fused to Gal4AD and β-TRCP as bait was performed. The yeast reporter strain MaV203 was assayed for histidine auxothrophy (Figure 3.18).

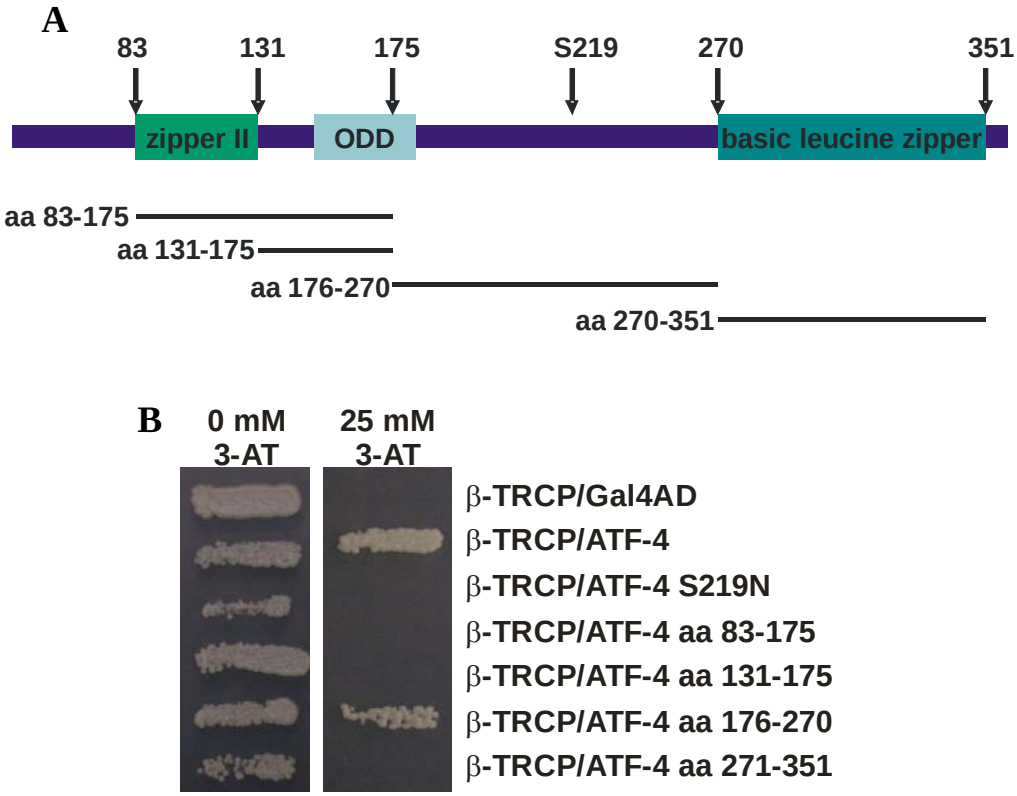

Fig. 3.18: ATF-4 interacts with β-TRCP. (A) Diagram of the used ATF-4 fragments fused to Gal4AD, which were analyzed in the yeast two-hybrid assay. (B) The yeast reporter strain MaV203 expressing Gal4BD β-TRCP and different variants of Gal4AD ATF-4 was assayed for histidine auxotrophy.

Analyzing the yeast two-hybrid assay showed that, aa 176-270 of ATF-4 are essential for the ATF-4 protein-interaction with β-TRCP. These residues are situated between the identified ODD domain and the C-terminal basic leucine zipper (Figure 3.18 A). The N-terminal zipper II domain together with the ODD domain (aa 83-175) or the ODD domain alone (aa 131-175) showed no interaction with β-TRCP. The basic leucine zipper (aa 271-351) is also not crucial for the interaction between ATF-4 and β-TRCP.

Other β-TRCP target proteins harbor a DSGXXS motif. The serine in this motif is essential for interaction with β-TRCP. ATF-4 aa 176-270 does contain a similar motif, which is DSGXXXS. Point mutation of ATF-4 serine 219 to asparagine within this motif abolished the protein-interaction with β-TRCP.

Our results indicated a PHD3-dependent normoxic degradation of ATF-4. To analyze if the protein interaction of ATF-4 and β-TRCP is dependent on PHD3, a MBP pull-down was performed (Figure 3.19). Recombinant ATF-4 and β-TRCP were preincubated with recombinant PHD3.

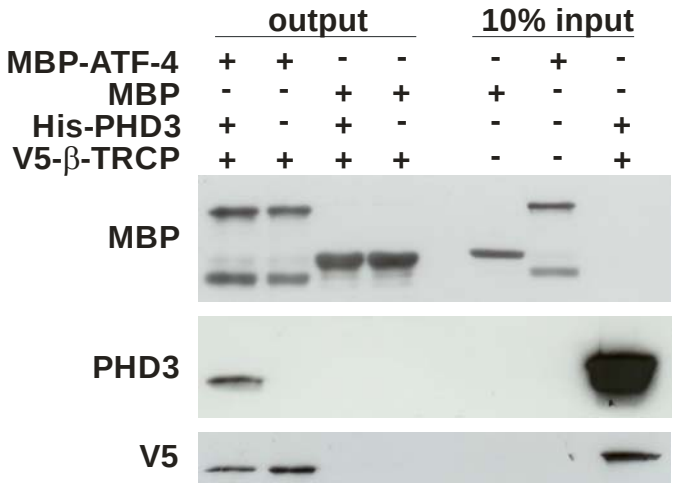

Fig. 3.19: The interaction of ATF-4 with β-TRCP is independent of PHD3. MBP-ATF-4 or MBP were bound to amylose resin and incubated with V5-β-TRCP for 1 hrs at 30°C in the presence of oxygen, ferrous iron, 2-oxoglutarate and ascorbate for an efficient hydroxylation reaction. The samples were incubated with or without His-PHD3. The binding to V5-β-TRCP was tested by MBP pull-down and immunoblots.

By analyzing the MBP pull-down it was observed that the protein-interaction of ATF-4 with β-TRCP is independent of incubation with PHD3. An interaction between β-TRCP and its target ATF-4 was observed with and without preincubation with His-PHD3.

To study if PHD3 regulates ATF-4 degradation by interacting with β-TRCP, the interaction between PHD3 and β-TRCP was analyzed by performing an additional yeast two-hybrid assay (Figure 3.20) and by MBP pull-down (Figure 3.21).

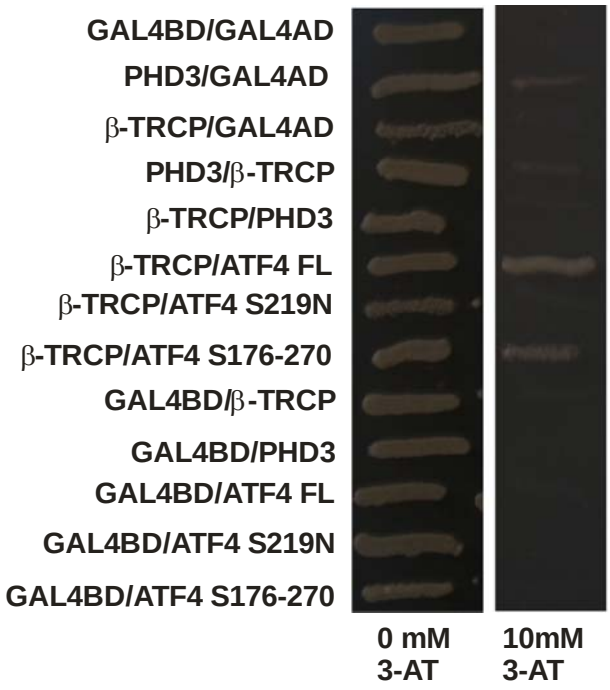

Fig. 3.20: β-TRCP interacts with ATF-4 but not with PHD3. The yeast reporter strain MaV203 expressing Gal4BD β-TRCP and different variants of Gal4AD-ATF-4, Gal4AD-PDHD3 or Gal4BD-PHD3, was assayed for histidine auxotrophy.

In the yeast two-hybrid assay only the interaction of full length ATF-4 (ATF-4 FL) and ATF-4 fragment aa 176-270 with β-TRCP was detected. A protein-interaction of β-TRCP with PHD3 was not observed in this assay.

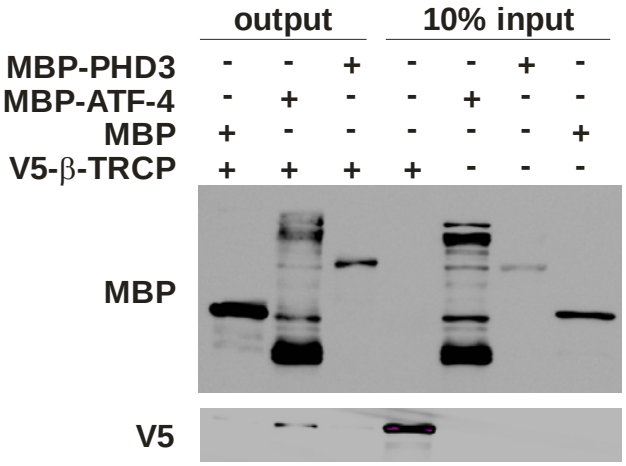

Fig. 3.21: β-TRCP interacts with ATF-4. MBP-ATF-4 or MBP-PHD3 were bound to amylose resin and incubated with V5-β-TRCP for 1 hrs at 30 °C in the presence of oxygen, ferrous iron, 2-oxoglutarate and ascorbate for an efficient hydroxylation reaction. The binding to V5-β-TRCP was tested by MBP pull-down and immunoblots.

An interaction between PHD3 and β-TRCP was also not observed in the MBP pull-down. This suggests that the interaction of ATF-4 with PHD3 and β-TRCP is independent of each other.

3.10 Normoxic degradation of ATF-4 is independent of β-TRCP

To strengthen the hypothesis that normoxic degradation of ATF-4 is independent of β-TRCP the β-TRCP expression was silenced by transiently transfecting HEK293T cells with siRNA against β-TRCP in normoxia (Figure 3.22). As a positive control for the normoxic stabilization of ATF-4, the expression of PHD3 was silenced, as a negative control a non-target control siRNA was transiently transfected.

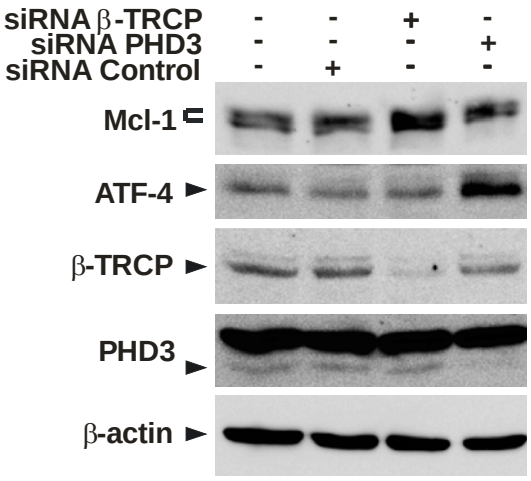

Fig. 3.22: Normoxic degradation of ATF-4 is independent of β-TRCP. HEK293T cells were transfected with siRNA against β-TRCP or PHD3 and a non-targeting control siRNA. The cells were incubated for 24 hrs in normoxia and the protein levels of MCL-1, ATF-4, β-TRCP, PHD3 and β-actin were analyzed by immunoblots.

As expected from the previous experiments, PHD3 silencing resulted in an elevated ATF-4 abundance even under normoxic conditions.

Bcl-2-like antiapoptotic protein myeloid cell leukemia 1 (MCL-1) is a known β-TRCP target (Ding et al., 2007). MCL-1 is rapidly degraded via the proteasome when cells undergo apoptosis. The degradation is mediated by β-TRCP-dependent ubiquitination. After silencing β-TRCP expression increased MCL-1 protein levels were observed demonstrating the functional downregulation of β-TRCP by siRNA. In contrast to this, β-TRCP silencing had no effect on the ATF-4 abundance.

The F-box protein β-TRCP is part of the multi-subunit RING finger type SCF (SKP1-CUL1-FBP) E3 ligases. The SCF E3 ligases contain a cullin (CUL1) subunit that functions as a scaffold and interacts via its N-terminus with the S-phase-kinase-associated protein-1 (SKP1), which functions as an adaptor subunit (Cardozo and Pagano, 2004). SKP1 interacts with one of the many F-box proteins (FBPs) that are characterized by their F-box domain, which is essential for SKP1-binding. The FBPs are responsible for the specific target recognition of the SCF E3 ligase.

To further exclude the involvement of β-TRCP or other SCF E3 ligases in the normoxic degradation of ATF-4, the expression of SKP1 was silenced under normoxic conditions by transient transfection of siRNA (Figure 3.23).

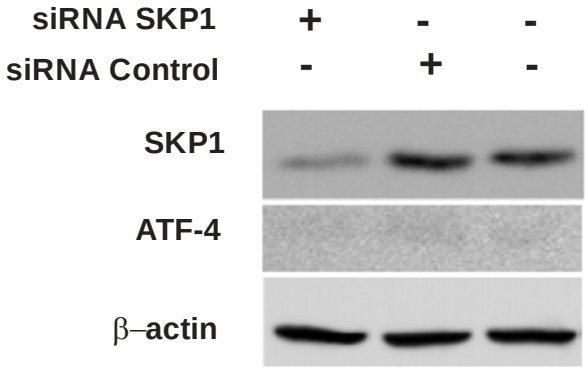

Fig. 3.23: ATF-4 stability in normoxia is not affected by SKP1 down-regulation. HeLa cells were transfected with siRNA against SKP1 and a non-targeting control siRNA. 24 hrs after transfection the cells were lysed and the protein levels of ATF-4, SKP1 and β-actin were analyzed by immunoblots.

Like silencing β-TRCP mRNA expression also SKP1 down-regulation had no influence on the ATF-4 protein level under normoxic conditions. In summary, ATF-4 interacts with β-TRCP and ATF-4 serine 219 is crucial for this interaction. However, β-TRCP is not responsible for the normoxic degradation of ATF-4.

3.11 Oxygen-dependent expression of ATF-4 target genes

Up to now more than one hundred HIF target genes have been characterized (Bernhardt et al., 2007). However, there are several genes including GADD153, for which a HIF-independent induction in hypoxia has been described (Carmeliet et al., 1998). GADD153 is an ATF-4 target gene. It is involved in regulating cell cycle progression and apoptosis (Hai et al., 1999; Kim et al., 2006). To further study the functional consequences of the oxygen-dependent regulation of ATF-4, GADD153 expression was analyzed in normoxia (20 % O_2) and hypoxia (1 % O_2). To this end, the hypoxia-inducible expression of GADD153 was confirmed in HEK293T cells (Figure 3.24). GADD153 was not detectable in 20 % O_2. Exposure to 1 % O_2 for 4 hrs and 24 hrs, however, resulted in enhanced ATF-4 and GADD153 levels, respectively.

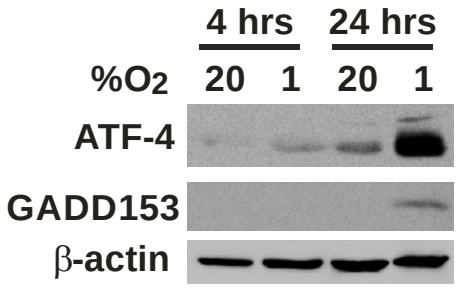

Fig. 3.24: GADD153 and ATF-4 protein levels are increased after exposure to hypoxia. HEK293T cells were incubated at 20 % or 1 % O_2 for 4 and 24 hrs. Subsequently cells were lysed and the protein levels of ATF-4, GADD153 and β-actin was analyzed by immunoblot.

To analyze the impact of the oxygen-dependent regulation of ATF-4 for the hypoxia-inducible GADD153 expression, ATF-4 was silenced by transiently transfecting HEK293T cells with siRNA targeting ATF-4 (Figure 3.25). As negative control a non-targeting control siRNA was transfected and the cells were harvested after 24 hrs of exposure to normoxic (20 % O_2) or hypoxic conditions (1 % O_2).

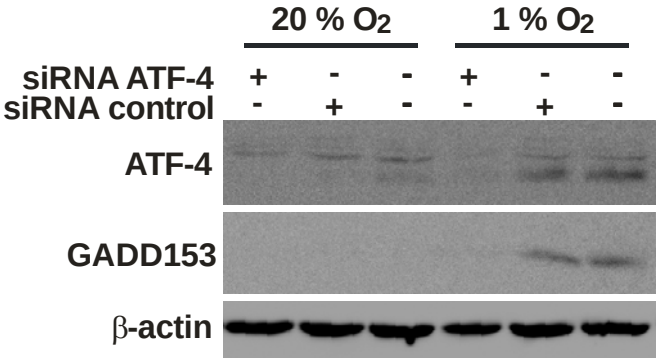

Fig. 3.25: Hypoxia-induced GADD153 expression is dependent on ATF-4. HEK293T cells were transiently transfected with siRNA against ATF-4 or non-targeting control siRNA. The cells were incubated at 20 % or 1 % O_2 for 24 hrs. Subsequently cells were lysed and the expression of ATF-4, GADD153 and β-actin was analyzed by immunoblot.

As expected, hypoxic induction of GADD153 was observed in untreated cells and in cells transfected with non-targeting siRNA. This effect was abolished after silencing ATF-4 expression, indicating an ATF-4-dependent upregulation of GADD153 expression in hypoxia. If ATF-4 is involved in the hypoxia-induced expression of GADD153, its regulator PHD3 should also affect the GADD153 expression. According to the previous experiments presented here, PHD3 downregulation but not PHD2 silencing, should lead to an enhanced ATF-4 protein level and additionally to an increased expression of ATF-4-target genes. The expression of PHD2 and PHD3 was silenced in HEK293T cells. After incubating the cells

under normoxic, conditions for 24 hrs the expression of ATF-4, GADD153, PHD3 and PHD2 was determined (Figure 3.26).

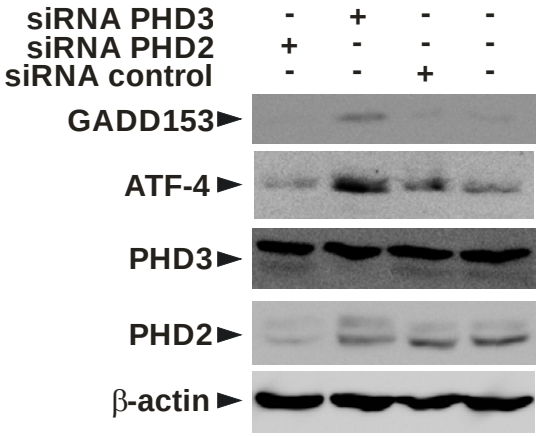

Fig. 3.26: GADD153 expression is induced as a consequence of PHD3 knockdown. HEK293T cells were transfected with siRNA against PHD2, PHD3 or a control siRNA. The cells were incubated at 20 % O_2 for 24 hrs. Subsequently cells were lysed and protein levels of ATF-4, PHD2, PHD3, GADD153 and β-actin were analyzed by immunoblots.

Like ATF-4, GADD153 expression was induced after silencing PHD3 expression but not after silencing PHD2 demonstrating a functional link between ATF-4 target genes and the cellular oxygen sensor PHD3.

4. Discussion

An adequate oxygen supply is essential for all multicellular organisms and an inadequate oxygen supply is termed hypoxia. The transcription factor HIF is the master regulator to respond to hypoxia. The regulation of HIF involves various posttranslational modifications. The most crucial step of HIF regulation is the oxygen-dependent proteasomal degradation of the HIF-α subunit. The degradation is regulated by prolyl hydroxylation mediated by PHD 1-3. By studying PHD knockout mice isoform specific physiological functions were observed. The enzymatic activity towards hydroxylating HIF-1α and HIF-2α is also isoform specific. Even the hydroxylation activity towards HIF-α differs within the three PHD isoforms. PHD3 exclusively hydroxylates proline 564 of HIF-α, whereas PHD1 and PHD2 hydroxylate proline 402 and 564 (Hirsila et al., 2003). Additionally several PHD protein-interaction partners were found to be isoform-specific. The knowledge about PHD isoform specific functions is important for the ongoing development of small molecule PHD inhibitors that are currently tested in preclinical and clinical trails for the treatment of anemia and for cytoprotection. PHD inhibition has been proven to activate the HIF pathway *in vitro* and *in vivo* (Warnecke et al., 2003). From this knowledge one can conclude that inhibition of PHDs stabilizes HIF-α and stimulates HIF-mediated pathways even under normoxic conditions. This approach activates the beneficial aspects of the HIF system. To this end, various PHD inhibitors were designed. These drugs are currently investigated for their efficacy to stimulate erythropoiesis in case of anemia caused by chronic kidney diseases, chronic inflammatory diseases or for treatment of chemotherapy-induced anemia (Katschinski, 2009). Additionally, HIF stabilizers may be useful for cytoprotection in case of tissue damage in the renal, cardiovascular or central nervous system. As mentioned above, PHDs have isoform-specific functions *in vivo*, therefore it will be important to develop PHD isoform-specific inhibitors that interact with distinct HIF-α isoforms and thus distinct HIF-target genes or other HIF independent signal transduction pathways to minimize adverse effects. Given the ubiquitous expression of PHDs and the large amount of HIF activated genes, otherwise even a short term use of PHD inhibitors may result in several unwanted side effects.

Therefore, yeast two-hybrid screens were performed in the Department of Cardiovascular Physiology by Dr. J. Nesper and Dr. J. Köditz to identify novel PHD interaction partners.

In this screen, ATF-4 was identified, besides others, as PHD3 protein-interaction partner. The aims of this thesis were to characterise the protein-interaction of ATF-4 with PHD3 and gain insight into the physiological function of this interaction.

4.1 ATF-4 is a novel PHD3 interaction partner

ATF-4 was identified as novel interaction partner of PHD3. To further check if this interaction is restricted to PHD3 or if ATF-4 also interacts with the other PHD isoforms or the asparaginyl hydroxylase FIH, yeast two-hybrid assays were performed. In these assays the exclusive protein-interaction of ATF-4 with PHD3 was observed (Fig. 3.2). For other PHD-interaction partners a PHD isoform specific protein-interaction has been reported by other groups, too. The inhibitor of the NF-κB (IκB) kinase-β (IKKβ) interacts exclusively with PHD1 and increased protein levels were found in hypoxia or after inhibition of PHD activity (Cummins et al., 2006). Additionally, the large subunit of RNA polymerase II (Rpb1) interacts with PHD1 and PHD2 only (Mikhaylova et al., 2008). Myogenin and kinesin family member 1B (KIF1Bβ) exclusively interacts with PHD3 (Fu et al., 2007; Schlisio et al., 2008).
Modelling studies and sequence comparisons of the PHD catalytic domain showed that it is highly conserved among the three human PHD isoforms and therefore is most likely not responsible for the substrate specificity (McDonough et al., 2006). In further studies a variability of the N- and the C-terminus of the PHDs was reported. Various motifs were identified in the PHD sequences, which are not conserved among the PHDs, like a β2-β3 finger motif and two N-terminal helices, α1 and α2, distant from the active site. It has been shown that the β2-β3 finger motif is likely to be responsible for the PHD-isoform substrate specificity (Villar et al., 2007).
The expression of ATF-4 is known to be upregulated upon exposure to several stress conditions like amino acid deprivation, oxidative stress or ER-stress (Rutkowski and Kaufman, 2003). The stress-induced upregulation of ATF-4 is mediated via translational control by two uORFs in the 5'-leader of the ATF-4 mRNA, whereas the mRNA itself is constitutively expressed (Harding et al., 2000). Additionally, elevated ATF-4 levels were found in cells exposed to severe hypoxia (0.1 % O_2) or anoxia (less than 0.1 % O_2) (Ameri et al., 2004). To further characterize the function of the ATF-4 PHD3 interaction, the expression of ATF-4 was studied after exposure to hypoxia. The enzymatic activity of PHDs is decreased under hypoxic conditions. Additionally, it can be inhibited by treatment with the 2-oxoglutarate analog DMOG. If PHD3 is involved in regulating ATF-4 expression, hypoxia or DMOG treatment would affect the ATF-4 protein levels. In various cell lines (HeLa, HepG2 and HEK293T) increased ATF-4 protein levels were indeed observed under hypoxic conditions (1 % O_2) or after inhibiting PHD activity by DMOG treatment indicating that besides the translational control ATF-4 protein levels are regulated by additional mechanisms

(Figure 3.3). Since hypoxia/DMOG-dependent increased ATF-4 levels were observed in various cell lines a cell line specific effect could be excluded.

Using MEF*Hif-1α*$^{+/+}$ and MEF*Hif-1α*$^{-/-}$ cells a HIF-1α-dependent mechanism for the ATF-4 regulation in hypoxia can be excluded (Figure 3.4). ATF-4 is not the only PHD protein-interaction partner known to be upregulated under hypoxia in a HIF-independent manner. As mentioned above, Rpb1, KIF1Bβ and IKKβ were also found to interact with PHDs. Similar to ATF-4 increased protein levels were observed in hypoxia or after DMOG treatment independent of HIF-α (Cummins et al., 2006; Mikhaylova et al., 2008; Schlisio et al., 2008). There are several genes, for which an upregulated RNA expression in hypoxia has been described. Not all of these are HIF-target genes supporting the hypothesis of an alternative HIF-independent transcriptional regulation in hypoxia. Even one of the most prominent HIF-α targets, VEGF, seems to be regulated via an additional HIF-independent pathway. In *Hif-1α*$^{-/-}$ ES cells the VEGF mRNA levels were reduced by just 50 % in hypoxia pointing to HIF-independent pathways regulating angiogenesis (Hopfl et al., 2002). In this regard it is interesting to note, that ATF-4 induces VEGF expression during oxidative stress (Roybal et al., 2005).

Luciferase reporter gene assays showed that similar to HIF-1 not only the ATF-4 protein levels are increased in hypoxia or after inhibition of PHD activity by DMOG treatment, but also its transactivation activity is increased (Figure 3.5). The ATF-4 protein is therefore present in an active form, in which ATF-4 is able to activate its target gene expression. This leads to the suggestion, that besides the described translational control via eIF2α phosphorylation, ATF-4 activity is regulated by an additional pathway.

The kinetic of ATF-4 stabilisation in hypoxia together with siRNA experiments revealed a specific role of PHD3 in regulating ATF-4 protein levels. A hypoxic stabilisation of ATF-4 was observed after a 4 hrs long hypoxic incubation. Upregulation of PHD3 after prolonged hypoxia (24 hrs) resulted in a decreased ATF-4 abundance (Figure 3.6). The expression of PHD2 and PHD3 are upregulated by HIF-1 in hypoxia limiting HIF-1α steady-state levels under hypoxic conditions and leading to its rapid degradation upon reoxygenation (Marxsen et al., 2004).

The specificity of PHD3 in regulating ATF-4 protein levels was further shown by siRNA experiments. Only the downregulation of PHD3 mRNA expression, but not PHD2 silencing, resulted in enhanced ATF-4 protein levels in normoxia and also after 24 hrs of hypoxia (Figure 3.7). After transient transfection of a combination of siRNAs against PHD2 and

PHD3 only a slight increase of ATF-4 was detectable. This can be explained by a decreased transfection efficiency of the PHD3 siRNA in combination with the PHD2 siRNA. In contrast to ATF-4, normoxic stabilization of HIF-1α has been shown after silencing of PHD2 expression by siRNA, whereas downregulation of PHD1 and PHD3 had no influence on HIF-1α stability in normoxia (Berra et al., 2003). In my experiments downregulation of PHD2 resulted as expected in an increased HIF-1α stabilization in normoxic conditions.

By analysing the ATF-4 mRNA levels after downregulation of PHD2 or PHD3 mRNA expression with siRNAs it could be excluded that the observed elevated ATF-4 protein levels are the result of an increased mRNA expression (Figure 3.8). The exposure to hypoxic conditions had no influence on the ATF-4 mRNA levels either. This is consistent with unchanged ATF-4 mRNA levels after exposure to anoxic conditions as described in the literature (Ameri et al., 2004). Previous studies in the Department of Cardiovascular Physiology performed by Dr. J. Köditz showed that DMOG treatment or exposure of cells to hypoxia do not lead to phosphorylation of eIF2α and therefore the observed increased ATF-4 protein levels are most likely not a result of an enhanced translation. Taken together, the presented data suggest that ATF-4 is regulated via an additional pathway besides the well described translational control, in which PHD3 might be specifically involved by regulating ATF-4 protein stability.

4.2 PHD3 regulates ATF-4 protein stability

The HIF-1α protein has a short half-life under normoxic conditions, which is about less than 5 min (Huang et al., 1998). In the HIF-1α protein sequence an ODD domain was identified where PHD-mediated prolyl hydroxylation takes place at two conserved proline residues. The hydroxylation marks HIF-1α for degradation via the ubiquitin proteasome system (Ivan et al., 2001; Jaakkola et al., 2001). Deletion of the ODD domain in HIF-1α results in an enhanced protein half-life of more than 45 min (Huang et al., 1998).

The protein stability of ATF-4 in normoxic conditions was analyzed to find out, if ATF-4 is similar to HIF-1α stabilized under hypoxic conditions and rapidly degraded upon reoxygenation. As described above, I found elevated ATF-4 protein levels under hypoxic conditions and after inhibition of PHD activity or expression, which might be a result of a decrease in protein degradation under these conditions. The presented reoxygenation experiments indeed showed an increased ATF-4 protein half-life after inhibition of PHD activity by DMOG treatment and after reducing the PHD3 expression by siRNA (Figure 3.9 and Figure 3.10). Inhibition of PHD activity by DMOG treatment resulted in a prolonged

ATF-4 half-life of about 21 min compared to 9 min. These results indicate that the ATF-4 protein stability is regulated by PHD activity and especially by PHD3.

Similar to HIF-1α, in the ATF-4 protein sequence an ODD domain was found, which includes 5 proline residues. These proline residues are potential targets for a PHD3-dependent hydroxylation. Deletion of the ODD domain or mutation of all 5 proline residues resulted in an increased ATF-4 protein stability (Köditz et al., 2007). Despite using different approaches like mass spectroscopy or 2-oxoglutarate turnover, a direct hydroxylation of ATF-4 was not detectable. Besides technical difficulties, the conditions for ATF-4 hydroxylation are also not known. The regulation of ATF-4 protein stability by PHD3 differs from the well studied regulation of HIF-1α in several aspects. HIF-1α is in contrast to ATF-4 not only dependent on PHD3 but also known to be hydroxylated by PHD2 and PHD1. Additionally, HIF-1α is also stabilized after prolonged hypoxia. Therefore, the conditions for an efficient hydroxylation of ATF-4 might be different from the conditions known for an efficient HIF-α hydroxylation and might explain the difficulties in measuring the hydroxylation of ATF-4.

A number of novel PHD protein interaction partners have been identified as putative targets for prolyl hydroxylation. Until now just for Rbp1 a PHD1-dependent hydroxylation was shown by immunoblotting using an antibody, which was generated with a hydroxylated proline in the Rpb1 peptide, but not by mass spectroscopy (Mikhaylova et al., 2008). Therefore, further efforts will be needed to detect hydroxylation modifications by mass spectroscopy or other techniques in the future.

4.3 ATF-4 is degradated via the ubiquitin proteasome system

The degradation of proteins via the ubiquitin proteasome system is done in two steps. First the protein is tagged for degradation by covalently attaching ubiquitin molecules and second the ubiquitinated protein is degraded by the 26S proteasome complex. The ubiquitination of a protein is tightly regulated and involves a cascade of three steps. The ubiquitin is activated by the E1 ubiquitin activating enzyme. This reaction consumes ATP and the thiol ester intermediate E1-S-ubiquitin is generated. The substrate specifically binds a member of the E3 ubiquitin protein ligase family via a defined recognition motif. These E3 ubiquitin ligases are responsible for the substrate recognition. The E2 ubiquitin conjugating enzyme transfers the activated ubiquitin from the E1 via the thiol ester intermediate or E2-S-ubiquitin directly to the E3-bound substrate. The ubiquitinated protein is then degraded via the proteasome (Glickman and Ciechanover, 2002).

The normoxic degradation of HIF-α is well studied. PHD-dependent prolyl hydroxylation marks HIF-α for degradation via the ubiquitin proteasome system (Ivan et al., 2001; Jaakkola et al., 2001). This is mediated by the pVHL-E3-ubiquitin-ligase complex, in which pVHL functions as F-box protein (Maxwell et al., 1999). ATF-4 is also regulated via its protein stability. SCF β-TRCP is one known E3 ubiquitin ligase, which is involved in the ubiquitination of ATF-4 (Lassot et al., 2001). β-TRCP is the responsible F-box protein for the target specificity in a multi-component E3 ubiquitin ligase complex composed of Skp1, Cullin and the F-box protein (SCF). Therefore, the normoxic destabilization of ATF-4, which was observed in reoxygenation experiments, was further studied, to clarify if ATF-4 is similar to HIF-1α regulated by the ubiquitin proteasome system.

By overexpressing V5-tagged ATF-4 in HeLa cells with an expression vector, which contains the not hypoxia-inducible CMV promoter, V5-ATF-4 accumulates in the cells under hypoxic and normoxic conditions after inhibiting the proteasome with MG-132 (Figure 3.12). This suggests that the normoxic degradation of ATF-4 is similar to HIF-1α mediated via the ubiquitin proteasome system. MG-132 is a peptide aldehyde proteasome inhibitor, which not only inhibits the proteasome but also the activity of lysosomal cysteine proteases and calpains (Rock et al., 1994). The ATF-4 protein contains one potential proline, glutamic acid, serine, threonine (PEST)-like sequence between the aa 209-234. PEST sequences function as putative intramolecular signals for proteolytic degradation by calpains (Rechsteiner and Rogers, 1996).

Therefore, an additional approach was used to exclude the involvement of proteases and calpains in the normoxic degradation of ATF-4. By studying the TS-20 cell line (Figure 3.13), which has a temperature-sensitive E1 ubiquitin activating enzyme defect, and by performing pull-down assays with His-ubiquitin (Figure 3.14), the normoxic degradation of ATF-4 was shown to be mediated via the ubiquitin proteasome system.

Further experiments showed that the ubiquitination of ATF-4 is decreased under hypoxic conditions resulting in a decrease of polyubiquitinated ATF-4 (Figure 3.15 and 3.16). Lactacystin instead of MG-132 was used to inhibit the proteasome in these experiments, because of its high specificity. Lactacystin acts as a pseudosubstrate, which is covalently linked to hydroxyl groups on the active site of the β subunit of the 26S proteasome and thereby inactivates the chymotryptic- and tryptic-like activities of the proteasome irreversibly (Fenteany et al., 1995). Taken together the results show that ATF-4 is rapidly degraded under normoxic conditions and similar to HIF-α inhibition of PHD activity by hypoxia results in accumulation of ATF-4 protein as a consequence of a decrease in ubiquitination.

Further studies will be needed to show if the observed normoxic degradation of ATF-4 is dependent on PHD3-mediated hydroxylation. The here presented data: hypoxia/DMOG leading to enhanced ATF-4 protein levels; reduction of PHD3 expression resulting in elevated ATF-4 abundance even in normoxia; unchanged ATF-4 mRNA levels in hypoxia; identification of an ODD domain which contains 5 prolyl residues in the ATF-4 protein sequence and decreased ubiquitination of ATF-4 under hypoxic conditions point to a PHD3-mediated hydroxylation-dependent regulation of ATF-4 degradation under normoxic conditions.

4.4 The E3 ubiquitin ligase, which is responsible for the normoxic degradation of ATF-4 is unknown

Many similarities in the regulation of ATF-4 and HIF-α protein stability under normoxic conditions were observed in the presented work. Contrary to HIF-α however, ATF-4 is not a target of pVHL-mediated ubiquitination (Figure 3.17).

Furthermore, the SCF E3 ubiquitin ligase β-TRCP, which has been reported to interact with ATF-4 (Lassot et al., 2001), is not involved in regulating the normoxic degradation of ATF-4 (Figure 3.18). Silencing β-TRCP expression by siRNA under normoxic conditions did not result in accumulation of ATF-4 (see Fig. 3.22). Additionally, the interaction of ATF-4 with β-TRCP is independent of PHD3 activity (see Fig. 3.19) and no interaction was observed between PHD3 and β-TRCP (see Fig. 3.20 and 3.21), indicating that β-TRCP and PHD3 are part of two different pathways regulating ATF-4 stability and activity. β-TRCP mediates the degradation of factors involved in signal transduction pathways and cell cycle progression like the inhibitor of nuclear factor-κB (IκB) or β-catenin. These known β-TRCP targets harbour the DSGXXS destruction motif (Megy et al., 2005; Yaron et al., 1997), similar to the DSGXXXS motif found in the ATF-4 sequence (Lassot et al., 2001).

The interaction of β-TRCP with its substrates requires the phosphorylation of serine residues within the DSGXXS motif. For ATF-4 the phosphorylation of the serine residue 219 within the DSGXXXS motif has been shown to be crucial for the interaction with β-TRCP, but until now the responsible kinase was not discovered.

These presented data suggest that ATF-4 ubiquitination is mediated by more than just one E3 ubiquitin ligase. The ubiquitination could be regulated by different stimuli. One could suggest that the phosphorylation-dependent ubiquitination of ATF-4 is mediated via β-TRCP whereas the normoxic presumably prolyl hydroxylation-dependent ubiquitination is accomplished by another so far unknown E3 ubiquitin ligase. ATF-4 is not the only protein known to be

stimuli-dependently regulated by different E3 ubiquitin ligases. In addition to the prolyl hydroxylation-dependent degradation via pVHL, HIF-1α is also oxygen-independently degraded via the receptor for activated C-kinase 1 (RACK1). RACK1 functions as a multi-functional scaffolding protein and links HIF-1α to Elongin-C, which is presumed to recruit the other members of the SCF ubiquitin ligase complex resulting in the degradation of HIF-1α (Liu et al., 2007). The spermidine/spermine N-acetyltransferase-1 is crucial for the interaction of RACK1 and HIF-1α (Baek et al., 2007).

A stimuli-dependent ubiquitination has also been described for the transcriptional co-activator of the canonical Wnt signal transduction pathway, β-catenin. The Wnt-β-catenin pathway is involved in regulating cell fate and proliferation. Besides phosphorylation-dependent ubiquitination mediated by β-TRCP in the absence of a Wnt ligand (Wu et al., 2003), β-catenin is also ubiquitinated in its phosphorylated and dephosphorylated state by the E3 ligases JADE-1 and pVHL (Chitalia et al., 2008). This allows a tight regulation of β-catenin protein levels in Wnt-on and Wnt-off phase.

To date over 500 different E3 ubiquitin ligases are proposed to exist in the human genome until date, which can be classified into two major classes based on the different mechanisms to transfer ubiquitin to the substrate. The HECT (homologous to E6AP C-terminus) domain E3 ligases contain a conserved active site cysteine residue near the C-terminus which forms the thioester intermediate with ubiquitin. Their variable N-terminal region is responsible for the substrate recognition. β-TRCP belongs to the RING- (really interesting new gene) type E3 ubiquitin ligase class. This class mediates the direct transfer of ubiquitin from the E2 ubiquitin conjugating enzyme to the substrate (Petroski, 2008; Sun, 2006). The SCF (SKP-Cullin-F-box) complex E3 ubiquitin ligases are the best studied member of the RING-type E3 ubiquitin ligases. Until now about 70 F-box proteins are known to interact with SKP1, which functions as scaffold of the SCF-ligase, in mammals (Schulman et al., 2000).

Most likely the unknown E3 ubiquitin ligase, responsible for the normoxic degradation of ATF-4, does not belong to the SCF E3 ubiquitin ligase family, since silencing of SKP1 expression by siRNA showed no influence on ATF-4 stability under normoxic conditions (Figure 3.23). Further studies will be needed to identify the corresponding E3 ligase involved in the normoxic degradation of ATF-4. The use of an E3 ubiquitin ligase siRNA library might be useful to identify the unknown E3 ligase.

4.5 Stabilized ATF-4 is involved in regulation of cell fate decision

The response to different stress conditions like amino acid deprivation or oxidative stress is tightly controlled by a number of stress-responsive transcription factors. Among these transcription factors ATF-4 has a key function.

ATF-4 has been shown to act as pro-death transcription factor as well as pro-survival transcription factor mediating cell survival under different stress conditions. In fibroblasts ATF-4 is essential for a successful response to ER-stress, amino acid starvation or exposure to oxidants (Harding et al., 2003). In line, knockdown of ATF-4 in neurons leads to smaller infarct areals and to a decrease in oxidative stress-induced cell death (Lange et al., 2008). ATF-4 has also been reported to play a role in activating autophagy via upregulation of microtuble-associated protein 1 light chain 3B expression in response to the antitumor agent Bortezomib. The induction of autophagy in tumor cells is thought to be a mechanism for resistance to antitumor agents (Milani et al., 2009).

The expression of several genes is increased by ER or oxidative stress via ATF-4. One of these ATF-4 target genes is the transcription factor GADD153, a member of the C/EBP family. GADD153 deficient mice show a decreased sensitivity to ER stress-induced apoptosis (Zinszner et al., 1998). Elevated GADD153 expression has been shown to lead to enhanced apoptosis of β-cells during ER stress-mediated diabetes (Oyadomari et al., 2002). This might be explained by a decrease in expression of the anti-apoptotic protein Bcl2 which consequently leads to an increased sensitivity to ER stress (McCullough et al., 2001). Additionally, GADD153 regulates the translocation of the Bax protein from the cytosol to mitochondria resulting in the release of pro-apoptotic molecules from the mitochondrial intermembrane space into the cytosol, where the apoptotic cascade is initiated (Gotoh et al., 2004). Finally, GADD153 induces cell cycle arrest in nutritional deprived cells (Barone et al., 1994). Besides the regulation by ER stress, GADD153 expression was also found to be upregulated under hypoxic conditions and in anoxia in a HIF-1-independent manner (Ameri et al., 2004; Carmeliet et al., 1998).

This hypoxic induction of GADD153 appears to be mediated by ATF-4. Silencing ATF-4 mRNA expression under hypoxic conditions abolished the expression of GADD153 (Figure 3.25). The expression seems to be linked to the oxygen sensor PHD3. Stabilizing ATF-4 by silencing PHD3 mRNA expression resulted in an increased GADD153 expression (Figure 3.26). These observations suggest that PHD3 and oxygen-dependent stabilization of ATF-4 might be involved in regulating cell fate decision.

4.6 Conclusions and outlook

In this presented thesis the protein-interaction of PHD3 with ATF-4 was characterized. The exclusive interaction of ATF-4 with PHD3 was revealed. Studying the ATF-4 abundance showed increased protein levels under hypoxic conditions and after inhibition of PHD activity in a HIF-independent manner. Exposure to hypoxia or silencing PHD3 mRNA expression with siRNA led to a slower degradation rate of the ATF-4 protein. The normoxic destabilisation of ATF-4 was shown to be mediated via PHD3-dependent degradation by the ubiquitin-proteasome system. Exposure of cells to hypoxia led to a decreased ubiquitination of ATF-4 and resulted in enhanced ATF-4 protein levels and transactivation activity.

Within this thesis it was not possible to identify the E3 ubiquitin ligase responsible for the normoxic destabilisation of ATF-4. It was shown that the ubiquitination of ATF-4 is independent of the E3 ubiquitin ligases pVHL and β-TRCP. Further studies will be needed to identify the E3 ubiquitin ligase which is involved in the normoxic degradation of ATF-4 to get a deeper insight into the regulation of ATF-4 and to understand the mechanisms how ATF-4 is involved in regulating cell fate.

A link was found between the hypoxic-stabilization of ATF-4 and cell fate decision. GADD153 was shown to be ATF-4-dependently expressed under hypoxic condition. It would be interesting to further study the connection between PHD3-mediated degradation of ATF-4 and cell fate via a HIF-independent pathway. Although there is an increasing list of hypoxia-inducible HIF-dependent target genes, there are several genes for which a HIF-independent expression under hypoxia has been described. One of theses genes is GADD153. GADD153 induces apoptosis or cell cycle arrest in response to different apoptotic stimuli. Since GADD153 is a well known ATF-4 target gene it would be interesting to further study ATF-4-dependent gene expression in response to changes in oxygen availability. This might help to understand the connection between PHD3-dependent normoxic destabilization of ATF-4 and cell fate decision.

The PHD1-3 enzymes have been identified based on their ability to regulate the stability of HIF-α subunits and thus to modify hypoxia-inducible gene expression. The presented thesis provides insight into a PHD3 isoform-specific HIF-independent regulation of ATF-4. This knowledge is important to deepen the understanding of the cellular oxygen sensing system. Furthermore, it is helpful for the ongoing development of small molecule PHD-inhibitors that are currently tested for the treatment of anaemia and cytoprotection.

5. Literature

Abastado, J.P., P.F. Miller, B.M. Jackson, and A.G. Hinnebusch. 1991. Suppression of ribosomal reinitiation at upstream open reading frames in amino acid-starved cells forms the basis for GCN4 translational control. Mol Cell Biol 11:486-96.

Agani, F., and G.L. Semenza. 1998. Mersalyl is a novel inducer of vascular endothelial growth factor gene expression and hypoxia-inducible factor 1 activity. Mol Pharmacol 54:749-54.

Ameri, K., and A.L. Harris. 2008. Activating transcription factor 4. Int J Biochem Cell Biol 40:14-21.

Ameri, K., C.E. Lewis, M. Raida, H. Sowter, T. Hai, and A.L. Harris. 2004. Anoxic induction of ATF-4 through HIF-1-independent pathways of protein stabilization in human cancer cells. Blood 103:1876-82.

Appelhoff, R.J., Y.M. Tian, R.R. Raval, H. Turley, A.L. Harris, C.W. Pugh, P.J. Ratcliffe, and J.M. Gleadle. 2004. Differential function of the prolyl hydroxylases PHD1, PHD2, and PHD3 in the regulation of hypoxia-inducible factor. J Biol Chem 279:38458-65.

Aprelikova, O., S. Pandolfi, S. Tackett, M. Ferreira, K. Salnikow, Y. Ward, J.I. Risinger, J.C. Barrett, and J. Niederhuber. 2009. Melanoma antigen-11 inhibits the hypoxia-inducible factor prolyl hydroxylase 2 and activates hypoxic response. Cancer Res 69:616-24.

Aragones, J., D.R. Jones, S. Martin, M.A. San Juan, A. Alfranca, F. Vidal, A. Vara, I. Merida, and M.O. Landazuri. 2001. Evidence for the involvement of diacylglycerol kinase in the activation of hypoxia-inducible transcription factor 1 by low oxygen tension. J Biol Chem 276:10548-55.

Arnesen, T., X. Kong, R. Evjenth, D. Gromyko, J.E. Varhaug, Z. Lin, N. Sang, J. Caro, and J.R. Lillehaug. 2005. Interaction between HIF-1α (ODD) and hARD1 does not induce acetylation and destabilization of HIF-1α. FEBS Lett 579:6428-32.

Bae, S.H., J.W. Jeong, J.A. Park, S.H. Kim, M.K. Bae, S.J. Choi, and K.W. Kim. 2004. Sumoylation increases HIF-1α stability and its transcriptional activity. Biochem Biophys Res Commun 324:394-400.

Baek, J.H., Y.V. Liu, K.R. McDonald, J.B. Wesley, H. Zhang, and G.L. Semenza. 2007. Spermidine/spermine N(1)-acetyltransferase-1 binds to hypoxia-inducible factor-1α (HIF-1α) and RACK1 and promotes ubiquitination and degradation of HIF-1α. J Biol Chem 282:33358-66.

Baek, J.H., P.C. Mahon, J. Oh, B. Kelly, B. Krishnamachary, M. Pearson, D.A. Chan, A.J. Giaccia, and G.L. Semenza. 2005. OS-9 interacts with hypoxia-inducible factor 1α and prolyl hydroxylases to promote oxygen-dependent degradation of HIF-1α. Mol Cell 17:503-12.

Barone, M.V., A. Crozat, A. Tabaee, L. Philipson, and D. Ron. 1994. CHOP (GADD153) and its oncogenic variant, TLS-CHOP, have opposing effects on the induction of G1/S arrest. Genes Dev 8:453-64.

Barth, S., J. Nesper, P.A. Hasgall, R. Wirthner, K.J. Nytko, F. Edlich, D.M. Katschinski, D.P. Stiehl, R.H. Wenger, and G. Camenisch. 2007. The peptidyl prolyl cis/trans isomerase FKBP38 determines hypoxia-inducible transcription factor prolyl-4-hydroxylase PHD2 protein stability. Mol Cell Biol 27:3758-68.

Berlanga, J.J., I. Ventoso, H.P. Harding, J. Deng, D. Ron, N. Sonenberg, L. Carrasco, and C. de Haro. 2006. Antiviral effect of the mammalian translation initiation factor 2α kinase GCN2 against RNA viruses. Embo J 25:1730-40.

Bernhardt, W.M., C. Warnecke, C. Willam, T. Tanaka, M.S. Wiesener, and K.U. Eckardt. 2007. Organ protection by hypoxia and hypoxia-inducible factors. Methods Enzymol 435:221-45.

Bernhardt, W.M., V. Campean, S. Kany, J.S. Jurgensen, A. Weidemann, C. Warnecke, M. Arend, S. Klaus, V. Gunzler, K. Amann, C. Willam, M.S. Wiesener, and K.U. Eckardt. 2006. Preconditional activation of hypoxia-inducible factors ameliorates ischemic acute renal failure. J Am Soc Nephrol 17:1970-8.

Berra, E., A. Ginouves, and J. Pouyssegur. 2006. The hypoxia-inducible-factor hydroxylases bring fresh air into hypoxia signalling. EMBO Rep 7:41-5.

Berra, E., D. Roux, D.E. Richard, and J. Pouyssegur. 2001. Hypoxia-inducible factor-1 α (HIF-1 α) escapes O_2-driven proteasomal degradation irrespective of its subcellular localization: nucleus or cytoplasm. EMBO Rep 2:615-20.

Berra, E., E. Benizri, A. Ginouves, V. Volmat, D. Roux, and J. Pouyssegur. 2003. HIF prolyl-hydroxylase 2 is the key oxygen sensor setting low steady-state levels of HIF-1α in normoxia. Embo J 22:4082-90.

Berta, M.A., N. Mazure, M. Hattab, J. Pouyssegur, and M.C. Brahimi-Horn. 2007. SUMOylation of hypoxia-inducible factor-1α reduces its transcriptional activity. Biochem Biophys Res Commun 360:646-52.

Bilton, R., N. Mazure, E. Trottier, M. Hattab, M.A. Dery, D.E. Richard, J. Pouyssegur, and M.C. Brahimi-Horn. 2005. Arrest-defective-1 protein, an acetyltransferase, does not alter stability of hypoxia-inducible factor (HIF)-1α and is not induced by hypoxia or HIF. J Biol Chem 280:31132-40.

Bishop, T., D. Gallagher, A. Pascual, C.A. Lygate, J.P. de Bono, L.G. Nicholls, P. Ortega-Saenz, H. Oster, B. Wijeyekoon, A.I. Sutherland, A. Grosfeld, J. Aragones, M. Schneider, K. van Geyte, D. Teixeira, A. Diez-Juan, J. Lopez-Barneo, K.M. Channon, P.H. Maxwell, C.W. Pugh, A.M. Davies, P. Carmeliet, and P.J. Ratcliffe. 2008. Abnormal sympathoadrenal development and systemic hypotension in PHD3-/- mice. Mol Cell Biol 28:3386-400.

Bruick, R.K. 2000. Expression of the gene encoding the proapoptotic Nip3 protein is induced by hypoxia. Proc Natl Acad Sci U S A 97:9082-7.

Bruick, R.K., and S.L. McKnight. 2001. A conserved family of prolyl-4-hydroxylases that modify HIF. Science 294:1337-40.

Caniggia, I., H. Mostachfi, J. Winter, M. Gassmann, S.J. Lye, M. Kuliszewski, and M. Post. 2000. Hypoxia-inducible factor-1 mediates the biological effects of oxygen on human trophoblast differentiation through TGFβ(3). J Clin Invest 105:577-87.

Cardozo, T., and M. Pagano. 2004. The SCF ubiquitin ligase: insights into a molecular machine. Nat Rev Mol Cell Biol 5:739-51.

Carmeliet, P., Y. Dor, J.M. Herbert, D. Fukumura, K. Brusselmans, M. Dewerchin, M. Neeman, F. Bono, R. Abramovitch, P. Maxwell, C.J. Koch, P. Ratcliffe, L. Moons, R.K. Jain, D. Collen, and E. Keshert. 1998. Role of HIF-1α in hypoxia-mediated apoptosis, cell proliferation and tumour angiogenesis. Nature 394:485-90.

Chan, D.A., P.D. Sutphin, S.E. Yen, and A.J. Giaccia. 2005. Coordinate regulation of the oxygen-dependent degradation domains of hypoxia-inducible factor 1α. Mol Cell Biol 25:6415-26.

Chandel, N.S., E. Maltepe, E. Goldwasser, C.E. Mathieu, M.C. Simon, and P.T. Schumacker. 1998. Mitochondrial reactive oxygen species trigger hypoxia-induced transcription. Proc Natl Acad Sci U S A 95:11715-20.

Chen, J.J. 2007. Regulation of protein synthesis by the heme-regulated eIF2α kinase: relevance to anemias. Blood 109:2693-9.

Chevray, P.M., and D. Nathans. 1992. Protein interaction cloning in yeast: identification of mammalian proteins that react with the leucine zipper of Jun. Proc Natl Acad Sci U S A 89:5789-93.

Chitalia, V.C., R.L. Foy, M.M. Bachschmid, L. Zeng, M.V. Panchenko, M.I. Zhou, A. Bharti, D.C. Seldin, S.H. Lecker, I. Dominguez, and H.T. Cohen. 2008. Jade-1 inhibits Wnt signalling by ubiquitylating β-catenin and mediates Wnt pathway inhibition by pVHL. Nat Cell Biol 10:1208-16.

Choi, Y.K., J.H. Kim, W.J. Kim, H.Y. Lee, J.A. Park, S.W. Lee, D.K. Yoon, H.H. Kim, H. Chung, Y.S. Yu, and K.W. Kim. 2007. AKAP12 regulates human blood-retinal barrier formation by downregulation of hypoxia-inducible factor-1α. J Neurosci 27:4472-81.

Chun, Y.S., J.Y. Hyun, Y.G. Kwak, I.S. Kim, C.H. Kim, E. Choi, M.S. Kim, and J.W. Park. 2003. Hypoxic activation of the atrial natriuretic peptide gene promoter through direct and indirect actions of hypoxia-inducible factor-1. Biochem J 370:149-57.

Cioffi, C.L., X.Q. Liu, P.A. Kosinski, M. Garay, and B.R. Bowen. 2003. Differential regulation of HIF-1 α prolyl-4-hydroxylase genes by hypoxia in human cardiovascular cells. Biochem Biophys Res Commun 303:947-53.

Cockman, M.E., D.E. Lancaster, I.P. Stolze, K.S. Hewitson, M.A. McDonough, M.L. Coleman, C.H. Coles, X. Yu, R.T. Hay, S.C. Ley, C.W. Pugh, N.J. Oldham, N. Masson, C.J. Schofield, and P.J. Ratcliffe. 2006. Posttranslational hydroxylation of ankyrin repeats in IκB proteins by the hypoxia-inducible factor (HIF) asparaginyl hydroxylase, factor inhibiting HIF (FIH). Proc Natl Acad Sci U S A 103:14767-72.

Counts, D.F., G.J. Cardinale, and S. Udenfriend. 1978. Prolyl hydroxylase half reaction: peptidyl prolyl-independent decarboxylation of α-ketoglutarate. Proc Natl Acad Sci U S A 75:2145-9.

Craiu, A., M. Gaczynska, T. Akopian, C.F. Gramm, G. Fenteany, A.L. Goldberg, and K.L. Rock. 1997. Lactacystin and clasto-lactacystin β-lactone modify multiple proteasome β-subunits and inhibit intracellular protein degradation and major histocompatibility complex class I antigen presentation. J Biol Chem 272:13437-45.

Cummins, E.P., E. Berra, K.M. Comerford, A. Ginouves, K.T. Fitzgerald, F. Seeballuck, C. Godson, J.E. Nielsen, P. Moynagh, J. Pouyssegur, and C.T. Taylor. 2006. Prolyl hydroxylase-1 negatively regulates IκB kinase-β, giving insight into hypoxia-induced NFκB activity. Proc Natl Acad Sci U S A 103:18154-9.

Deng, J., H.P. Harding, B. Raught, A.C. Gingras, J.J. Berlanga, D. Scheuner, R.J. Kaufman, D. Ron, and N. Sonenberg. 2002. Activation of GCN2 in UV-irradiated cells inhibits translation. Curr Biol 12:1279-86.

Ding, Q., X. He, J.M. Hsu, W. Xia, C.T. Chen, L.Y. Li, D.F. Lee, J.C. Liu, Q. Zhong, X. Wang, and M.C. Hung. 2007. Degradation of Mcl-1 by β-TrCP mediates glycogen synthase kinase 3-induced tumor suppression and chemosensitization. Mol Cell Biol 27:4006-17.

Ebert, B.L., J.D. Firth, and P.J. Ratcliffe. 1995. Hypoxia and mitochondrial inhibitors regulate expression of glucose transporter-1 via distinct Cis-acting sequences. J Biol Chem 270:29083-9.

Elefteriou, F., M.D. Benson, H. Sowa, M. Starbuck, X. Liu, D. Ron, L.F. Parada, and G. Karsenty. 2006. ATF4 mediation of NF1 functions in osteoblast reveals a nutritional basis for congenital skeletal dysplasiae. Cell Metab 4:441-51.

Ema, M., S. Taya, N. Yokotani, K. Sogawa, Y. Matsuda, and Y. Fujii-Kuriyama. 1997. A novel bHLH-PAS factor with close sequence similarity to hypoxia-inducible factor 1α regulates the VEGF expression and is potentially involved in lung and vascular development. Proc Natl Acad Sci U S A 94:4273-8.

Epstein, A.C., J.M. Gleadle, L.A. McNeill, K.S. Hewitson, J. O'Rourke, D.R. Mole, M. Mukherji, E. Metzen, M.I. Wilson, A. Dhanda, Y.M. Tian, N. Masson, D.L. Hamilton, P. Jaakkola, R. Barstead, J. Hodgkin, P.H. Maxwell, C.W. Pugh, C.J. Schofield, and P.J. Ratcliffe. 2001. *C. elegans* EGL-9 and mammalian homologs define a family of dioxygenases that regulate HIF by prolyl hydroxylation. Cell 107:43-54.

Fedulova, N., J. Hanrieder, J. Bergquist, and L.O. Emren. 2007. Expression and purification of catalytically active human PHD3 in *Escherichia coli*. Protein Expr Purif 54:1-10.

Feldman, D.E., V. Thulasiraman, R.G. Ferreyra, and J. Frydman. 1999. Formation of the VHL-elongin BC tumor suppressor complex is mediated by the chaperonin TRiC. Mol Cell 4:1051-61.

Fenteany, G., R.F. Standaert, W.S. Lane, S. Choi, E.J. Corey, and S.L. Schreiber. 1995. Inhibition of proteasome activities and subunit-specific amino-terminal threonine modification by lactacystin. Science 268:726-31.

Firth, J.D., B.L. Ebert, C.W. Pugh, and P.J. Ratcliffe. 1994. Oxygen-regulated control elements in the phosphoglycerate kinase 1 and lactate dehydrogenase A genes: similarities with the erythropoietin 3' enhancer. Proc Natl Acad Sci U S A 91:6496-500.

Flamme, I., T. Frohlich, M. von Reutern, A. Kappel, A. Damert, and W. Risau. 1997. HRF, a putative basic helix-loop-helix-PAS-domain transcription factor is closely related to hypoxia-inducible factor-1 α and developmentally expressed in blood vessels. Mech Dev 63:51-60.

Forsythe, J.A., B.H. Jiang, N.V. Iyer, F. Agani, S.W. Leung, R.D. Koos, and G.L. Semenza. 1996. Activation of vascular endothelial growth factor gene transcription by hypoxia-inducible factor 1. Mol Cell Biol 16:4604-13.

Fu, J., K. Menzies, R.S. Freeman, and M.B. Taubman. 2007. EGLN3 prolyl hydroxylase regulates skeletal muscle differentiation and myogenin protein stability. J Biol Chem 282:12410-8.

Gachon, F., C. Devaux, and J.M. Mesnard. 2002. Activation of HTLV-I transcription in the presence of Tax is independent of the acetylation of CREB-2 (ATF-4). Virology 299:271-8.

Garcia, M.A., J. Gil, I. Ventoso, S. Guerra, E. Domingo, C. Rivas, and M. Esteban. 2006. Impact of protein kinase PKR in cell biology: from antiviral to antiproliferative action. Microbiol Mol Biol Rev 70:1032-60.

Gerald, D., E. Berra, Y.M. Frapart, D.A. Chan, A.J. Giaccia, D. Mansuy, J. Pouyssegur, M. Yaniv, and F. Mechta-Grigoriou. 2004. JunD reduces tumor angiogenesis by protecting cells from oxidative stress. Cell 118:781-94.

Gerber, H.P., F. Condorelli, J. Park, and N. Ferrara. 1997. Differential transcriptional regulation of the two vascular endothelial growth factor receptor genes. Flt-1, but not Flk-1/KDR, is up-regulated by hypoxia. J Biol Chem 272:23659-67.

Glickman, M.H., and A. Ciechanover. 2002. The ubiquitin-proteasome proteolytic pathway: destruction for the sake of construction. Physiol Rev 82:373-428.

Goldberg, M.A., S.P. Dunning, and H.F. Bunn. 1988. Regulation of the erythropoietin gene: evidence that the oxygen sensor is a heme protein. Science 242:1412-5.

Gotoh, T., K. Terada, S. Oyadomari, and M. Mori. 2004. hsp70-DnaJ chaperone pair prevents nitric oxide- and CHOP-induced apoptosis by inhibiting translocation of Bax to mitochondria. Cell Death Differ 11:390-402.

Gradin, K., C. Takasaki, Y. Fujii-Kuriyama, and K. Sogawa. 2002. The transcriptional activation function of the HIF-like factor requires phosphorylation at a conserved threonine. J Biol Chem 277:23508-14.

Gu, Y.Z., S.M. Moran, J.B. Hogenesch, L. Wartman, and C.A. Bradfield. 1998. Molecular characterization and chromosomal localization of a third α-class hypoxia inducible factor subunit, HIF3α. Gene Expr 7:205-13.

Guzy, R.D., B. Hoyos, E. Robin, H. Chen, L. Liu, K.D. Mansfield, M.C. Simon, U. Hammerling, and P.T. Schumacker. 2005. Mitochondrial complex III is required for hypoxia-induced ROS production and cellular oxygen sensing. Cell Metab 1:401-8.

Hai, T., C.D. Wolfgang, D.K. Marsee, A.E. Allen, and U. Sivaprasad. 1999. ATF3 and stress responses. Gene Expr 7:321-35.

Harding, H.P., Y. Zhang, and D. Ron. 1999. Protein translation and folding are coupled by an endoplasmic-reticulum-resident kinase. Nature 397:271-4.

Harding, H.P., I. Novoa, Y. Zhang, H. Zeng, R. Wek, M. Schapira, and D. Ron. 2000. Regulated translation initiation controls stress-induced gene expression in mammalian cells. Mol Cell 6:1099-108.

Harding, H.P., Y. Zhang, H. Zeng, I. Novoa, P.D. Lu, M. Calfon, N. Sadri, C. Yun, B. Popko, R. Paules, D.F. Stojdl, J.C. Bell, T. Hettmann, J.M. Leiden, and D. Ron. 2003. An integrated stress response regulates amino acid metabolism and resistance to oxidative stress. Mol Cell 11:619-33.

He, C.H., P. Gong, B. Hu, D. Stewart, M.E. Choi, A.M. Choi, and J. Alam. 2001. Identification of activating transcription factor 4 (ATF4) as an Nrf2-interacting protein. Implication for heme oxygenase-1 gene regulation. J Biol Chem 276:20858-65.

Hinnebusch, A.G. 2005. Translational regulation of GCN4 and the general amino acid control of yeast. Annu Rev Microbiol 59:407-50.

Hirsila, M., P. Koivunen, V. Gunzler, K.I. Kivirikko, and J. Myllyharju. 2003. Characterization of the human prolyl 4-hydroxylases that modify the hypoxia-inducible factor. J Biol Chem 278:30772-80.

Hogenesch, J.B., W.K. Chan, V.H. Jackiw, R.C. Brown, Y.Z. Gu, M. Pray-Grant, G.H. Perdew, and C.A. Bradfield. 1997. Characterization of a subset of the basic-helix-loop-helix-PAS superfamily that interacts with components of the dioxin signaling pathway. J Biol Chem 272:8581-93.

Hopfer, U., H. Hopfer, K. Jablonski, R.A. Stahl, and G. Wolf. 2006. The novel WD-repeat protein Morg1 acts as a molecular scaffold for hypoxia-inducible factor prolyl hydroxylase 3 (PHD3). J Biol Chem 281:8645-55.

Hopfl, G., R.H. Wenger, U. Ziegler, T. Stallmach, O. Gardelle, R. Achermann, M. Wergin, B. Kaser-Hotz, H.M. Saunders, K.J. Williams, I.J. Stratford, M. Gassmann, and I. Desbaillets. 2002. Rescue of hypoxia-inducible factor-1α-deficient tumor growth by wild-type cells is independent of vascular endothelial growth factor. Cancer Res 62:2962-70.

Hsieh, M.M., N.S. Linde, A. Wynter, M. Metzger, C. Wong, I. Langsetmo, A. Lin, R. Smith, G.P. Rodgers, R.E. Donahue, S.J. Klaus, and J.F. Tisdale. 2007. HIF prolyl hydroxylase inhibition results in endogenous erythropoietin induction, erythrocytosis, and modest fetal hemoglobin expression in rhesus macaques. Blood 110:2140-7.

Huang, J., Q. Zhao, S.M. Mooney, and F.S. Lee. 2002. Sequence determinants in hypoxia-inducible factor-1α for hydroxylation by the prolyl hydroxylases PHD1, PHD2, and PHD3. J Biol Chem 277:39792-800.

Huang, L.E., J. Gu, M. Schau, and H.F. Bunn. 1998. Regulation of hypoxia-inducible factor 1α is mediated by an O_2-dependent degradation domain via the ubiquitin-proteasome pathway. Proc Natl Acad Sci U S A 95:7987-92.

Ivan, M., K. Kondo, H. Yang, W. Kim, J. Valiando, M. Ohh, A. Salic, J.M. Asara, W.S. Lane, and W.G. Kaelin, Jr. 2001. HIFalpha targeted for VHL-mediated destruction by proline hydroxylation: implications for O2 sensing. Science 292:464-8.

Iyer, N.V., L.E. Kotch, F. Agani, S.W. Leung, E. Laughner, R.H. Wenger, M. Gassmann, J.D. Gearhart, A.M. Lawler, A.Y. Yu, and G.L. Semenza. 1998. Cellular and developmental control of O_2 homeostasis by hypoxia-inducible factor 1 α. Genes Dev 12:149-62.

Jaakkola, P., D.R. Mole, Y.M. Tian, M.I. Wilson, J. Gielbert, S.J. Gaskell, A. Kriegsheim, H.F. Hebestreit, M. Mukherji, C.J. Schofield, P.H. Maxwell, C.W. Pugh, and P.J. Ratcliffe. 2001. Targeting of HIF-α to the von Hippel-Lindau ubiquitylation complex by O_2-regulated prolyl hydroxylation. Science 292:468-72.

Jeong, J.W., M.K. Bae, M.Y. Ahn, S.H. Kim, T.K. Sohn, M.H. Bae, M.A. Yoo, E.J. Song, K.J. Lee, and K.W. Kim. 2002. Regulation and destabilization of HIF-1α by ARD1-mediated acetylation. Cell 111:709-20.

Jiang, B.H., J.Z. Zheng, S.W. Leung, R. Roe, and G.L. Semenza. 1997. Transactivation and inhibitory domains of hypoxia-inducible factor 1α. Modulation of transcriptional activity by oxygen tension. J Biol Chem 272:19253-60.

Jiang, H.Y., and R.C. Wek. 2005. Phosphorylation of the α-subunit of the eukaryotic initiation factor-2 (eIF2α) reduces protein synthesis and enhances apoptosis in response to proteasome inhibition. J Biol Chem 280:14189-202.

Kallio, P.J., K. Okamoto, S. O'Brien, P. Carrero, Y. Makino, H. Tanaka, and L. Poellinger. 1998. Signal transduction in hypoxic cells: inducible nuclear translocation and recruitment of the CBP/p300 coactivator by the hypoxia-inducible factor-1α. Embo J 17:6573-86.

Katschinski, D.M. 2009. In vivo functions of the prolyl-4-hydroxylase domain oxygen sensors: direct route to the treatment of anaemia and the protection of ischaemic tissues. Acta Physiol (Oxf) 195:407-14.

Kim, R., M. Emi, K. Tanabe, and S. Murakami. 2006. Role of the unfolded protein response in cell death. Apoptosis 11:5-13.

Köditz, J., J. Nesper, M. Wottawa, D.P. Stiehl, G. Camenisch, C. Franke, J. Myllyharju, R.H. Wenger, and D.M. Katschinski. 2007. Oxygen-dependent ATF-4 stability is mediated by the PHD3 oxygen sensor. Blood 110:3610-7.

Lancaster, D.E., L.A. McNeill, M.A. McDonough, R.T. Aplin, K.S. Hewitson, C.W. Pugh, P.J. Ratcliffe, and C.J. Schofield. 2004. Disruption of dimerization and substrate phosphorylation inhibit factor inhibiting hypoxia-inducible factor (FIH) activity. Biochem J 383:429-37.

Lando, D., D.J. Peet, J.J. Gorman, D.A. Whelan, M.L. Whitelaw, and R.K. Bruick. 2002. FIH-1 is an asparaginyl hydroxylase enzyme that regulates the transcriptional activity of hypoxia-inducible factor. Genes Dev 16:1466-71.

Lange, P.S., J.C. Chavez, J.T. Pinto, G. Coppola, C.W. Sun, T.M. Townes, D.H. Geschwind, and R.R. Ratan. 2008. ATF4 is an oxidative stress-inducible, prodeath transcription factor in neurons *in vitro* and *in vivo*. J Exp Med 205:1227-42.

Lassot, I., E. Estrabaud, S. Emiliani, M. Benkirane, R. Benarous, and F. Margottin-Goguet. 2005. p300 modulates ATF4 stability and transcriptional activity independently of its acetyltransferase domain. J Biol Chem 280:41537-45.

Lassot, I., E. Segeral, C. Berlioz-Torrent, H. Durand, L. Groussin, T. Hai, R. Benarous, and F. Margottin-Goguet. 2001. ATF4 degradation relies on a phosphorylation-dependent interaction with the SCF(βTrCP) ubiquitin ligase. Mol Cell Biol 21:2192-202.

Le, N.T., and D.R. Richardson. 2002. The role of iron in cell cycle progression and the proliferation of neoplastic cells. Biochim Biophys Acta 1603:31-46.

Lebkowski, J.S., S. Clancy, and M.P. Calos. 1985. Simian virus 40 replication in adenovirus-transformed human cells antagonizes gene expression. Nature 317:169-71.

Lee, Y.Y., R.C. Cevallos, and E. Jan. 2009. An upstream open reading frame regulates translation of GADD34 during cellular stresses that induce eIF2α phosphorylation. J Biol Chem 284:6661-73.

Li, F., Z.Z. Chong, and K. Maiese. 2004. Erythropoietin on a tightrope: balancing neuronal and vascular protection between intrinsic and extrinsic pathways. Neurosignals 13:265-89.

Lieb, M.E., K. Menzies, M.C. Moschella, R. Ni, and M.B. Taubman. 2002. Mammalian EGLN genes have distinct patterns of mRNA expression and regulation. Biochem Cell Biol 80:421-6.

Liu, J., J.D. Farmer, Jr., W.S. Lane, J. Friedman, I. Weissman, and S.L. Schreiber. 1991. Calcineurin is a common target of cyclophilin-cyclosporin A and FKBP-FK506 complexes. Cell 66:807-15.

Liu, Y., S.R. Cox, T. Morita, and S. Kourembanas. 1995. Hypoxia regulates vascular endothelial growth factor gene expression in endothelial cells. Identification of a 5' enhancer. Circ Res 77:638-43.

Liu, Y.V., J.H. Baek, H. Zhang, R. Diez, R.N. Cole, and G.L. Semenza. 2007. RACK1 competes with HSP90 for binding to HIF-1α and is required for O_2-independent and HSP90 inhibitor-induced degradation of HIF-1α. Mol Cell 25:207-17.

Lok, C.N., and P. Ponka. 1999. Identification of a hypoxia response element in the transferrin receptor gene. J Biol Chem 274:24147-52.

Lopez-Barneo, J., R. Pardal, and P. Ortega-Saenz. 2001. Cellular mechanism of oxygen sensing. Annu Rev Physiol 63:259-87.

Luo, Y., C. Jiang, A.J. Belanger, G.Y. Akita, S.C. Wadsworth, R.J. Gregory, and K.A. Vincent. 2006. A constitutively active hypoxia-inducible factor-1α/VP16 hybrid factor activates expression of the human B-type natriuretic peptide gene. Mol Pharmacol 69:1953-62.

Mahon, P.C., K. Hirota, and G.L. Semenza. 2001. FIH-1: a novel protein that interacts with HIF-1α and VHL to mediate repression of HIF-1 transcriptional activity. Genes Dev 15:2675-86.

Makino, Y., R. Uenishi, K. Okamoto, T. Isoe, O. Hosono, H. Tanaka, A. Kanopka, L. Poellinger, M. Haneda, and C. Morimoto. 2007. Transcriptional up-regulation of inhibitory PAS domain protein gene expression by hypoxia-inducible factor 1 (HIF-1): a negative feedback regulatory circuit in HIF-1-mediated signaling in hypoxic cells. J Biol Chem 282:14073-82.

Mansfield, K.D., R.D. Guzy, Y. Pan, R.M. Young, T.P. Cash, P.T. Schumacker, and M.C. Simon. 2005. Mitochondrial dysfunction resulting from loss of cytochrome c impairs cellular oxygen sensing and hypoxic HIF-α activation. Cell Metab 1:393-9.

Marxsen, J.H., P. Stengel, K. Doege, P. Heikkinen, T. Jokilehto, T. Wagner, W. Jelkmann, P. Jaakkola, and E. Metzen. 2004. Hypoxia-inducible factor-1 (HIF-1) promotes its degradation by induction of HIF-α-prolyl-4-hydroxylases. Biochem J 381:761-7.

Masson, N., R.J. Appelhoff, J.R. Tuckerman, Y.M. Tian, H. Demol, M. Puype, J. Vandekerckhove, P.J. Ratcliffe, and C.W. Pugh. 2004. The HIF prolyl hydroxylase PHD3 is a potential substrate of the TRiC chaperonin. FEBS Lett 570:166-70.

Masuoka, H.C., and T.M. Townes. 2002. Targeted disruption of the activating transcription factor 4 gene results in severe fetal anemia in mice. Blood 99:736-45.

Maxwell, P.H., M.S. Wiesener, G.W. Chang, S.C. Clifford, E.C. Vaux, M.E. Cockman, C.C. Wykoff, C.W. Pugh, E.R. Maher, and P.J. Ratcliffe. 1999. The tumour suppressor protein VHL targets hypoxia-inducible factors for oxygen-dependent proteolysis. Nature 399:271-5.

Mazure, N.M., M.C. Brahimi-Horn, M.A. Berta, E. Benizri, R.L. Bilton, F. Dayan, A. Ginouves, E. Berra, and J. Pouyssegur. 2004. HIF-1: master and commander of the hypoxic world. A pharmacological approach to its regulation by siRNAs. Biochem Pharmacol 68:971-80.

McCullough, K.D., J.L. Martindale, L.O. Klotz, T.Y. Aw, and N.J. Holbrook. 2001. Gadd153 sensitizes cells to endoplasmic reticulum stress by down-regulating Bcl2 and perturbing the cellular redox state. Mol Cell Biol 21:1249-59.

McDonough, M.A., V. Li, E. Flashman, R. Chowdhury, C. Mohr, B.M. Lienard, J. Zondlo, N.J. Oldham, I.J. Clifton, J. Lewis, L.A. McNeill, R.J. Kurzeja, K.S. Hewitson, E. Yang, S. Jordan, R.S. Syed, and C.J. Schofield. 2006. Cellular oxygen sensing: Crystal structure of hypoxia-inducible factor prolyl hydroxylase (PHD2). Proc Natl Acad Sci U S A 103:9814-9.

Megy, S., G. Bertho, J. Gharbi-Benarous, F. Baleux, R. Benarous, and J.P. Girault. 2005. Solution structure of a peptide derived from the oncogenic protein β-Catenin in its phosphorylated and nonphosphorylated states. Peptides 26:227-41.

Melillo, G., T. Musso, A. Sica, L.S. Taylor, G.W. Cox, and L. Varesio. 1995. A hypoxia-responsive element mediates a novel pathway of activation of the inducible nitric oxide synthase promoter. J Exp Med 182:1683-93.

Metzen, E., D.P. Stiehl, K. Doege, J.H. Marxsen, T. Hellwig-Burgel, and W. Jelkmann. 2005. Regulation of the prolyl hydroxylase domain protein 2 (*phd*2/*egln*-1) gene: identification of a functional hypoxia-responsive element. Biochem J 387:711-7.

Metzen, E., U. Berchner-Pfannschmidt, P. Stengel, J.H. Marxsen, I. Stolze, M. Klinger, W.Q. Huang, C. Wotzlaw, T. Hellwig-Burgel, W. Jelkmann, H. Acker, and J. Fandrey. 2003. Intracellular localisation of human HIF-1 α hydroxylases: implications for oxygen sensing. J Cell Sci 116:1319-26.

Mikhaylova, O., M.L. Ignacak, T.J. Barankiewicz, S.V. Harbaugh, Y. Yi, P.H. Maxwell, M. Schneider, K. Van Geyte, P. Carmeliet, M.P. Revelo, M. Wyder, K.D. Greis, J. Meller, and M.F. Czyzyk-Krzeska. 2008. The von Hippel-Lindau tumor suppressor protein and Egl-9-Type proline hydroxylases regulate the large subunit of RNA polymerase II in response to oxidative stress. Mol Cell Biol 28:2701-17.

Milani, M., T. Rzymski, H.R. Mellor, L. Pike, A. Bottini, D. Generali, and A.L. Harris. 2009. The role of ATF4 stabilization and autophagy in resistance of breast cancer cells treated with Bortezomib. Cancer Res 69:4415-23.

Monney, L., I. Otter, R. Olivier, H.L. Ozer, A.L. Haas, S. Omura, and C. Borner. 1998. Defects in the ubiquitin pathway induce caspase-independent apoptosis blocked by Bcl-2. J Biol Chem 273:6121-31.

Mylonis, I., G. Chachami, M. Samiotaki, G. Panayotou, E. Paraskeva, A. Kalousi, E. Georgatsou, S. Bonanou, and G. Simos. 2006. Identification of MAPK phosphorylation sites and their role in the localization and activity of hypoxia-inducible factor-1α. J Biol Chem 281:33095-106.

Nakayama, K., S. Gazdoiu, R. Abraham, Z.Q. Pan, and Z. Ronai. 2007. Hypoxia-induced assembly of prolyl hydroxylase PHD3 into complexes: implications for its activity and susceptibility for degradation by the E3 ligase Siah2. Biochem J 401:217-26.

Nakayama, K., I.J. Frew, M. Hagensen, M. Skals, H. Habelhah, A. Bhoumik, T. Kadoya, H. Erdjument-Bromage, P. Tempst, P.B. Frappell, D.D. Bowtell, and Z. Ronai. 2004. Siah2 regulates stability of prolyl-hydroxylases, controls HIF1alpha abundance, and modulates physiological responses to hypoxia. Cell 117:941-52.

Nakayama, K.I., and K. Nakayama. 2005. Regulation of the cell cycle by SCF-type ubiquitin ligases. Semin Cell Dev Biol 16:323-33.

Nietfeld, J.J., and A. Kemp. 1981. The function of ascorbate with respect to prolyl 4-hydroxylase activity. Biochim Biophys Acta 657:159-67.

Novoa, I., H. Zeng, H.P. Harding, and D. Ron. 2001. Feedback inhibition of the unfolded protein response by GADD34-mediated dephosphorylation of eIF2alpha. J Cell Biol 153:1011-22.

Oehme, F., W. Jonghaus, L. Narouz-Ott, J. Huetter, and I. Flamme. 2004. A nonradioactive 96-well plate assay for the detection of hypoxia-inducible factor prolyl hydroxylase activity. Anal Biochem 330:74-80.

Oehme, F., P. Ellinghaus, P. Kolkhof, T.J. Smith, S. Ramakrishnan, J. Hutter, M. Schramm, and I. Flamme. 2002. Overexpression of PH-4, a novel putative proline 4-hydroxylase, modulates activity of hypoxia-inducible transcription factors. Biochem Biophys Res Commun 296:343-9.

Ord, D., and T. Ord. 2003. Mouse NIPK interacts with ATF4 and affects its transcriptional activity. Exp Cell Res 286:308-20.

Oyadomari, S., A. Koizumi, K. Takeda, T. Gotoh, S. Akira, E. Araki, and M. Mori. 2002. Targeted disruption of the Chop gene delays endoplasmic reticulum stress-mediated diabetes. J Clin Invest 109:525-32.

Ozer, A., L.C. Wu, and R.K. Bruick. 2005. The candidate tumor suppressor ING4 represses activation of the hypoxia inducible factor (HIF). Proc Natl Acad Sci U S A 102:7481-6.

Pan, Y., K.D. Mansfield, C.C. Bertozzi, V. Rudenko, D.A. Chan, A.J. Giaccia, and M.C. Simon. 2007. Multiple factors affecting cellular redox status and energy metabolism modulate hypoxia-inducible factor prolyl hydroxylase activity in vivo and in vitro. Mol Cell Biol 27:912-25.

Pescador, N., Y. Cuevas, S. Naranjo, M. Alcaide, D. Villar, M.O. Landazuri, and L. Del Peso. 2005. Identification of a functional hypoxia-responsive element that regulates the expression of the egl nine homologue 3 (*egln3*/*phd3*) gene. Biochem J 390:189-97.

Petroski, M.D. 2008. The ubiquitin system, disease, and drug discovery. BMC Biochem 9 Suppl 1:S7.

Pugh, C.W., J.F. O'Rourke, M. Nagao, J.M. Gleadle, and P.J. Ratcliffe. 1997. Activation of hypoxia-inducible factor-1; definition of regulatory domains within the α subunit. J Biol Chem 272:11205-14.

Rechsteiner, M., and S.W. Rogers. 1996. PEST sequences and regulation by proteolysis. Trends Biochem Sci 21:267-71.

Richard, D.E., E. Berra, E. Gothie, D. Roux, and J. Pouyssegur. 1999. p42/p44 mitogen-activated protein kinases phosphorylate hypoxia-inducible factor 1α (HIF-1α) and enhance the transcriptional activity of HIF-1. J Biol Chem 274:32631-7.

Rock, K.L., C. Gramm, L. Rothstein, K. Clark, R. Stein, L. Dick, D. Hwang, and A.L. Goldberg. 1994. Inhibitors of the proteasome block the degradation of most cell proteins and the generation of peptides presented on MHC class I molecules. Cell 78:761-71.

Rolfs, A., I. Kvietikova, M. Gassmann, and R.H. Wenger. 1997. Oxygen-regulated transferrin expression is mediated by hypoxia-inducible factor-1. J Biol Chem 272:20055-62.

Roybal, C.N., L.A. Hunsaker, O. Barbash, D.L. Vander Jagt, and S.F. Abcouwer. 2005. The oxidative stressor arsenite activates vascular endothelial growth factor mRNA transcription by an ATF4-dependent mechanism. J Biol Chem 280:20331-9.

Rutkowski, D.T., and R.J. Kaufman. 2003. All roads lead to ATF4. Dev Cell 4:442-4.

Ryan, H.E., J. Lo, and R.S. Johnson. 1998. HIF-1 α is required for solid tumor formation and embryonic vascularization. Embo J 17:3005-15.

Salnikow, K., S.P. Donald, R.K. Bruick, A. Zhitkovich, J.M. Phang, and K.S. Kasprzak. 2004. Depletion of intracellular ascorbate by the carcinogenic metals nickel and cobalt results in the induction of hypoxic stress. J Biol Chem 279:40337-44.

Sambrook, J., P. MacCallum, and D. Russell. 2000. Molecular Cloning: A Laboratory Manual. Cold Spring Harbor Laboratory Press.

Schlisio, S., R.S. Kenchappa, L.C. Vredeveld, R.E. George, R. Stewart, H. Greulich, K. Shahriari, N.V. Nguyen, P. Pigny, P.L. Dahia, S.L. Pomeroy, J.M. Maris, A.T. Look, M. Meyerson, D.S. Peeper, B.D. Carter, and W.G. Kaelin, Jr. 2008. The kinesin KIF1B*b* acts downstream from EglN3 to induce apoptosis and is a potential 1p36 tumor suppressor. Genes Dev 22:884-93.

Schulman, B.A., A.C. Carrano, P.D. Jeffrey, Z. Bowen, E.R. Kinnucan, M.S. Finnin, S.J. Elledge, J.W. Harper, M. Pagano, and N.P. Pavletich. 2000. Insights into SCF ubiquitin ligases from the structure of the Skp1-Skp2 complex. Nature 408:381-6.

Semenza, G.L. 1998. Hypoxia-inducible factor 1: master regulator of O2 homeostasis. Curr Opin Genet Dev 8:588-94.

Semenza, G.L., P.H. Roth, H.M. Fang, and G.L. Wang. 1994. Transcriptional regulation of genes encoding glycolytic enzymes by hypoxia-inducible factor 1. J Biol Chem 269:23757-63.

Semenza, G.L., B.H. Jiang, S.W. Leung, R. Passantino, J.P. Concordet, P. Maire, and A. Giallongo. 1996. Hypoxia response elements in the aldolase A, enolase 1, and lactate dehydrogenase A gene promoters contain essential binding sites for hypoxia-inducible factor 1. J Biol Chem 271:32529-37.

Seth, P., I. Krop, D. Porter, and K. Polyak. 2002. Novel estrogen and tamoxifen induced genes identified by SAGE (Serial Analysis of Gene Expression). Oncogene 21:836-43.

Shemer, R., A. Meimoun, T. Holtzman, and D. Kornitzer. 2002. Regulation of the transcription factor Gcn4 by Pho85 cyclin PCL5. Mol Cell Biol 22:5395-404.

Siu, F., P.J. Bain, R. LeBlanc-Chaffin, H. Chen, and M.S. Kilberg. 2002. ATF4 is a mediator of the nutrient-sensing response pathway that activates the human asparagine synthetase gene. J Biol Chem 277:24120-7.

Song, H., J. Luo, W. Luo, J. Weng, Z. Wang, B. Li, D. Li, and M. Liu. 2008. Inactivation of G-protein-coupled receptor 48 (Gpr48/Lgr4) impairs definitive erythropoiesis at midgestation through down-regulation of the ATF4 signaling pathway. J Biol Chem 283:36687-97.

Sood, R., A.C. Porter, K. Ma, L.A. Quilliam, and R.C. Wek. 2000. Pancreatic eukaryotic initiation factor-2α kinase (PEK) homologues in humans, *Drosophila melanogaster* and *Caenorhabditis elegans* that mediate translational control in response to endoplasmic reticulum stress. Biochem J 346 Pt 2:281-93.

Sun, Y. 2006. E3 ubiquitin ligases as cancer targets and biomarkers. Neoplasia 8:645-54.

Tacchini, L., L. Bianchi, A. Bernelli-Zazzera, and G. Cairo. 1999. Transferrin receptor induction by hypoxia. HIF-1-mediated transcriptional activation and cell-specific post-transcriptional regulation. J Biol Chem 274:24142-6.

Takeda, K., A. Cowan, and G.H. Fong. 2007. Essential role for prolyl hydroxylase domain protein 2 in oxygen homeostasis of the adult vascular system. Circulation 116:774-81.

Takeda, K., V.C. Ho, H. Takeda, L.J. Duan, A. Nagy, and G.H. Fong. 2006. Placental but not heart defects are associated with elevated hypoxia-inducible factor α levels in mice lacking prolyl hydroxylase domain protein 2. Mol Cell Biol 26:8336-46.

Tan, C., R.G. de Noronha, A.J. Roecker, B. Pyrzynska, F. Khwaja, Z. Zhang, H. Zhang, Q. Teng, A.C. Nicholson, P. Giannakakou, W. Zhou, J.J. Olson, M.M. Pereira, K.C. Nicolaou, and E.G. Van Meir. 2005. Identification of a novel small-molecule inhibitor of the hypoxia-inducible factor 1 pathway. Cancer Res 65:605-12.

Tan, S. 2001. A Modular Polycistronic Expression System for Overexpressing Protein Complexes in *Escherichia coli*. Protein Expression and Purification 21:224-234.

Tazuke, S.I., N.M. Mazure, J. Sugawara, G. Carland, G.H. Faessen, L.F. Suen, J.C. Irwin, D.R. Powell, A.J. Giaccia, and L.C. Giudice. 1998. Hypoxia stimulates

insulin-like growth factor binding protein 1 (IGFBP-1) gene expression in HepG2 cells: a possible model for IGFBP-1 expression in fetal hypoxia. Proc Natl Acad Sci U S A 95:10188-93.

Tian, H., S.L. McKnight, and D.W. Russell. 1997. Endothelial PAS domain protein 1 (EPAS1), a transcription factor selectively expressed in endothelial cells. Genes Dev 11:72-82.

Tuckerman, J.R., Y. Zhao, K.S. Hewitson, Y.M. Tian, C.W. Pugh, P.J. Ratcliffe, and D.R. Mole. 2004. Determination and comparison of specific activity of the HIF-prolyl hydroxylases. FEBS Lett 576:145-50.

Unruh, A., A. Ressel, H.G. Mohamed, R.S. Johnson, R. Nadrowitz, E. Richter, D.M. Katschinski, and R.H. Wenger. 2003. The hypoxia-inducible factor-1 α is a negative factor for tumor therapy. Oncogene 22:3213-20.

Vallejo, M., D. Ron, C.P. Miller, and J.F. Habener. 1993. C/ATF, a member of the activating transcription factor family of DNA-binding proteins, dimerizes with CAAT/enhancer-binding proteins and directs their binding to cAMP response elements. Proc Natl Acad Sci U S A 90:4679-83.

Villar, D., A. Vara-Vega, M.O. Landazuri, and L. Del Peso. 2007. Identification of a region on hypoxia-inducible-factor prolyl 4-hydroxylases that determines their specificity for the oxygen degradation domains. Biochem J 408:231-40.

Wang, G.L., and G.L. Semenza. 1993. General involvement of hypoxia-inducible factor 1 in transcriptional response to hypoxia. Proc Natl Acad Sci U S A 90:4304-8.

Wang, G.L., B.H. Jiang, E.A. Rue, and G.L. Semenza. 1995. Hypoxia-inducible factor 1 is a basic-helix-loop-helix-PAS heterodimer regulated by cellular O_2 tension. Proc Natl Acad Sci U S A 92:5510-4.

Warnecke, C., W. Griethe, A. Weidemann, J.S. Jurgensen, C. Willam, S. Bachmann, Y. Ivashchenko, I. Wagner, U. Frei, M. Wiesener, and K.U. Eckardt. 2003. Activation of the hypoxia-inducible factor-pathway and stimulation of angiogenesis by application of prolyl hydroxylase inhibitors. Faseb J 17:1186-8.

Wu, G., G. Xu, B.A. Schulman, P.D. Jeffrey, J.W. Harper, and N.P. Pavletich. 2003. Structure of a β-TrCP1-Skp1-β-catenin complex: destruction motif binding and lysine specificity of the SCF(β-TrCP1) ubiquitin ligase. Mol Cell 11:1445-56.

Wykoff, C.C., N.J. Beasley, P.H. Watson, K.J. Turner, J. Pastorek, A. Sibtain, G.D. Wilson, H. Turley, K.L. Talks, P.H. Maxwell, C.W. Pugh, P.J. Ratcliffe, and A.L. Harris. 2000. Hypoxia-inducible expression of tumor-associated carbonic anhydrases. Cancer Res 60:7075-83.

Yamaguchi, S., H. Ishihara, T. Yamada, A. Tamura, M. Usui, R. Tominaga, Y. Munakata, C. Satake, H. Katagiri, F. Tashiro, H. Aburatani, K. Tsukiyama-Kohara, J. Miyazaki, N. Sonenberg, and Y. Oka. 2008. ATF4-mediated induction of 4E-BP1 contributes to pancreatic beta cell survival under endoplasmic reticulum stress. Cell Metab 7:269-76.

Yang, X., K. Matsuda, P. Bialek, S. Jacquot, H.C. Masuoka, T. Schinke, L. Li, S. Brancorsini, P. Sassone-Corsi, T.M. Townes, A. Hanauer, and G. Karsenty. 2004. ATF4 is a substrate of RSK2 and an essential regulator of osteoblast biology; implication for Coffin-Lowry Syndrome. Cell 117:387-98.

Yaron, A., H. Gonen, I. Alkalay, A. Hatzubai, S. Jung, S. Beyth, F. Mercurio, A.M. Manning, A. Ciechanover, and Y. Ben-Neriah. 1997. Inhibition of NF-κ-B cellular function via specific targeting of the I-κ-B-ubiquitin ligase. Embo J 16:6486-94.

Yu, V.W., G. Ambartsoumian, L. Verlinden, J.M. Moir, J. Prud'homme, C. Gauthier, P.J. Roughley, and R. St-Arnaud. 2005. FIAT represses ATF4-mediated transcription to regulate bone mass in transgenic mice. J Cell Biol 169:591-601.

Zinszner, H., M. Kuroda, X. Wang, N. Batchvarova, R.T. Lightfoot, H. Remotti, J.L. Stevens, and D. Ron. 1998. CHOP is implicated in programmed cell death in response to impaired function of the endoplasmic reticulum. Genes Dev 12:982-95.

Acknowledgment

Ganz herzlich möchte ich mich bei Prof. Dr. Dörthe Katschinski bedanken, die diese Arbeit erst möglich gemacht hat. Vielen Dank für die umfassende Betreuung und das stete Interesse an meiner Arbeit. Bedanken möchte ich mich auch für die ganze Unterstützung während meiner Promotionszeit und dafür, dass sie immer die Zeit für Ratschläge und Anregungen gefunden hat.

Des Weiteren bedanke ich mich ganz herzlich bei Dr. Jens Köditz, von dem ich zu Beginn meiner Arbeit viel gelernt habe und der mir mit seinem umfassenden fachlichen Wissen immer ein guter Ansprechpartner war.

Bei den Mitglieder meines Thesis Committees, Prof. Dr. Gerhard Braus und Prof. Dr. Frauke Melchior, möchte ich mich für das stete Interesse an meiner Arbeit sowie die unterstützenden Anmerkungen und Ratschläge bedanken. Des Weiteren möchte ich mich bei Herrn Prof. Dr. Braus für die Übernahme des Referats und bei Frau Prof. Dr. Melchior für die Übernahme des Koreferats bedanken.

Des Weiteren möchte ich mich bei den Mitgliedern der Prüfungskommission, Prof. Dr. Frauke Alves, Prof. Dr. Matthias Dobbelstein, Prof. Dr. Dr. Hannelore Ehrenreich und Prof. Dr. Jürgen Wienands, bedanken.

Ganz besonders möchte ich mich auch bei Dr. Sabine Vogel bedanken, die mein Interesse für die Arbeit der Herz- und Kreislaufphysiologie geweckt hat und immer als Ansprechpartner für mich da war. Vielen Dank auch für alle Korrekturen während meiner gesamten Promotionszeit. Und bei meiner Büronachbarin Dr. Anke Zieseniß möchte ich mich für die große Unterstützung und die vielen Anregungen bedanken. Vielen Dank für die Korrektur der Arbeit. Bei Melanie von Ahlen möchte ich mich für die vielen praktischen Tipps im Labor bedanken und bei Sabine Krull für ihre große Hilfsbereitschaft. Des Weiteren möchte ich mich bei allen weiteren Mitarbeiten des Arbeitskreises für das echt tolle Arbeitsklima und die große Hilfsbereitschaft bedanken. Und auch bei den ehemaligen Mitarbeitern des Arbeitskreises, Dr. Sonja Hägele und Dr. Malte Kleinschmitdt, möchte ich mich für ihre Hilfe und Unterstützung ganz herzlich bedanken. Dank für die gute Stimmung im Labor und die schönen Jahre in Göttingen.

Vielen Dank auch an Shivangi Gupta und Nina Schnedler, ohne die es in Göttingen nicht halb so schön geworden wäre! Thanks for the nice time in Göttingen.

Besonders möchte ich mich aber auch bei meinen Eltern und meinem Bruder bedanken, die mich alle die Jahre immer unterstützt haben und so zum Gelingen dieser Arbeit beigetragen haben.

Publications

Articles in peer-reviewed journals

Year	Publication
2009	**Normoxic destabilization of ATF-4 depends on proteasomal degradation.** Wottawa M[1], Köditz J, Katschinski DM (Manuscript under revision)
2007	**Oxygen-dependent ATF-4 stability is mediated by the PHD3 oxygen sensor**. Köditz J, Nesper J, Wottawa M[1], Stiehl DP, Camenisch G, Franke C, Myllyharju J, Wenger RH, Katschinski DM. Blood. 2007 Nov 15;110(10):3610-7.
2007	**Impact of ammonium permeases mepA, mepB, and mepC on nitrogen-regulated secondary metabolism in *Fusarium fujikuroi*.** Teichert S, Rutherford JC, Wottawa M[2], Heitman J, Tudzynski B. Eukaryot Cell. 2008 Feb;7(2):187-201.
2006	**Role of the *Fusarium fujikuroi* TOR kinase in nitrogen regulation and secondary metabolism.** Teichert S, Wottawa M[2], Schönig B, Tudzynski B. Eukaryot Cell. 2006 Oct;5(10):1807-19.

[1]Department of Cardiovascular Physiology, Center for Physiology and Pathophysiology, Georg-August-University Goettingen, Germany.
[2] Department of Botany, Faculty of Biology. Westfälischen Wilhelms University, Münster, Germany

Conferences

Conference	Organization	Location	Date	Contribution
87th Congress of the DPG	Deutsche Physiologische Gesellschaft (DPG)	Köln, Germany	02.03.-05.03.08	poster presentation
88th Congress of the DPG	Deutsche Physiologische Gesellschaft (DPG)	Gießen, Germany	22.03.-25.03.09	oral presentation

Biography

Name	Marieke Claudia Wottawa
Date of birth	19.11.1980
Place of birth	Kaufbeuren, Germany

1991 to June 2000	Marienschule Münster, bischöfliches Mädchen-gymnasium Münster, Germany
June 2000	Abitur
September 2000 to January 2006	Diploma Biology, Westfälischen Wilhelms-University Münster, Germany Thesis title: Molecular studies on the nitrogen regulation of *Fusarium fujikuroi*
April 2006 to July 2006	research assistent, Department of Botany, Westfälischen Wilhelms-University, Münster, Germany
October 2007 to September 2009	PhD student at the Department of Cardiovascular Physiology, Georg-August-University, Göttingen, Germany